Function and regulation of Death-associated protein kinase1 (DAPK) in colon cancer cells and macrophage-like cell line

Identification of p38 as a novel DAPK interacting partner during TNFα-mediated apoptosis in colon cancer

Dissertation

zur Erlangung des akademischen Grades

doctor rerum naturalium

(Dr. rer. nat.)

genehmigt durch die Fakultät für Naturwissenschaften

der Otto-von-Guericke-Universität Magdeburg

von Dipl.-Biol. Khuloud Bajbouj

geb. am 10.03.1980 in Om AlQwain, Vereinigte Arabische Emirate

Gutachter: Prof. Dr. Regine Schneider-Stock

Prof. Dr. Arndt Hartmann

eingereicht am: 12.12.2007

verteidigt am: 11.02.2008

Acknowledgments

This work was carried out at the institute of pathology, Otto-von-Guericke University, Magdeburg.

First of all I would like to express my gratitude to Professor Dr. med. Albert Roessner, Director of the institute of pathology for his friendly reception of this undertaking and the opportunity to develop my thesis in his institute.

I am extremely grateful to Professor Dr. Regine Schneider-Stock, the best group leader, who gave me a primary opportunity to attend research work, for her continuous support and guidance.

I am very thankful to my colleagues, especially Diana Walluscheck, Kathrin Haase, Thomas Drewes, and Dr. Roland Hartig and all other members of the institute of pathology and as well as institute of immunology for their intellectual support, friendship, help and cooperation.

I would like to thank Hiltraud Scharfenort, Simone Staeck, Uta Schönborn, and Antje Schinlauer for their support and excellent technical assistance.

My friends Kathrin Gruss, Evelyn Busse and Susanne Bonifatius, thank you for your friendship and support.

I would also like to thank my family (my mother, sisters, and my brother) for their continuous support in my whole life, their love and friendship.

My husband, you deserve a special thank you.

Finally, I dedicate this thesis to my father.

Table of Contents

1. Abstract

Death-associated protein kinase (DAPK) is a serine/threonine kinase that contributes to pro-apoptotic signalling upon cytokine exposure. Recently, it has been found that a high DAPK expression in colorectal tumor cells and tumor-associated macrophages (TAMs) was correlated with a high apoptotic rate in tumor cells but not in TAMs suggesting a new function of DAPK in apoptosis induction during the interaction between colorectal tumor cells and TAMs. However, the role of DAPK regulation in macrophage-associated tumor cell death is still elusive. We used a cell-culture model with conditioned supernatants of differentiated/activated macrophages (U937) and HCT116 colorectal tumor cells to recapitulate DAPK-associated tumor cell death that might reflect the *in vivo* tumor setting. We measured Cytokines in differentiated/activated macrophage supernatants ELISA. DAPK expression and DAPK activity were determined by *real-time* RT-PCR, Western Blotting, and DAPK *in vitro* kinase assay. Co-immunoprecipitation and triple immunofluorescence labelling were used to show protein interactions. For detection of protein-dependent apoptosis induction, we used the Annexin V-binding assay, caspase 3/7 activity ELISA, Western Blotting and siRNA-transfection. Here, we show that *in vitro* DAPK induction and apoptosis in tumor cells was due to TNF-α release from the activated macrophages. p53 was found to act down-stream of DAPK in this scenario. Simultaneously, an early phosphorylation of p38 MAPK was observed. We identified for the first time that p-p38 MAPK co-localizes and interacts with DAPK and triggers DAPK-mediated apoptosis in the HCT116 cells. We addressed the physiological relevance of our findings and showed that supernatants of freshly isolated human macrophages were also able to induce DAPK, p-p38, and caspase 3 cleavage in HCT116 cells. We further verified the co-localization of DAPK and p-p38 proteins by immunohistochemistry analysis of human colon cancer slices. Moreover, the observed apoptosis resistance in the macrophages was mediated by DAPK. Finally, we suggest that, the cytoprotective effect of DAPK impacts the mitochondrial signalling pathway by inhibiting the caspase 3 cleavage.

Altogether, we are the first to show p-p38 triggering of DAPK-activation in TNFα-induced apoptosis. Our findings highlight the mechanisms underlying DAPK regulation in tumor cell death evoked by immune cells.

2. Zusammenfassung

Die death-associated protein kinase (DAPK) ist eine Ca^{2+}/Calmodulin regulierte Serin-Threonin-Kinase, die nach Zytokinstimulation eine proapoptotische Funktion hat. Neuesten Berichten zufolge exprimieren nicht nur kolorektale Tumorzellen sondern auch die sie umgebenden tumor-assozierten Makrophagen die DAPK. Dabei war eine erhöhte DAPK-Expression in den Tumorzellen mit einer verstärkten Apoptose assoziiert, während DAPK-positive Makrophagen keine TUNEL-Färbung zeigten. Über die Rolle der DAPK bei der immunzell-vermittelten Apoptose ist bisher jedoch nichts bekannt.

Um die *in vivo* Bedingungen zu simulieren und die DAPK-assozierte Tumorzell-Apoptose näher zu untersuchen, wurde ein Zellkulturmodell mit konditionierten Überständen der ausdifferenzierten/aktivierten Makrophagen (U937) und der kolorektalen Tumor-Zelllinie HCT116 verwendet. Gleichzeitig sollte geprüft werden, ob die DAPK eine Rolle bei der Apoptoseresistenz der Makrophagen spielt.

Zunächst wurden die in den Überständen von ausdifferenzierten/aktivierten Makrophagen enthaltenen Zytokine mittels ELISAs gemessen. Die DAPK-Expression und die DAPK-Aktivität wurden über *real-time* RT-PCR, Western Bloting und DAPK in-vitro Kinase-Assay untersucht. Die Methoden der Co-Immunopräzipitation und der Dreifach-Immunfluoreszenzfärbung wurden verwendet, um Protein-Protein-Interaktionen nachzuweisen. Der Annexin V-binding Assay, die Caspase 3 und 7 Aktivitäts-ELISAs, der Nachweis von aktiven Spaltprodukten im Western Blot sowie die siRNA-Transfektion wurden verwendet, um eine DAPK-abhängige Apoptoseinduktion zu untersuchen. Wir konnten zeigen, dass in-vitro die DAPK-Regulation und die Apoptoseinduktion in den Tumorzellen von der TNFα-Freisetzung der aktivierten Makrophagen abhängig sind. Weiterhin stellte sich heraus, dass p53 dabei downstream von DAPK agierte. Gleichzeitig wurde eine frühe Phosphorylierung von p38-MAPK beobachtet. Wir konnten erstmalig die Co-Lokalisation und Interaktion von p-p38-MAPK mit DAPK in den HCT116-Zellen nach TNFα-Behandlung beschreiben. Ferner induziert p-p38 die katalytische Aktivierung der DAPK und vermittelt somit die DAPK-abhängige Apoptose. Um die physiologische Relevanz unserer Daten zu zeigen, untersuchten wir das DAPK- und

p-p38-Expressionsmuster in humanen Normal-Gewebe und Gewebe von Kolonkarzinomen. Die immunhistochemische Analyse zeigte nur in den Tumoren eine DAPK-p-p38 Co-lokalisation. Auch frisch isolierte humane Makrophagen vermögen nach Akivierung den apopotischen Zelltod in der HCT116 Zellinie auszulösen. Ferner stellten wir fest, dass die beobachtete Apoptoseresistenz in den Makrophagen DAPK-abhängig war. Schließlich postulieren wir, dass die DAPK-vermittelten Resistenz in den Makrophagen über den Caspase 3 Weg realisiert ist.

Zusammenfassend zeigte unsere Studie erstmalig, dass die TNFα-induzierte Apoptose über eine DAPK-Aktivierung durch p-p38 ausgelöst wird. Unsere Ergebnisse haben eine weitreichende Bedeutung für die Erklärung der durch Immunzellen ausgelösten Tumorzellapoptose sowie einer Termination der Makrophagenantwort.

3. Introduction

3.1 Protein kinases

A protein kinase is a kinase enzyme that modifies other proteins by chemically adding phosphate groups to them (phosphorylation). This class of proteins is further separated into subsets such as PKC alpha, PKC beta, and PKC gamma, each with specific functions. Phosphorylation usually results in a functional change of the target protein (substrate) by changing enzyme activity, cellular location, or association with other proteins. Up to 30% of all proteins may be modified by kinase activity, and kinases are known to regulate the majority of cellular pathways, especially those involved in signal transduction, the transmission of signals within the cell. The human genome contains about 500 protein kinase genes; they constitute about 2% of all eukaryotic genes. The chemical activity of a kinase involves removing a phosphate group from ATP and covalently attaching it to one of three amino acids that have a free hydroxyl group. Most kinases act on both serine and threonine, others act on tyrosine, and a number (dual specificity kinases) act on all three. Because protein kinases have profound effects on a cell, their activity is highly regulated. Kinases are turned on or off by phosphorylation (sometimes by the kinase itself - *cis*-phosphorylation/autophosphorylation), by binding of activator proteins or inhibitor proteins, or small molecules, or by controlling their location in the cell relative to their substrates (Anderson *et al*., 1990, Keranen *et al*., 1995, and Konishi *et al*., 1997). Disregulated kinase activity is a frequent cause of disease, particularly cancer, where kinases regulate many aspects that control cell growth, movement and death (Pawson et al., 2000).

3.1.1 DAPK family

Death-associated protein kinase1 (DAPK) is a calmodulin (CaM)-regulated serine/threonine protein kinase. DAPK features a multidomain structure (Fig. 1), comprising eight ankyrin repeats (a 33-amino acid repeat that has been implicated in mediating protein−protein interactions), P-loops (a mononucleotide-binding sequence motif), a cytoskeleton-binding region, a death-domain and a catalytic (kinase) domain (Cohen et al., 1997; Kimchi et al., 1998; Cohen et al., 1999; Raveh et al., 2000) that has high sequence similarity to vertebrate myosin light chain kinase (MLCK). Like MLCK, DAPK does not require phosphorylation for activation.

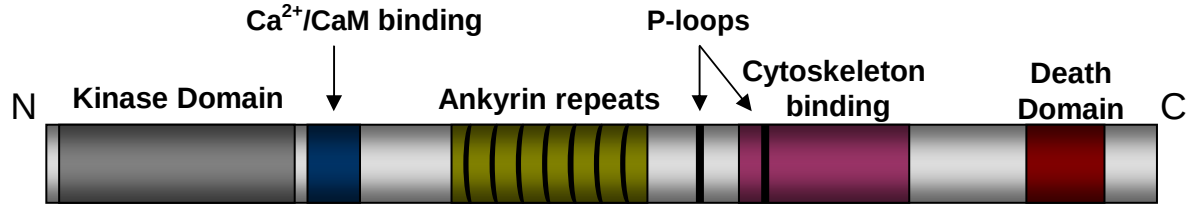

FIG. 1. Schematic diagram of DAP-kinase1 protein structure. The 160 kDa Ca2+/calmodulin (CaM)-regulated Ser/Thr kinase bears a multiple domain structure. The catalytic and the calmodulin regulatory domains determine substrate specificity and regulation of kinase catalytic activity, respectively. The non-catalytic association domains, involved in subcellular localization or interactions with other proteins, include the ankyrin repeats, two nucleotide-binding P-loops, a cytoskeleton-binding region, and a death domain.

Four additional kinases that show a significant homology in their catalytic domain to DAPK have been recently identified (Inbal et al., 2000). ZIP(Dlk)-kinase and DRP-1 are the closest family members, as their catalytic domains share approximately 80% identity to that of DAPK. Two more distant DAPK-related proteins are DRAK1 and DRAK2 (Fig. 2). Phylogenetic analyses, based on multiple sequence alignment of the catalytic domains of 16 proteins, show that DAPK, ZIP(Dlk)-kinase and DRP-1 may be grouped into a distinct clade with high bootstrap probabilities. DRAK1 and DRAK2 form another clade sharing a putative common ancestor to the other DAPK related proteins. Interestingly, the extracatalytic domains of these five members differ considerably from each other (Fig. 2). Additionally, ZIPkinase, DRAK1 and DRAK2 were shown to be nuclear proteins that do not require Ca2 +/CaM for activation. DRP-1, however, is a cytoplasmic kinase, containing a typical CaM-regulatory domain similar to that of DAPK and a short C-terminal segment required for homodimerization.(Inbal et al., 2000 and Shani et al ., 2001). Interestingly, DRP-1 can promote cell death upon its ectopic expression and it shares with DAPK many of the induced subcellular events including membrane blebbing and the formation of autophagic vesicles (Inbal et al., 2002).

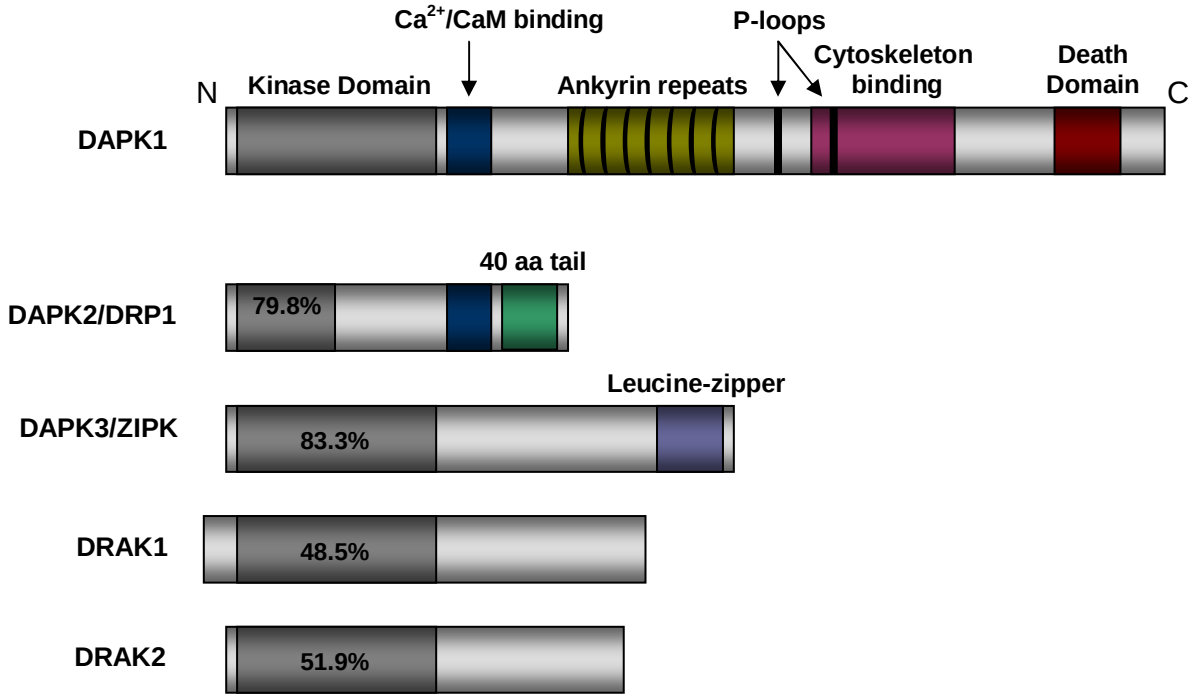

FIG. 2. Schematic diagram of Death associated protein kinase family: DAP Kinase 1 (DAPK), DAP kinase related protein 1/DAP kinase 2 (DRP-1/DAPK2), DAP kinase 3 (DAPK3/ZIPK), DAP kinase related apoptosis inducing protein kinase 1 und 2 (DRAK1 und DRAK2).

3.1.1.1 DAPK function

Death-Associated Protein Kinase1 (DAPK) is a 160 kDa-Ca2+ /Calmodulin-dependent, cytoskeletal-associated protein kinase the expression of which is implicated in the sensitivity of cells to apoptotic effects of cytokines such as Interferon-γ, TNFα, and TGF-β (Deiss et al., 1995; Cohen et al., 1999; Jang et al., 2001). It has been found that DAPK exerts an apoptotic effect by inside-out inactivation of integrin ß1, thereby suppressing the matrix survival signal and activating a p53-dependent apoptosis pathway (Wang et al., 2002). Accordingly, the proapoptotic activity of DAPK is largely dependent on the existence of functional p53 protein, and several p53-deficient cell lines either escape from cell death (Wang et al., 2002) or undergo autophagic death in response to DAPK overexpression (Inbal et al., 2002). However, given the broad involvement of DAPK in tumor suppression and the frequent loss or mutation of p53 in various tumors, we postulate that DAPK elicits the second, apoptosis-unrelated mechanism to suppress tumor progression. Notably, the effects of DAPK on integrin inactivation (Wang et al., 2002) and actin cytoskeleton reorganization (Kuo et al., 2003; Bialik et al., 2004) raise the possibility of DAPK involvement in motility regulation. It has been demonstrated that DAPK

interferes with directional persistence during random migration and with cell polarization during directed migration and that these effects of DAPK are mainly mediated by its suppression of the integrin–Cdc42 signaling axis. Even in tumor cells that are resistant to DAPK-induced apoptosis, DAPK can elicit this motility-inhibitory effect and functions as a determining factor in tumor cell invasion (Kuo et al., 2006).

3.1.1.2 DAPK signal transduction

It has been shown that TGFβ activates DAPK promoter through the action of the transcription factors Smad2, Smad3, and Smad4 (Jang et al., 2001). Futhuremore, Martoriati et al. (2005) demonstrates that *DAPK* is a target of the transcription factor p53. DAPK is up-regulated by hyperproliferative signals, and operates upstream of $p19^{ARF}$ and p53 to induce apoptosis. Whereas the inactivation or loss of DAPK significantly reduces the p53 responses to c-Myc or E2F-1, it does not completely eliminate them, indicating that DAPK is not an exclusive player upstream of $p19^{ARF}$/p53 (Raveh et al., 2001). Recent studies showed several mechanisms influencing DAPK activity. These include; the phosphorylation by RSK at Ser289, which triggers a suppression of DAPK proapoptotic function (Anjum et al., 2005), the autophosphorylation site, which was mapped to Ser308 within the CaM-regulatory domain (Shohat et al., 2002), ERK-phosphorylation of DAPK at Ser735, which stimulates DAPK-mediated apoptosis (Chen et al., 2005), phosphorylation of DAPK by SRC at Tyr491/492, which induces DAPK intra-/intermolecular interaction and inactivation, and 5) dephosphorylation by LAR at pTyr491/492 to stimulate the catalytic, proapoptotic, and antiadhesion/antimigration activities of DAPK (Wang et al., 2007). Furthermore, cathepsin B can directly interact with DAPK, forming a stable immune complex mediated by TNFR-1 induction of the changing of DAPK localization (Lin et al., 2007). It has been also found that inhibition of HSP90 results in degradation of active dephosphorylated DAPK via the ubiquitin proteasome pathway. Also DAPK can form heterocomplexes composed of HSP90 and CHIP or DIP1/Mib1, indicating that the heightened surveillance and modulation of DAPK activities is critical to accurate regulation of apoptosis and cellular homeostasis (Zhang et al., 2007). Several substrates of DAPK have been identified shown in table 1.

Substrate	**Mechanism of action**	**Reference**
myosin II regulatory light chain (MLC)	Mediation of membrane blebbing	Jin et al., 2001
Syntaxin	Syntaxin regulation in response to intracellular [Ca2+] and synaptic activity	Tian et al., 2003
$p19^{ARF}$	Linkage of certain oncogenes to the $p19^{ARF}$/p53-mediated apoptotic checkpoint	Raveh et al., 2001
ZIPK	Regulation of ZIPK intracellular localization and association with changes in cell motility and cell death	Shani el al., 2004
Mammalian 40S ribosomal protein S6	Reduction of protein synthesis	Schumacher et al., 2006
Protein kinase D (PKD)	Activation of JNK signalling under oxidative stress	Eisenberg-Lerner et al., 2007

Table 1: Substrates of DAPK

3.1.1.3 DAPK in cancer

A role for DAPK in the activation of a $p19^{ARF}$/p53 cell cycle checkpoint has been established (Raveh et al. 2001), thus providing a mechanism whereby loss might lead to inactivation of this critical apoptotic pathway in tumorigenesis. Indeed, several studies have suggested that loss of DAPK expression or methylation of its associated CpG islands (CGI) may be characteristics of highly invasive or metastatic tumours (Simpson et al., 2002). More than 100 reports from different laboratories were published on DAPK gene methylation in various human tumors. The absence of DAPK expression in highly metastatic variants of mouse lung cancer cell lines, in contrast to its presence in the low metastatic variants of those same cell lines, led to

the study of the role of DAPK expression in lung tumor growth and metastasis (Inbal et al., 1997). Additional analysis of primary tumor samples from patients with colon cancer revealed that the DAPK gene was methylated in 26% of these tumors (Raveh et al., 2001). In an in vivo model of experimental metastasis, reintroduction of DAPK by stable transfection in the highly metastatic clones that lost DAPK expression, attenuated the metastatic capacities of these cells. A recent study reported that DAPK expression in colorectal carcinoma was associated with high apoptotic rate. On the other hand this study showed that the DAPK expressing tumor-associated macrophages were TUNEL-negative, suggesting a dual function of DAPK (Schneider-Stock et al., 2006).

3.1.2 MAPKs

Cells recognize and respond to extracellular stimuli by engaging specific intracellular programs, such as the signalling cascade that leads to activation of the mitogen-activated protein kinases (MAPKs). All eukaryotic cells possess multiple MAPK pathways, which co-ordinately regulate diverse cellular activities running the gamut from gene expression, mitosis, and metabolism to motility, survival and apoptosis, and differentiation. To date, five distinct groups of MAPKs have been characterized in mammals: extracellular signal-regulated kinases (ERKs) 1 and 2 (ERK1/2), c-Jun amino-terminal kinases (JNKs) 1, 2, and 3, p38 isoforms α, β, γ, and δ, ERKs 3 and 4, and ERK5 (Chen et al., 2001 and Kyriakis et al., 2001). Since *Saccharomyces cerevisiae* possesses six different MAPKs, the relative complexity of the human genome suggests that there are probably several additional vertebrate MAPK subfamilies (Madhani et al., 1998). The most extensively studied groups of vertebrate MAPKs to date are the ERK1/2, JNKs, and p38 kinases. MAPKs can be activated by a wide variety of different stimuli, but in general, ERK1 and ERK2 are preferentially activated in response to growth factors and phorbol esters, while the JNK and p38 kinases are more responsive to stress stimuli ranging from osmotic shock and ionizing radiation to cytokine stimulation (Pearson et al., 2001)

3.1.2.1 P38

The most well-known role of the p38 family is as a transducer of responses to environmental stress such as hyperosmolarity, UV irradiation, heat shock, and inhibition of protein synthesis, as well as to receptor occupancy by pro-inflammatory

molecules such as endotoxin, TNFα, and IL-1 (Raingeaud et al., 1995; Derijard et al., 1994; Han et al., 1994). p38 signaling has been implicated in responses ranging from apoptosis, cell survival (protection from apoptosis), induction of cytokine genes, differentiation, and activation of effector functions (Zarubin et al., 2005). The best-characterized mechanism for activating p38 is dual phosphorylation of a Thr-Gly-Tyr motif by upstream MAPK kinases (MAPKK). A major question is how these ubiquitous kinases carry out specific biological effects while seemingly being activated by a single mechanism. p38 substrates are numerous and continue to be identified; which subsets are phosphorylated in response to different stimuli, how they are activated, and their roles in cell-specific p38 signaling remain to be sorted out (Schaeffer et al., 2000).

p38 was shown to be present in both the nucleus and cytoplasm of quiescent cells, but upon cell stimulation, the cellular localization of p38 is not well understood. Some evidence suggests that, following activation, p38 translocates from the cytoplasm to the nucleus (Raingeaud et al., 1995), but other data indicate that activated p38 is also present in the cytoplasm of stimulated cells (Ben-Levy et al., 1998).

3.1.2.2 P38 in cancer

p38 has recently gained attention as a tumor suppressor. A comparison of 20 human hepatocellular carcinomas with adjacent nonneoplastic tissue showed that p38 was significantly less active in tumors; additionally, the larger the tumor, the less p38 activity was detected (Iyoda et al., 2003). Other studies showed that oncogenic Ras cannot induce transformation unless p38 is silenced (Pruitt et al., 2002; Ellinger-Ziegelbauer et al., 1999). Overall, these studies indicate that sustained p38 activity is consistent with dormancy behavior and inconsistent with proliferation and growth of primary tumors in vivo. Thus it appears that p38 activation ought to suppress oncogenesis. Indeed, when p38 activity was forced in rhabdomyosarcoma cells, it induced terminal differentiation (Puri et al., 2000). Similarly, deletion of a p38-inhibitory phosphatase blocked Hras1- and erbB2-induced carcinogenesis in vivo, whereas inhibition of p38 promoted tumor formation (Bulavin et al., 2004). Imposed p38 activation in HeLa cells specifically suppressed their tumor-forming ability in vivo (Timofeev et al., 2005). Other studies have evaluated p38 activity in the response to chemotherapy. The results indicate that diverse chemotherapeutic agents stimulate apoptosis in a p38-dependent manner. For example, microtubule-perturbing drugs

such as vinblastine, vincristine and taxol induce tumor cell apoptosis that is inhibited by treatment with SB203580 (Deacon et al., 2003). In these cells, the basal level of apoptosis is 2%, but can be raised to 54% by activating p38 (Deacon et al., 2003). Cisplatinin, a DNA damaging agent, also induced p38-dependent apoptosis in several cells lines (Losa et al., 2003). Thus, p38 appears to promote tumor cell apoptosis, at least in some cases. However, this should not be construed as a universal relationship, since p38 activity can also block apoptosis. For example, the anthrax lethal factor promotes macrophage apoptosis by inhibiting p38 activity (Park et al., 2002). Furthermore, the p38 MAPK inhibitor SB239063 significantly reduced TNFα production from LPS-stimulated human lung macrophages (Smith et al., 2006).

3.2 Colorectal carcinoma

Colorectal cancer, also called colon cancer or bowel cancer, includes cancerous growths in the colon, rectum and appendix. According to the World Health organization (WHO), it is the third most common form of cancer and the second leading cause of cancer-related death in the Western world. Colorectal cancer causes 655,000 deaths worldwide per year. It is now generally accepted that colorectal cancer develops by genetic alterations. Analysis of the molecular mechanism makes it possible to develop a more targeted approach to prevention and treatment of this cancer. There are two major pathways in colorectal carcinogenesis. One is the chromosomal instability pathway (adenoma-carcinoma sequence), which is characterized by allelic losses, and the other is a pathway involving microsatellite instability (MSI), described below.

3.2.1 Risk factors and causes

Most cases of colorectal cancer are due to sporadic factors, namely older age, ureterocolic anastomosis, diet (rich in meat and fat, and poor in fibre, folate, and calcium), obesity, diabetes mellitus, smoking, previous irradiation, and high alcohol intake. Another category of colorectal cancer risk factor is inflammatory bowel disease, including ulcerative colitis and crohn's colitis. Finally, Hereditary factors are also colorectal cancer risk factors. Roughly 5–10% of all colorectal cancers develop in the setting of defined hereditary cancer syndromes. The two main forms are

hereditary nonpolyposis colorectal cancer (HNPCC) and familial adenomatous polyposis (FAP).

3.2.1 Pathogenesis

The majority of colorectal cancers develop from adenomas. The progression from an adenoma to a cancer passes through a series of defined histological stages referred to as the adenoma-carcinoma sequence (Fig. 3) (Vogelstein et al., 1988). The colorectal tumour initiation requires several different somatic changes before a cell can develop into a carcinoma (Kinzler et al., 1996).

3.2.1.1 Chromosomal instability pathway

Fearon and Vogelstein et al. (1990) proposed a multistep model of colorectal carcinogenesis, in which mutations in the adenomatous polyposis coli (*APC*) gene occur early during the development of polyps, *K-ras* mutations arise during the adenomatous stage, and mutations of *p53* and deletions on chromosome 18q occur concurrently with the transition to malignancy. This pathway is characterized by allelic losses on chromosome 5q (*APC*), 7p (*p53*), and 18q (*DCC/SMAD4*), and is therefore called the chromosomal instability (CIN) pathway. One of the cornerstones of the CIN pathway is the model represented by FAP, in which multiple small adenomas form as a result of initiation of tumorigenesis, namely, two hits in the *APC* gene, followed by mutations of *K-ras*, and subsequently mutations of *p53* and deletion on chromosome 18q. Furthermore, it has been shown that DAPK promotor methylation is an early event in colorectal carcinogenesis (Mittag et al., 2005). It has been suggested that, the same mechanism is also applicable to sporadic colorectal carcinogenesis.

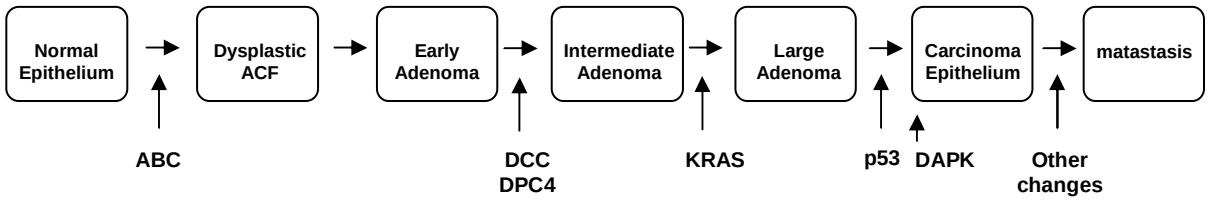

FIG. 3. Main events in the adenoma-carcinoma sequence (Vogelstein et al., 1988; Boland et al., 1995)

3.2.1.2 Microsatellite instability pathway

Microsatellite instability (MSI) is characterized by expansions or contractions in the number of tandem repeats of simple DNA sequences (microsatellites). MSI has been identified in colorectal cancer associated with HNPCC syndrome (Ionov et al., 1993, Thibodeau et al., 1993, and Aaltonen et al., 1993), and DNA mismatch repair (MMR) enzymes, including hMSH2, hMLH1, hPMS1, hPMS2, and hMSH6, have since been shown to be responsible for MSI (Fishel et al., 1993, Bronner et al., 1994, Nicolaides et al., 1994, Nicolaides et al., 1995, and Papdopoulos et al.,1995). Moreover, mutations in microsatellites of target genes such as the transforming growth factor-β (*TGF*-b) gene have also been identified in MSI positive tumors (Markowitz et al., 1995).

3.3 Tumor-associated macrophages (TAMs)

It is widely accepted that tumour-associated macrophages (TAMs) represent a major and important component of the leukocyte infiltrates of many tumours and metastatic deposits (Mantovani et al., 1986 and Volodko et al., 1998). It has been established that TAMs have pleiotropic functions, which can influence tumour growth, both in terms of progression and regression. This differential effect of TAMs is believed to be regulated by modulation of the host immune system (Mills et al., 1992 and Elgert et al., 1998). Tumour growth reduction by TAMs can be mediated by non-specific anti-tumour cytotoxic mechanisms or induction of specific cell lytic effects (Grabbe et al., 1994 and Blachere et al., 1997). On the other hand, there is convincing data for TAMs demonstrating tumour cell growth-promoting effects through release of various cytokines and prostanoids (Sunderkotter et al., 1994 and Parajuli et al., 1996). Also, macrophages have been shown to suppress many T cell (Alleva et al., 1994 and Aoe et al., 199) and NK cell (Aso et al., 1992) anti-tumour responses. What determines the outcome of these competing interactions and subsequent defined macrophage functions during tumour growth, as yet, is still poorly defined. An understanding of the complex regulatory mechanisms, therefore, that control macrophage functions during tumour growth is critical to planning therapeutic approaches to achieving improvement of patient well being and control of the malignant process.

3.3.1 TAM repression of Tumor Growth

Macrophages, particularly when activated, can be cytostatic or cytotoxic for tumour cell growth (Fidler et al., 1988; Owen et al., 1998 and Killion et al., 1998). In 1959, Biozzie observed that Bacille Calmette-Guérin (BCG)- a non-specific activator of the 'reticulo-endothelial system-when inoculated into mice, was able to decrease the growth of certain tumours. Since these early observations, many reports have demonstrated that non-specific stimulants, known to activate macrophages, may inhibit tumour growth in animals when administered at an appropriate time interval in relation to inoculation of tumour cells. Also, it was observed that when grafts of tumour cells, transfected with the genes encoding for interferon (IFN)-g, IL-2 and TNFα, were rejected, activated macrophages were present in the tissues at the sites of inoculation. Furthermore, specific antibodies that blocked the recruitment of macrophages inhibited the rejection response (Colombo et al., 1992).

Macrophage-derived cytokines have been shown to be cytotoxic against a range of tumour cells (Bonta et al., 1991 and Ben-Efraim et al., 1994). IL-1 has been demonstrated to be cytotoxic and cytostatic for tumour cells (Ichinose et al., 1988). Also, it has been demonstrated that IL-1 can act synergistically or additively with TNFα in killing tumour cells. TNFα is capable of causing haemorrhagic necrosis of certain transplantable tumors in vivo (Carswell et al., 1975), and capable of direct tumour cytotoxicity in vitro. TNFα is produced primarily by monocytes and macrophages. This has led to the postulate that TNFα is involved in the delivery of the lethal hit of some tumours (Klostergaard et al., 1987 and DeMarco et al., 1992). A crucial role for TNFα in macrophage-mediated anti-tumour cell cytotoxicity has been demonstrated in two experimental studies. The first series of investigations demonstrated that UV-induced tumour clones, selected for resistance to macrophages, were resistant to TNFα (Urban et al., 1988). The second series of experiments showed that anti-TNFα antibodies inhibited macrophage cytotoxicity. More definitive experiments should now be possible with the advent of knockout mice in which the genes for TNFα and its receptors are deleted (Erickson et al., 1994). Numerous cells of immunosurveillance are known to microscopically infiltrate in cancers. These infiltrating immunosurveillance cells, including mast cell (MCs) and tumor associated macrophagel (TAMs), have been found to reflect a tumor-related immune response (Ghiara et al., 1985, Hensweson et al., 1981, Alleva et al., 1993,

and Tani et al., 2001). Although TAMs have the potential to mediate tumor cytotoxicity and to stimulate antitumor lymphocytes[3], it is still unclear whether TAMs can predict tumor prognosis. MC and TAM count were found to have a direct relationship with clinical outcome in patients with colorectal cancer. In this study, authors showed that, MCs and TAMs may play an important role in the enhancement of host immunity against cancer cells and that an increase in MCs and TAMs may improve the postoperative prognosis of patients with colorectal cancer. It is beneficial for estimating biological character of colorectal carcinoma to combine MC and TAM counts, thus enhancing immunosurveillance. Finally, in advanced gastric carcinoma, the number of TAMs in close proximity to tumor cells in tumor cell nests correlates positively with tumor cell apoptosis, suggesting that TAMs or TAM effector cells are actively involved in tumor cell destruction. Notably, tumors that have large numbers of "nest TAM" are associated with a significant increase in 10-year disease-free survival (Ohno et al., 2003).

3.3.2 TAM induction of Tumour Growth

TAMs have been shown to play a key role in tumour growth and dissemination and in some of the systematic manifestations of neoplasia. Mononuclear phagocytes can produce a range of growth factors, including platelet-derived growth factor (PDGF), epidermal growth factor (EGF) and transforming growth factor (TGF)-b, as well as cytokines such as TNFα and IL-1, that have been shown to enhance metastatic spread in several animal tumour models (Opdenakker et al., 1992; Leek et al., 1996; Salvesen et al., 1999 and Takanami et al., 1999). It is not surprising, therefore, that TAMs can promote the growth of tumour cells, an activity best observed in vitro at low effector to target cell ratios or with tumour cells in suboptimal culture conditions (Auger et al., 1992 and Mantovani et al., 1986).

There are several evidence demonstrating that, unlike macrophages from healthy tissues, which are capable of presenting tumor-associated antigens, lysing tumor cells, and stimulating the antitumor functions of T cells and NK cells, TAMs in the tumor microenvironment lack these activities, leaving the host without the ability to mount an effective antitumor immune response. A number of studies have shown that tumor-derived molecules, like cytokines, growth factors, chemotactic molecules, and

proteases, influence TAM functions (Elgert et al., 1998, Sunderkotter et al., 1991, and Ben-Baruch et al., 2005). For example, tumor cells secrete IL-4, IL-6, IL-10, MDF, TGF-ß1, and PGE_2, which inhibit the cytotoxic activity of TAMs (Elgert et al., 1998 and Ben-Baruch et al., 2005). Moreover, TGF-ß1, IL-10, and PGE_2 may suppress the expression of MHC class II molecules by macrophages in the tumor microenvironment as well as distant sites like the spleen and peritoneum. This effect may limit the ability of TAMs to present tumor-associated antigens to T cells effectively in these areas (Elgert et al., 1998). Thus, tumors undergo immunoediting to down-regulate macrophage functions that are potentially dangerous to the tumor even in circumstances where recognizable tumor antigens are presented. It should be noted that the tumoricidal activity of TAMs may vary markedly in different tumor microenvironments.

4. Thesis aims and proposal

Recently, Schneider-Stock et al. (2006) demonstrated that a high DAPK1 expression in colorectal tumors and surrounding macrophages was associated with a high apoptotic rate in in tumor cells but not in TAMs, suggesting a new function of DAPK1 in apoptosis induction during the cross talk between colorectal tumor cells and TAMs. However, the role of DAPK1 regulation in macrophages-induced tumor cell death and macrophage survival is still unknown.

The objective of the thesis was to establish an *in vitro* model, using conditioned supernatants of differentiated/activated macrophages and HCT116 colorectal tumor cells, which recapitulates the above *in vivo* observed findings and reflects the *in vivo* tumor settings (Fig. 4).

- **Supernatant study**

  Principle :
  Collect supernatants of the differentiated and activated macrophages (U937)
  Collect supernatants of the HCT116p53+/+ and HCT116p53-/-

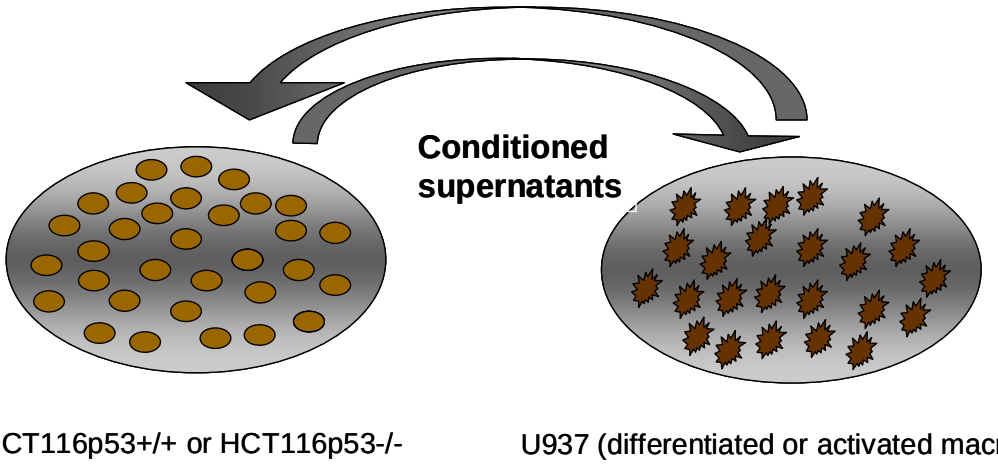

FIG. 4. Thesis Proposal: Effects of HCT116- and macrophages-conditioned supernatants on DAPK expression and function.

The aims of the thesis were to study DAPK function and regulation in two directions:

1- Macrophage ⟶ Tumor cell

- To understand the mechanisms underlying the apoptosis induction in the tumor cells and whether it is mediated by the macrophages-supernatants.
- To investigate which mediator(s), released from macrophages, is/are involved in DAPK induction.
- To study if the apoptosis induction is DAPK1-dependent.
- To examine the upstream signalling pathway, which contributes to the DAPK1/apoptosis induction.
- To verify the physiological relevance of DAPK regulation in the *in vivo* settings.

2- Tumor cell ⟶ Macrophage

- To demonstrate whether the apoptosis resistance in macrophages is mediated by DAPK1.
- To study the effects of tumor cells-supernatants on the differentiated/activated macrophages.
- To investigate upstream/downstream mechanisms in DAPK-triggered macrophage survival.

5. Materials and Methods

5.1 Materials

5.1.1 Laboratory equipment

0.45 µm sterile filters	BD Falcon, France
–20ºC Freezer	Siemens AG, Germany
4ºC Fridge	Siemens AG, Germany
5 ml FACS tubes	BD Biosciences, Belgium
–80ºC Freezer	Heraeus, Hanau, Germany
Automatic pipettes	Gilson, Middleton, WI, USA
AxioCam MRc5 camera	Carl Zeiss GmbH, Germany
Blotting chamber	Bio-rad, Munich, Germany
Coulter Counter ZII	Coulter Immunotech, Germany
Centrifuges	Eppendorf, Germany
CO2 Incubators	Heraeus, Rodenbach, Germany
Digital Precision Scale	KERN & Sohn GmbH, Germany
Fluorescence-activated cell sorter (FACS)	BD Biosciences, Belgium
Gel electrophoresis systems	Bio-rad, Munich, Germany
Heating block	Biometra, Germany
Hyperfilm	Amersham Biosciences, Germany
Kinetic microplate reader	Molecular Devices, Sunnyvale, USA
Laminar flow hoods	Heraeus, Hanau, Germany
Liquid nitrogen tank	MVE, New Prague, MN, USA
Light Cycler	Roche Diagnostics GmbH, Germany
Microscopes	Carl Zeiss GmbH, Germany
pH-meter	WTW, Weilheim, Germany
Photometer	Eppendorf, Germany
PTC-200 Peltier Thermal Cycler	MJ Research, Germany
Rocking Platforms	Biometra GmbH, Göttingen, Germany
Rotary microtome	Leica Microsystems GmbH, Germany
Semi-Dry Electrophoretic Transfer Cell	Bio-rad, Munich, Germany
Sterile cell scrapers	TPP, Switzerland
Sterile tissue culture plastic flasks, plates, dishes	NUNC, Denmark
Sterile tissue culture plastic tubes, pipets	Eppendorf, Germany
Vortex	IKA Works, Wilmington, NC, USA

Water bath	GFL, Burgwedel, Germany
X-ray film developing machine	AGFA, Germany

5.1.2 Chemical reagents and other research solutions

2-Mercaptoethanol	Merck, Darmstadt, Germany
3,3′,5,5′-Tetramethylbenzidine tablets (TMB)	Sigma-Aldrich GmbH, Germany
3-(4,5-dimethylthiazol-2-yl)-2,5-diphenyltetrazolium bromide (MTT)	Sigma-Aldrich GmbH, Germany
30% Acrylamide/Bis Solution	Roth, Karlsruhe, Germany
4',6-diamino-2-phenylindole (DAPI)	Molecular Probes, USA
D,1-Dithiothreitol (DTT)	Sigma-Aldrich GmbH, Germany
Acetic acid 96%	Sigma-Aldrich GmbH, Germany
Ammonium Persulfate	Sigma-Aldrich GmbH, Germany
Aprotinin	Roche Diagnostics GmbH, Germany
γ^{32}-ATP	Amersham Biosciences, Germany
Biotinylated Protein Ladder	Cell Signaling Inc., Germany
Bovine serumalbumin (BSA)	Sigma-Aldrich GmbH, Germany
DNA Molecular weight Marker VIII	Roche Diagnostics GmbH, Germany
Dimethylsulfoxide (DMSO)	Sigma-Aldrich GmbH, Germany
EDTA	Sigma-Aldrich GmbH, Germany
Ethanol	Merck, Darmstadt, Germany
Glycerol	Merck, Darmstadt, Germany
Glycine for electrophoresis	Merck, Darmstadt, Germany
Griess Reagent	Sigma-Aldrich GmbH, Germany
HEPES	NeoLab GmbH, Germany
Isopropanol	Merck, Darmstadt, Germany
Leupeptin A	Roche Diagnostics GmbH, Germany
LPS	Sigma-Aldrich GmbH, Germany
Magnesium Chloride	Merck, Darmstadt, Germany
Methanol	Merck, Darmstadt, Germany
Nonidet P-40	Roche Diagnostics GmbH, Germany
Phenylmethylsulfonyl fluoride (PMSF)	Sigma-Aldrich GmbH, Germany
PMA	Sigma-Aldrich GmbH, Germany
Polyethylenglycol 6000 P.E.G	FERAK LABORAT GmbH, Germany

Ponceau S	Sigma-Aldrich GmbH, Germany
Protease inhibitor cocktail Set	Calbiochem, Germany
Skim milk powder (blotting grade)	Sigma-Aldrich GmbH, Germany
Sodium Chloride	Merck, Darmstadt, Germany
Sodium Citrate	Sigma-Aldrich GmbH, Germany
Sodium Hydroxide	Sigma-Aldrich GmbH, Germany
Sodium Vanadate	Sigma-Aldrich GmbH, Germany
Sodiumdodecylsulfat (SDS)	Biorad, Munich, Germany
Sulphuric Acid	Merck, Darmstadt, Germany
Tetramethylethylendiamine (TEMED) ICN	Biomedicals Inc, Aurora, USA
Tris base	Sigma-Aldrich GmbH, Germany
Triton-X100	Sigma-Aldrich GmbH, Germany
Trizol	Invitrogen Corporation, Germany
Human fibronectin	Sigma-Aldrich GmbH, Germany
Tween 20	Merck, Darmstadt, Germany

5.1.3 Cell lines

Five human Colorectal cancer cell lines were used and one human pre-monocytic cell line (U937). All cell lines were purchased from either DSMZ (DSMZ Braunschweig, Germany) or ATCC (ATCC, Manassas, VA).

Cell line	Histological origin	Medium	Source
HCT116 p53 +/+	colorectal carcinoma	RPMI	ATCC
HCT116 p53 -/-	colorectal carcinoma	DMEM	ATCC
HT29	colorectal adenocarcinoma	RPMI	DSMZ
CaCo	colorectal adenocarcinoma	RPMI	ATCC
SW480	colorectal adenocarcinoma	RPMI	DSMZ
U937	histiocytic lymphoma	RPMI	DSMZ

5.1.4 Media and supplements

Trypsin-EDTA	PAN, Germany
RPMI 1640	PAN, Germany
Dulbecco´s Modified Eagle Medium (D-MEM)	PAN, Germany
Fetal Bovine Serum (FBS)	PAN, Germany
Fetal Calf Serum	PAN, Germany

Penicillin-streptomycin mixture	PAA, Germany

5.1.5 Kits and other research products

Avidin-biotinylated Horseradish	
Immobilon Western Chemiluminescence	Pierce, Rockford, USA
Bio-Rad Dc Protein	Biorad, Munich, Germany
DeadEnd™ Fluorometric TUNEL System	Promega, Madison, WS, USA
ECL® Western Blotting Detection System	Amersham Biosciences, Germany
Enhanced Chemiluminescence System	Amersham Biosciences, UK
CpGenome^{TM} DNA Modification Kit	Chemicon International, USA
Human TNFα Immunoassay Kit	R&D Systems, Minneapolis, MN, USA
Human IFNγ Immunoassay Kit	ImmunoTools, Germany
Immunoprecipitation Kit	Amersham Biosciences, Germany
Restore™ Western Blot Stripping Buffer	Pierce, Rockford, IL, USA
Annexin-V-FLOUS	Roche Diagnostics GmbH, Germany
Omnia Plate IP Kit (p38 MAPK)	BioSource, USA
Caspase-Glo™ 3/7 Assay kit	Promega, Madison, WS, USA

5.1.6 Antibodies

Anti-DAPK monoclonal	BD Biosciences, Belgium
Anti–p83	Cell Signaling Inc., Germany
Anti–phospho-p38	Cell Signaling Inc., Germany
Santa Cruz Biotechnology, CA, USA	
Anti-ERK1/2	Cell Signaling Inc., Germany
Anti-phospho-ERK1/2	Cell Signaling Inc., Germany
Anti-SAPK/JNK	Cell Signaling Inc., Germany
Anti–phospho-SAPK/JNK	Cell Signaling Inc., Germany
Anti–phospho-p38	Cell Signaling Inc., Germany
Anti–RSK1	Cell Signaling Inc., Germany
Anti-p53	Oncogene, San Diego, CA
Anti–caspase 3	Cell Signaling Inc., Germany
Anti-ß-actin monoclonal	Sigma-Aldrich GmbH, Germany
Goat anti-mouse	Sigma-Aldrich GmbH, Germany
Goat anti–rabbit	Sigma-Aldrich GmbH, Germany

Goat anti–rabbit	Cell Signaling Inc., Germany

5.1.7 Software

Adobe Acrobat 5.0	Adobe Systems Inc., USA
Adobe Acrobat Distiller 5.0	Adobe Systems Inc., USA
Adobe Photoshop 5.0	Adobe Systems Inc., USA
AxioVision 4.4	Carl Zeiss GmbH, Germany
SOFTmax 2.32	Molecular Devices Corp., USA
Gene Tools	Syngene, Cambridge, UK
Windows XP Professional	Microsoft Corporation, USA

5.1.8 Database

http://www.ncbi.nlm.nih.gov/entrez/query.fcgi

5.1.9 Buffers

PBS Wash Buffer, 1X

140 mM NaCl
2.7 mM KCl
10 mM Na_2HPO_4
1.8 mM KH_2PO_4
High purity dH2O, pH 7.4

PBS-T

1X PBS
0.1% Tween-20

DAP Kinase Buffer, 1X

60 mM HEPES-NaOH, pH 7.5
3 mM $MgCl_2$
3 mM $MnCl_2$
0.003 M sodium orthovanadate
1.2 mM DTT
2.5 µg/µl PEG

Protein Lysis Buffer

4 M	*Urea*
0.5%	*SDS*
62.5 mM	*Tris, pH 6.8*

RIPA Lysis Buffer, 1X

50 mM	*Tris-HCl, pH 7.4*
150 mM	*NaCl*
1% Nonidet	*P-40*
0.5%	*Sosium deoxycolate (DOC)*
1 mM	*PMSF*
1 µg/ml	*Aprotinin*
1 µg/ml	*Leupeptin*

Protease and phosphatase inhibitors were added freshly before cell lysis.

Laemmli Buffer, 2X

1.25 M	*Tris-HCl, pH 6.8*
1 M	*DTT*
0.1%	*Bromophenol Blue*
20%	*Glycerol*
4%	*SDS*

IP Wash Buffer

50 mM	*Tris, pH 8.0*

Loading Buffer, 5X

4 M	*Urea*
10%	*SDS*
62.5	*mM Tris*
20%	*DTT*

Towbin Transfer Buffer, 1X

25 mM	*Tris-HCl, pH 8.3*
192 mM	*Glycine*

20% *Methanol*

High purity dH2O

Tris Buffered Saline (TBS) Buffer, 10X

1M *Tris-HCl, pH 7.4*

1.5M *NaCl*

TBS-T Buffer

1X *TBS*

0.1% *Tween-20*

SDS Electrophoresis Buffer, 10X

0.25 M *Tris*

1.92 M *Glycine*

1% *SDS*

High purity dH2O, pH 8.3 to 1000 ml

OLD-T Puffer

40 mM *Tris/HCl, pH7.5*

150 mM *NaCl*

25 mM *EDTA, pH7,5*

Separating gel Buffer

1.875 M *Tris*

1% *SDS*

High purity dH2O, pH 8.8 to 200 ml

Stacking gel Buffer

1.875 M *Tris*

0.5% *SDS*

High purity dH2O, pH 6.8 to 200 ml

Solutions for Casting One 10% Separating and One Stacking Gel

	Separating gel, 10%	Stacking gel
H2O	4.67 ml	6.33 ml
30% Acrylamide/Bis Solution	3.33 ml	1.65 ml
Separating gel Buffer	2 ml	-
Stacking gel Buffer	-	2 ml
10% Ammonium Persulfate	0.075 ml	0.075 ml
TEMED	0.008 ml	0.008 ml

Milk Blocking Solution

5% w/v nonfat dry milk dissolved in TBS-T buffer

Ponceau S Staining Solution

0.5 g of Ponceau S was dissolved in 1 ml of glacial acetic acid and the volume was adjusted to 100 ml with H2O.

TMB Substrate Solution

One tablet of the HRP substrate TMB was dissolved in 10 ml of phosphate citrate buffer with 2 µl of 30% H2O2.

Coating buffer

0.1 M *Sodium carbonate*

8.4 g *$NaHCO_3$*

3.56 g *$Na2CO_3$*

High purity dH2O, pH 9.5 to 1000 ml

Assay Diluent

1X *PBS*

10% *FCS, pH 7.0*

Phosphate-Citrate buffer

0.2 M *$Na_2HPO_4*H_2O$*

0.1 M *$C_6H_8O_7*H_2O$*

ELISA stop solution

1 M H_3PO_4

5.2 Methods

5.2.1 Cell biological methods

5.2.1.1 Cell culture techniques

The cells were cultivated under aseptic conditions in 75-cm2 tissue culture flasks. All tissue culture flasks have caps with filters which allow gaseous exchange, allowing maintenance of correct pH (which is monitored by the colour of the phenol red present in the medium) and the right percentage of CO_2 (5%). The optimal atmosphere conditions are allowed by CO_2 incubator, which automatically control temperature and pCO2; it operates with a try of water on the base in an attempt to maintain more than 98% relative humidity. Temperature of the incubator was set at 37℃ and regularly controlled. The five human color ectal cancer cells maintained as monolayer cultures in RPMI1640 medium, except the HCT116 p53-/- cells in DMEM meium, and supplemented with 10% FBS and 1% penicillin-streptomycin mixture. Cells of the U937 monocyte/macrophage cell line were also maintained in RPMI 1640. Growth medium was changed every 2-3 days. The cells were split into the new culture flasks when they reached 80-90% confluence. Old medium was removed and the cells were washed twice with sterile PBS buffer. Then 1 ml of trypsin-EDTA solution was added, the culture flask was incubated at 37℃ and observed under the microscope until cells detached from the surface of the flask. Then 10 ml of complete fresh medium was added to inactivate the activity of trypsin. Medium was discarded and the cells were re-suspended in fresh growth medium.

5.2.1.2 Adapting HCT116 p53 $^{-/-}$ to RPMI 1640 medium

To adapt the HCT116 p53-/- to grow in RPMI 1640 medium, cell were subcultured at a 1:2 split ratio into two identical culture vessels with one vessel containing the DMEM medium and the other containing a mixture of 50% DMEM and 50% RPMI 1640. The effects of the new medium formulation on the cells were observed by comparing the growth in the cultures with the medium mixture with the culture containing only the DMEM medium formulation. When the cells in the mixed culture became confluent, the process was repeated by again splitting the mixed culture at a

1:2 ratio into two identical vessels. The vessel then was containing 50% original medium and 50% new medium while the second culture had 25% original medium and 75% new medium. Once second culture became confluent the cells were subcultured into 100% new medium of RPMI1640.

5.2.1.3 Cell stimulation with different factors

Monocytes monocytic cell line U937 cells (DSMZ Braunschweig, Germany) were maintained in RPMI with 10% fetal bovine serum and 1% penicillin-streptomycin mixture in a humidified 5% CO2 atmosphere at 37℃.

For PMA/LPS induction experiment, U937 (4×10^6/ml) cells were first differentiated into macrophages in the presence of 16 nM phorbol 12-myristate 13-acetate (PMA) for 72 hours and then washed 3 times with PBS and recovered for 24 hours. Undifferentiated floating Cells and dead cells were washed away with three rinses of warm PBS. The attached macrophages were then stimulated with 1-10 ng/ml lipopolysaccharide (LPS) for 1-24 hours in the growth media. The culture supernatants were later centrifuged at 12000 rpm and collected as conditioned medium.

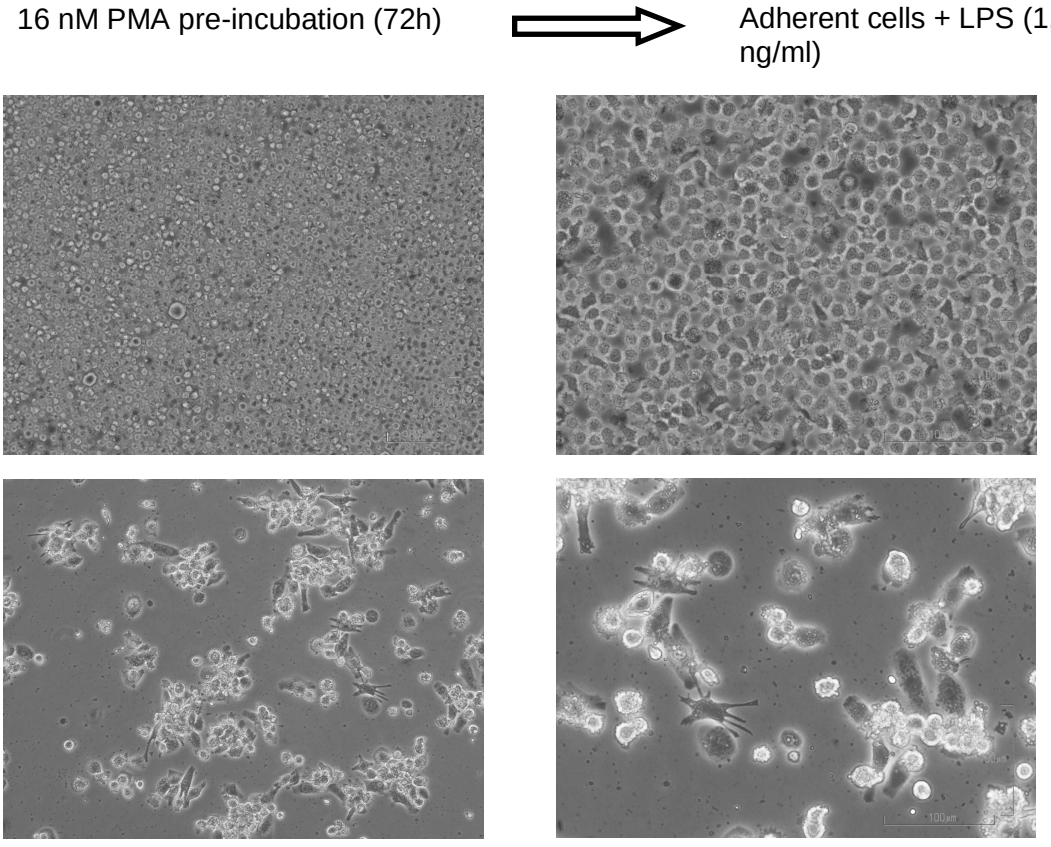

FIG 5. Morphology of U937; monocytes and differentiated macrophages after incubation with 16 nM PMA for 72h.

Human Monocyte isolation, differentiation and culture. PBMCs were isolated from freshly drawn human blood using Ficoll-Plaque technique and Density gradient Centrifugation. The monocytes were separated by negative selection with an AutoMACS magnetic cell isolation system according to the manufacturer´s instructions (Miltenyi). Monocyte purity was evaluated by immunofluorescent staining and flow cytometry using a monoclonal antibody for CD14 (BD Pharmingen). 4 x 10^5 Cells per ml were cultured in RPMI-1640 medium including FCS and Pen/Strep. Monocytes were activated with or without 10 ng/ml LPS for 4 h in 50mm culture dishes (Corning). Culture medium supernatants were collected for determination of TNFα concentrations (ELISA) and applied to HCT116 p53 +/+ cells for 6h or 24 h.

Colorectal cancer cell lines

Cells were maintained in RPMI with 10% FBS and 1% penicillin-streptomycin mixture in a humidified 5% CO2 atmosphere at 37℃. Cells (1 .2 x 10^6) were cultured for 6-72 hours in either normal, or macrophages-conditioned medium, or with cytokines, TNF-α and IFN-γ (Immunotools, Germany).

5.2.1.4 Storage of cells

In order to minimize the cellular injury induced by freezing and thawing procedures (intracellular ice crystals and osmotic effects), a cryoprotective agent DMSO was added. A variable number of cells (between 1-2 x 106) was spin down and resuspended in 10% DMSO solution (DMSO diluted in FBS). Afterwards, 1 ml aliquots of cell suspension were dispensed into criotubes (1.8 ml). The tubes were placed into wells of a brass block pre-cooled at 4°C. The block was then kept at –80℃ for 24 h after which the ampoules of cells wer e transferred to liquid nitrogen for long-term storage. For revival of cells a frozen ampoule was thawed rapidly in a 37℃ water bath, disinfected and the content was put in a cell culture flask with pre-warmed medium. After 6 hours the medium was discarded and fresh pre-warmed medium was added.

5.2.2 Biochemical methods

5.2.2.1 DNA extraction

It is a liquid-liquid extraction technique in biochemistry and molecular biology for purifying DNA contaminated by histones and other proteins. Equal volumes of a phenol:chloroform mixture and the aqueous DNA sample are mixed, forming a biphasic mixture. The proteins will partition into the organic phase while the DNA (as well as other contaminants such as salts, sugars, etc.) remain in the aqueous phase. This is usually repeated at least once and often more, depending on the requirements of the downstream processes, and then followed by precipitation with ethanol. OLD-T-buffer, 10% SDS, and Proteinase K were added to cell pellets. Cell pellets were then incubated overnight by 50 ℃ on t he thermoshaker. On the next day phenol was added two times to the tubes and the upper layer was collected by centrifugation (7500 rpm, 4 ℃). Choloroform/Isoamy alcohol (24:1) was added to the tubes and then they were centrifuged (7500 rpm, 4 °C). the supernatants were then collected and DNA wasd then precipitated with 3 M Sodium Acetate and 100% alcohol.

5.2.2.2 Methylation-specific PCR (MSP)

The initial step of both bisulfite genomic sequencing and MSP is to perform a bisulfite modification of the DNA sample. MSP then involves PCR amplification with specific primers designed to distinguish methylated from unmethylated DNA. The CpGenome™ Fast DNA Modification Kit contains the reagents for the initial bisulfite modification of the DNA required for both methodologies.

MSP requires an initial bisulfite reaction, using 200 to 500 ng genomic DNA (CpGenome DNA Modification Kit, Chemicon), in which all unmethylated cytosines are deaminated and converted to uracils, whereas 5-methylcytosines remain unaltered. Modified DNA was used as a template for MSP, using primers specific for either methylated or modified unmethylated sequences. CpGenome universal methylated DNA (QBiogene) was used as a positive control for methylated alleles. DNA from normal lymphocytes was used as a negative control for methylated alleles. Modified DNA was subjected to MSP using DAPK specific primers for methylated sequences (sense 5′-GGATAGTCGGATCGAGTTAACGTC-3′ and antisense 5′-CCCTCCCAAACGCCGA-3′) and for unmethylated sequences (sense 5′-GGAGGATAGTTGGATTGAGTTAATGTT-3′ and antisense 5′-

CAAATCCCTCCCAAACACCAA-3′), which generates polymerase chain reaction (PCR) products of 114 and 116 bp, respectively. The total 25 µl of PCR mix contained 2 µl of bisulfite-modified DNA, 1x PCR buffer, 3 mM $MgCl_2$, 12.5 pmol of each primer, 160 µM dNTPs, and 0.5 U of Hot-Goldstar Taq polymerase (Eurogentec, Seraing, Belgium). PCR conditions were as follows: 95℃ for 10 minutes, 35 cycles of 95℃ for 1 minute, annealing with 60℃ for 1 minute and 72℃ for 1 minute, followed by a final extension step at 72℃ for 10 minutes. Methylated standard DNA (Intergen) was used as a positive control for methylation, and placenta DNA was used as a negative control.

5.2.2.3 Measuring of RNA concentration

DNA was quantified by spectrophotometric analysis on the basis of its extinction using 1 OD_{260} = 40 µg/ml and diluted 5:65 with DEPC-H_2O. The absorbance was checked at 260 and 280 nm for determination of sample concentration and purity. The A_{260}/A_{280} ratio was between 1.7 and 2.1 for pure DNA. All DNA stock solutions were stored at -20℃.

5.2.2.4 Visualizing PCR products

The PCR products (7µl) along with a DNA marker were resolved on 8% polyacrylamide gels with silver nitrate staining. Briefly, the silver staining method involved; treatment with 3% HNO_3 for 2 to 3 min followed by a 5-min rinse in water; impregnation of the gel with 0.2% $AgNO_3$ for 20 min and water rinse for 2-3 min; developing of the gel with developer (3% Na_2CO_3 and 0.75 ml of 37% formaldehyde) for 2.5 min, followed by a brief rinse in water and 2 min in 10% citric acid stop solution; post fixation with 5% glycerol for 20 min. The gels were dried at room temprature.

5.2.2.5 RNA extraction

Total RNA extraction was preformed using Trizol reagent (invitrogen). Cell pellets were homogenized and re-suspended in 1ml of Trizol and incubated for 5 minutes at room temperature. Chloroform (0.5ml) was added to the suspension, which was incubated for 5 minutes at room temperature and centrifuged at 15,000 rpm to achieve phase separation (organic phase from aqueous phase). The aqueous phase,

containing the RNA, was transferred to a new tube, and RNA was recovered by precipitation with isopropyl alcohol. The precipitated RNA was dissolved in 50-200 µl DEPC-H_2O.

5.2.2.6 Measuring of RNA concentration

RNA was quantified by spectrophotometric analysis on the basis of its extinction using 1 OD_{260} = 40 µg/ml and diluted 1:70 with DEPC-H_2O. The absorbance was checked at 260 and 280 nm for determination of sample concentration and purity. The A_{260}/A_{280} ratio was between 1.7 and 2.1 for pure RNA. All RNA stock solutions were stored at -80℃.

5.2.2.7 *Real-time* RT-PCR

The reverse transcription polymerase chain reaction (RT-PCR) is used detect expression of a specific gene. RT-PCR involves the use of gene-specific primers and reverse transcriptase to synthesize a cDNA sequence to the mRNA. The cDNA is then amplified by multiple rounds of polymerase-mediated transcription of this template cDNA. There are several types of RT-PCR and the most precise one in terms of quantification is the real-time RT-PCR method, which requires an automated system able to detect fluorescence induced during the RT-PCR reaction. During RT-PCR, the expression of a certain gene can be deduced by comparing it to constitutively expressed genes, also known as "housekeeping" genes.

cDNA synthesis was done in a 20 µl reaction mix starting with 1 µg of total RNA using the reverse transcription system of Promega (Madison, WI; 42 ℃ for 30 min; 99 ℃ for 5 min, and 4 ℃ for 5 min). Real-time RT- PCR was performed using a LightCycler (Roche Diagnostics, Mannheim, Germany), and threshold cycle numbers were determined using the LightCycler software, version 3.5. DAPK primer sequences were sense 5'-CCTTGCAAGACTTCGAAAGGATA-3' and antisense 5'-GATTCCCGAGTGGCCAAA3', the two hybridization probes were CTTAATTCTTGGCTGCAGGTTCTGTG-FL and LC Red640-GTCGGAGCTGCTGGATGAAGAGTC-ph. P53 primer sequences were sense 5'-ATGAGCCGCCTGAGGTTG-3' and antisense 5'-AGCTGTTCCGTCCCAGTAGATTA-3', the two hybridization probes were GGCATGAACCGGAGGCCCA-FL and LC Red640-CCTCACCATCATCACACTGGAAGACTCC–ph. The *real-time* RT-PCR was

performed in a final volume of 20 µl. The final reaction mixture contained the forward and reverse primer at 10 pmol each, the LC Red640 probe at 40 pmol, the FL probe at 20 pmol, 4 mM $MgCl_2$, and 1 x Master Amp hybridization mix. PCR was performed under the following conditions: 95 ℃ for 30 s, followed by 45 cycles of 95 ℃ for 0 s, 57 ℃ (DAPK) or 62 ℃ (p53) for 10 s, and 72 ℃ for 5 s. We used serial dilutions of the positive control cDNA of HCT116 cells to create a standard curve. PCR was performed in triplicate, and the threshold cycle numbers were averaged. Fold induction was calculated according to the formula $2^{(Rt-Et)}/2^{(Rn-En)}$, where Rt is the threshold cycle number for the *ß*2-M gene in the treated cells, Et is the threshold cycle number for the experimental gene in treated cells, Rn is the threshold cycle number for the *ß*2-M gene in non-treated cells, and En is the threshold cycle number for the experimental gene in non-treated cells.

5.2.2.8 Preparation of total protein from cells

Whole-cell lysates were prepared from cell pellets and were lysed by the addition of protein lysis buffer containing 4 M Urea, 0.5% SDS, 62.2 mM Tris (pH 6.8), 1 mM PMSF, and 1:100 of Protease Inhibitor Cocktail Set III (Calbiochem). The cells were lysed by vortexing every 10 minutes in total time of 1 hour. The mixture was centrifuged at 14000 rpm at 4º C for 20 minutes to remove the cell debris. Cell lysates were stored at -80º C. Total protein concentration of the samples was determined as described below (5.2.2.9).

5.2.2.9 Preparation of cellular extracts using RIPA buffer

For Immunoprecipitation experiments, cells were lysed with RIPA buffer. During RIPA lysis intracellular and membrane proteins are solubilized due to the presence of detergent and high salt concentration in the lysis buffer. Nonsolubilized proteins are precipitated by centrifugation. Protease inhibitor cocktail is included in the lysis buffer to prevent proteolysis, phosphotase inhibitor cocktail - to maintain the phopsphorylation status of phosphoproteins, EDTA - to chelate divalent ions that are essential for metalloproteases. Cells (10^7) were washed twice with ice cold PBS, lysed with 1.5 ml RIPA buffer supplemented with the cocktail of protease/phosphotase inhibitors and incubated on ice for 15 minutes with occasional rocking. Lysates were then collected by centrifugation at 12000 rpm for 10 minutes at 4℃. Cell lysates were than briefly sonicated. Cells were incubated on ice for 10 min

and centrifuged at 12000 rpm at 4℃ for 10 min. The supernatant containing total cellular proteins was collected and stored at –20℃. Total protein concentration in the supernatant was determined as described below (5.2.2.10).

5.2.2.10 Determination of protein concentrations

Protein concentration was determined using Bio-Rad Dc Protein Assay (BioRad Laboratories, Hercules, CA). The Bio-Rad *DC* (detergent compatible) protein assay is a colorimetric assay for protein concentration following detergent solubilization. The reaction is similar to the well-documented Lowry assay (Lowry et al. 1951). The standard assay is used with samples having protein concentrations between 0.1 and 2.0 mg/ml. After plating five µl of standards and protein laysates in duplicates into a 96-well plate, 25 µl of (Reagent A and S) and 200 µl of Reagent B were plated to each well and incubated 15 minutes at room temperature. The Bio-Rad *DC* protein assay was measured at 650–750 nm with a microplate reader. A standard curve was prepared by plotting the average Blank-corrected 562 nm measurement for each BSA standard *vs.* its concentration in mg/ml. The standard curve was used to determine the protein concentration of each unknown sample.

5.2.2.11 Immunoprecipitation of proteins from cellular lysates

In this approach, specific antibody is added to the cellular lysate to bind protein of interest. Antibody-protein complexes are then precipitated using solid-phase matrix. Bacterial proteins A and G which have specific binding sites for Fc-parts of antibodies, covalently coupled to crosslinked agarose, are usually used as solid-phase matrix to precipitate protein-antibody complexes. Samples were pre-cleared at 4℃ for 1 h using protein G or A-Sepharose beads. Cellular lysates containing 0.5-1 mg of total protein were mixed with about 1 µg of antibody in pre-chilled 1.5 ml tubes on ice. Volumes of the mixture were adjusted to 400-500 µl to obtain equal protein concentrations in each sample. Tubes were incubated overnight at 4℃ with constant rotation. 70-75 µl of Protein A or G coupled agarose was added to each sample and tubes were incubated for additional 4 hours at 4℃ with constant rotation. Following incubation with Protein A or G sepharose, immuno-complexes were pelleted by centrifugation at 12000 rpm at 4℃ for 1 minute and washed 3 times with ice-cold RIPA lysis buffer and one time with ice-cold wash buffer. Each time complexes were collected by centrifugation at 12000 rpm at 4℃ for 1 minute. Five-10 µl of the wash

buffer used for the last wash were left above the agarose pellet. Thirty µl of 2X Laemmli loading buffer were added to the samples and proteins were denatured by heating to 95℃ for 5 minutes. Samples were cooled down on ice and analyzed immediately or frozen at –20℃ for later analyses. Protein A or G sepharose was pelleted by centrifugation at 12000 rpm at 4℃ for 2 minutes and supernatants, containing immunoprecipitated proteins were analyzed by SDS-PAGE electrophoresis (5.2.2.13).

5.2.2.12 In vitro kinase assay.

The In Vitro Kinase Assay provides a simple and straightforward method to assay kinase activity without performing time-consuming transfections. This assay helps to determine whether the kinase of interest is able to phosphorylates its specific substrate. Immunoprecipitation carried out as described above as shown in Figure 6. Sepharose-bound immune complexes in lysis buffer were washed and resuspended in kinase buffer (60 mM HEPES, pH 7.5, 3 mM $MnCl_2$, 3 mM $MgCl_2$, 3 µM sodium orthovanadate, 1.2 mM DTT, 2.5 µg/µl PEG) before incubation with 7.5 µCi [γ^{32}-P] ATP (GE Healthcare, Amersham Biosciences) and 2 µg RB-S6P (Biomol) at 25℃ for 80 min. Samples were boiled at 95℃ for 5 min and separated on a 10% gel by SDS-PAGE prior to autoradiography.

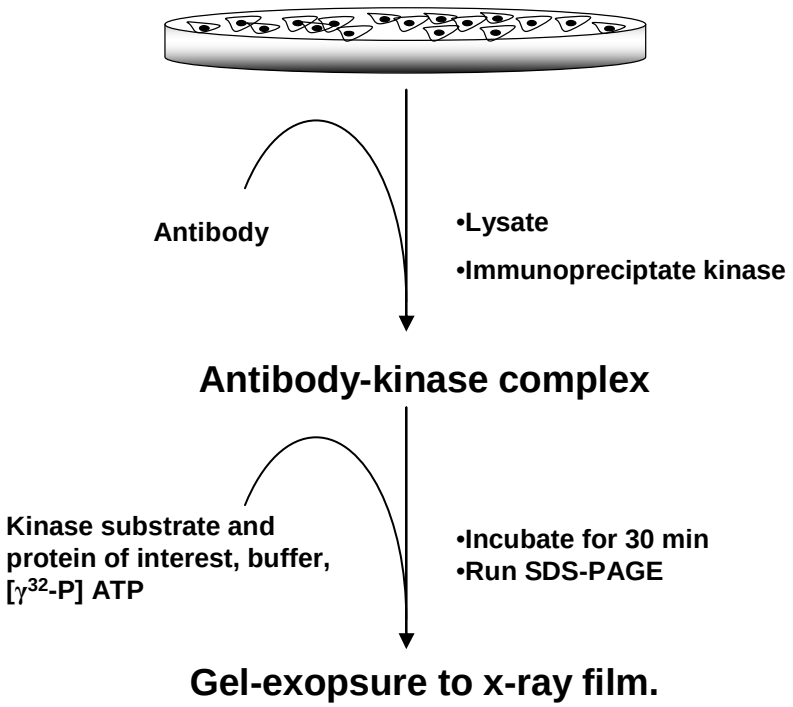

FIG. 6. Principle of the in vitro kinase assay.

5.2.2.13 SDS-PolyAcrylamide Gel Electrophoresis

In this approach proteins in the mixture are denatured by heating in the presence of DTT and SDS. Denatured polypeptides bind SDS and become negatively charged. The amount of bound SDS is almost always proportional to the molecular weight of a polypeptide, and is independent of its sequence. Therefore proteins and protein subunits are separated according to their size during migration through the pores in the gel matrix in response to an electrical field. The protein samples were mixed with 5x loading puffer and with 2x loading puffer to achieve equal loading amounts. Proteins were boiled for 5 minutes for complete denaturation. This mixture was loaded along with the Biotinylated protein Ladder, which was heated at 99° C for two minutes. Separation gels with the following dimensions were used: thickness 1.0 mm, length 7.3 cm and width 8.3 cm. TEMED was used for the catalysis of the polymerization reaction, which was initiated by adding APS. The stacking gel was composed similar to the running gel, only Tris-HCl with pH 6.8 was used and the acrylamid had a final concentration of 3%. Proteins were separated at 30-50 mA until the dye front has reached the end of the separation gel.

5.2.2.14 Transfer of proteins to Nitrocellulose membrane

electrophoresed Immunoblotting was performed utilising the semi dry transfer method. Nitrocellulose membrane (Schleisser and Schuell, Germany) and 2 layers of 2 papers were cut exactly to the size of the gel and soaked in transfer buffer, shown in figure 7. A stack was made with 2 papers on the top and bottom of the gel and membrane and placed in between the graphite plates of the transfer apparatus (Biometra, Germany). Transfer was performed at 17 V for 1 hour. In semi-dry blotting the electrodes are placed directly in contact with the gel/nitrocellulose membrane sandwich to provide a fast, efficient transfer. Because of this direct contact there is a minimum of transfer buffer required for this process. The membrane was soaked in transfer for a few minutes and then transferred to a container with Towbin transfer buffer. Gel and attached membrane were sandwiched between two pieces of Whatman paper and soaked in the transfer buffer.

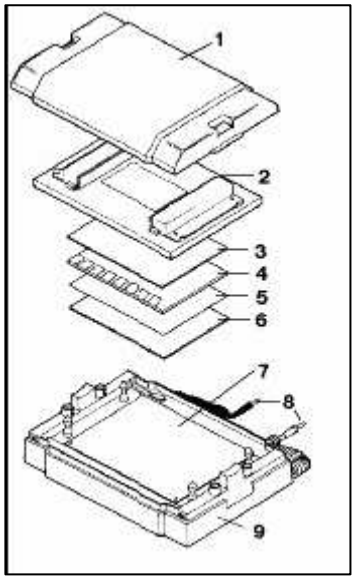

FIG. 7. An exploded view of the Trans-Blot SD cell: 1, safety lid; 2, cathode assembly with latches; 3, filter paper; 4, gel; 5, membrane; 6, filter paper; 7, spring-loaded anode platform, mounted on four guide posts; 8, power cables; 9, base. The prestained protein ladder served as a control for the transfer.

5.2.2.15 Ponceau S staining of proteins on PVDF membrane

Staining with Ponceau S was used to provide visiual evidence that electrophoretic transfer of proteins has taken place. Ponceau S is a negative stain which binds to the positively charged amino groups of the protein. The proteins bans were visiulized by incubating the membrane for 5-10 seconds in a 0.1% solution (containing 1% acetic acid) of Ponceau S staining solution. The excess stain was washed with TBST.

5.2.2.16 Analysis of proteins by immunoblotting

In this method, specific antibodies are used to identify proteins transferred to blotted membrane. First, membrane is immersed in blocking buffer to fill all protein binding sites with non-reactive protein. Then membrane is incubated in a solution containing antibody directed against the antigen(s) in the protein to be detected. Primary antibody bound to the protein of interest is recognized by secondary antobody conjugated with horseradish peroxidase (HRP). The complex containing the antigen, primary antibody and secondary antibody-HRP conjugate is detected by chem luminescent visualization using ECL detection system. The membranes were blocked in the blocking solution either for at lease one hour at room temperature. After blocking membranes were incubated with antibodies appropriately diluted in either

5% BSA or 5% milk blocking buffer in TBS-T overnight at 4℃ with agitation. After incubation with primary antibodies, membranes were washed three times each 10 minutes, then transferred to the containers with secondary antibody-HRP conjugates in 5% milk blocking buffer in TBS-T and incubated for 1 hour at room temperature shaking gently. Membranes were then rinsed twice and washed with agitation three times for 30 minutes. Bound antibodies were detected by incubating the blots in West Pico chemiluminescent substrate (Pierce, Rockford, IL). The level of immunoreactivity was then measured as peak intensity using an image capture and analysis system (GeneGnome, Syngene, UK). Hybridization with anti-β-actin was used to control equal loading and protein quality.

5.2.2.17 Stripping and re-probing of western blot

The blotted membranes were stripped and re-probed using Restore™ Western Blot Stripping Buffer. Twenty ml of Restore™ Western Blot Stripping Buffer were warmed to room temperature. Membranes were placed in the buffer to be stripped and incubated for 10 minutes at 42° C. After incubation , the blots were removed from the buffer and washed 2 times for 15 minutes in TBS-T. After determining that the membranes were properly stripped, next immunoprobing experiments were performed.

5.2.2.18 siRNA transfection

siRNA is sometimes known as short interfering RNA or silencing RNA, are a class of 20-25 nucleotide-long double-stranded RNA molecules that play a variety of roles in biology. Most notably, siRNA is involved in the RNA interference (RNAi) pathway where the siRNA interferes with the expression of a specific gene. In addition to their role in the RNAi pathway, siRNAs also act in RNAi-related pathways. Small/short interfering RNA (siRNA) transfection is an exciting new method for introducing foreign genetic information by inducing RNA interference. siRNA works by silencing key sequences on messenger RNA, which turns off specific genes by cleaving to them on the RNA strand. siRNA is dsRNA chemically cut into specific segments so that the entire strand or a portion of the dsRNA can cleave to the mRNA without causing a viral response, shown in figure 8. siRNA transfection is the introduction of the siRNA into the cell through chemical and biologic reagents. We followed the siRNA

transfection protocol of the manufacturer with only minor modifications (SantaCruz, USA). The optimal amount of siRNA was determined as 8 and/or 30 µl siRNA diluted in 6 µl transfection reagent were added together with transfection medium and incubated for 45 minutes in dark at room temperature. The mixture was add then to the cells for 6 hours. The cells were then assayed for different experiments. siRNA efficiency reached in the HCT116 cells a complete DAPK protein down-regulation and reduction of p38 protein level by 50%. In the U937 DAPK and RSK specific siRNA resulted in 50% protein reduction.

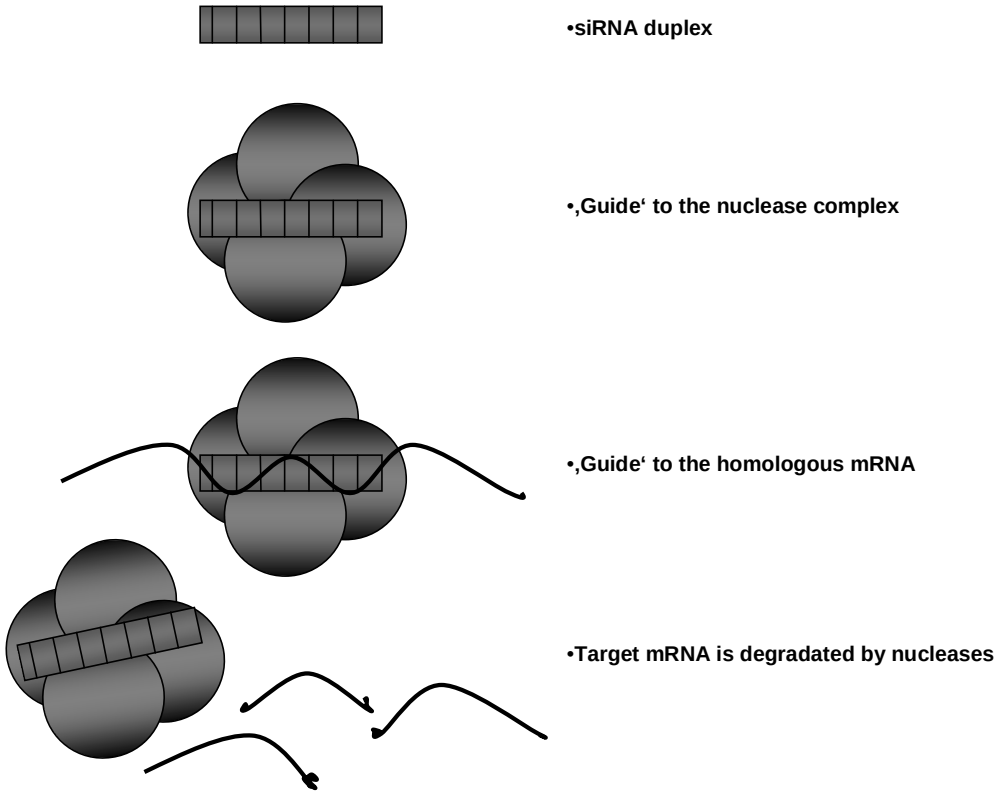

FIG. 8. Principle of siRNA transfection.

5.2.3 Quantification of apoptosis

5.2.3.1 Annexin V-binding and PI staining

In the early stages of apoptosis, changes occur at the cell surface. One of these plasma membrane alterations is the translocation of phosphatidylserine (PS) from the inner side of the plasma membrane to the outer layer, exposing PS at the surface of

the cell. Macrophages specifically recognize PS exposed on the cell surface of lymphocytes during the development of apoptosis. The recognition and phagocytosis of apoptotic cells and bodies protects organisms from exposure to cellular compounds that lead to inflammation, which usually accompanies necrosis. Annexin V is a Ca^{2+}-dependent phospholipid-binding protein with a high affinity for PS, making labeled annexin an excellent detection agent.

To detect apoptosis the Annexin-V-FLOUS kit (Roche Diagnostics) was used. Cells stimulated for 24-72 hours with the above mentioned conditions. Growth media of the cells were collected and the cell were washed two times with PBS. Cells were then trypsinized and collected by centrifugation at 200xg for 15 minutes. $1x10^6$ cells were stained with 100 µl annexin V staining solution, consisting of 20 µl fluorescein isothiocyanate (FITC)-conjugated annexin V reagent (20 µg/ml), 20 µl sotonic propidium iodide (50 µg/ml) and 1000 µl of 1 M HEPES buffer, for 15 min at room temperature. Cells were analyzed on a FACScan flow cytometer (Becton-Dickinson, CA, USA) using a 488-nm excitation and 515-nm band pass filter for fluorescein detection and a filter >600 nm for propidium iodide detection after electronic compensation. Since positive annexin V staining is seen for apoptotic and necrotic cells, propidium iodide-positive cells were used to measure late apoptotic and necrotic, whereas annexin V-positive and propidium iodide-negative cells were counted as early apoptotic cells.

5.2.3.2 Caspase 3/7 activity assay

The Caspase-Glo® 3/7 Assay is a luminescent assay that measures caspase-3 and -7 activities in purified enzyme preparations or cultures of adherent or suspension cells. The assay provides a proluminescent caspase-3/7 substrate, which contains the tetrapeptide sequence DEVD. This substrate is cleaved to release aminoluciferin, a substrate of luciferase used in the production of light. The Caspase-Glo® 3/7 Reagent has been optimized for caspase activity, luciferase activity and cell lysis. The addition of the single Caspase-Glo® 3/7 Reagent in an "add-mix-measure" format results in cell lysis, followed by caspase cleavage of the substrate and generation of a “glow-type” luminescent signal. The Caspase-Glo® 3/7 Assay is used for screening of caspase activity or apoptosis. Cells were seeded at in 96-well white-walled plates and incubated overnight. After treatment, Caspase-Glo 3/7 reagent was added for 1.5 h. Caspase activity was analyzed using a luminometer and quantified

as relative light units according to manufacturer's instructions. Caspase activation is shown as the ratio between the caspase activity of the treated sample and the activity of the corresponding untreated cells (relative caspase activity index).

5.2.4 Enzyme-linked immunoassays

5.2.4.1 Determination of human TNFα and IFNγ concentrations in cell culture supernates

This assay employs the quantitative sandwich enzyme immunoassay technique. A monoclonal antibodies specific for TNFα and IFNγ have been pre-coated onto a 96-well microplate separately. Standards and samples are pipetted into the wells and any TNFα and IFNγ present are bound by the immobilized antibody. After washing away any unbound substances, an enzyme-linked polyclonal antibody specific for TNFα and IFNγ is added to the wells. Following a wash to remove any unbound antibody-enzyme reagent, a substrate solution is added to the wells and color develops in proportion to the amount of TNFα and IFNγ bound in the initial step. The color development is stopped and the intensity of the color is measured. The level of TNFα and IFNγ were measured in cell culture supernates collected at 1, 2, 3, 4, 8, 24 h after stimulating with (1, 5, 10 ng/ml) LPS. The assay was performed according to the manufacturer's recommendations. Absorbance at 450 nm was measured and corrected using the 540-nm reading on the microplate reader. TNFα and IFNγ contents were calculated according to the parameter of the calibration curve. Calibration curves with a correlation coefficient at least 0.998 were used. All experiments were replicated three times.

5.2.4.2 p38 MAPK activity Assay

The Omnia^{TM} Plate-Based IP Kinase Assay Kit for p38 MAPK is designed to measure the kinase activity of p38 MAPK in cell lysates. This kit uses a p38 MAPK specific antibody to capture the target and separate it from the complex mixture of proteins in a crude cell lysate. The phosphotransferase (kinase) activity of the captured p38 MAPK is measured by using a cascade reaction, which uses an inactive MAPKAPK2 enzyme and a MAPKAPK2 substrate peptide (OmniaTM Ser/Thr Peptide 3). In the presence of ATP, the active p38 MAPK will phosphorylate and activate MAPKAPK2.

The activity of MAPKAPK2 is measured using a novel peptide substrate which contains the chelation-enhanced fluorophore, 8-hydroxy-5-(N,N-dimethylsulfoanamido)-2-methylquinoline (referred to as SOX7) in a real-time kinetic measurement mode. Sox is an unnatural amino acid that can be prepared as an Fmoc protected derivative and has been incorporated into the MAPKAPK2 substrate peptide (OmniaTM Ser/Thr Peptide 3) using standard solid-phase peptide chemistry. Upon phosphorylation of the peptide by MAPKAPK2, Mg++ is chelated to form a bridge between the Sox moiety and the phosphate group that is added by MAPKAPK2 to the serine residue within the peptide, resulting in an instantaneous increase in fluorescence when the kinase reaction mixture is excited at 360 nm and the emission is measured at 485 nm8. The fluorescence intensity generated at a given time is directly proportional to the concentration of active p38 MAPK present in the sample. 100 µg of cell lysates (control or stimulated/treated) where plated in a 96-well plate together with active p38 as a positive control. The unbound laysate was rinsed 4 times with wash buffer. The inactive substrate together with the reaction mixture were added to the bound p38. finally the plate was transferred to a fluorescent microplate reader. The measured values where adjusted to the controls.

5.2.5 Immunohistochemical analyses

5.2.5.1 Immunohistochemistry of paraffin embedded tissues

5.2.5.1.1 Haematoxylin and Eosin staining

Staining of the nucleus of the cells was done with haematoxylin; eosin was used for the cytoplasm staining. Samples were deparaffinized by incubation in xylene for 20 min, 2 minutes in 100%, one minute in 96 %, one minute in 75% ethanol and finally washed in distilled water. The samples were then rinsed in haematoxylin for one minute, washed in distilled water and incubated with eosin for 2 minutes. After washing the slides were mounted with Mayer gel.

5.2.5.1.2 Staining of DAPK and phosphp-p38

Immunohistochemical studies were performed using the avidin-biotin complex immunostaining method and the automated immunohistochemistry slide staining system by Ventana NexES (Ventana Medical System, Strasbourg, France). Immunohistochemical studies were performed on 3 µm thick, formalin-fixed, paraffin-

embedded serial tissue sections. Samples obtained from cases of methylated and unmethylated colorectal carcinoma (6 cases each) and 12 additional normal colon samples without pathological findings were analyzed for DAPK and phosphor-p38 protein expressions. Formalin-fixed paraffin-embedded serial tissue sections (3 µm thick) were dewaxed in xylol and rehydrated by descending concentrations of ethanol. For antigen retrieval, pre-treatment was performed by microwave heating in 1 mM sodium citrate puffer (30 minutes, 600 W, pH 6.0). Incubation of each one series with anti-DAPK (mouse monoclonal antibody, dilution 1:500, BD Transduction Laboratories, Heidelberg, Germany) and anti-Phospho-p38 MAPK (rabbit monoclonal antibody, dilution 1:100, Cell Signaling Technology, Boston, MA, USA) was conducted at room temperature for 12h and followed by PBS-washing. Positive immunohistochemical reactions were revealed using the iVIEW™ DAB Detection Kit (Ventana, Germany) as chromogen substrate. Specimens were counterstained with hematoxylin and mounted with DEPEX™. Samples were examined by two different reviewers blinded to other data.

5.2.5.2 Triple Immunofluorescence staining of cells

Immunofluorescence staining methods are used successfully for labeling multiple antigens in the same preparation. These methods are especially useful for co-localization of antigens in the same compartment of a cell.

The co-localization of DAPK and phospho-p38 or RSK was carried out on cells. DAPK was stained with anti-DAPK (BD Transduction, Laboratories, Lexington NY), phospho-p38 (Cell Signalling. Technology Inc.), or RSK (Cell Signalling. Technology Inc) and nucleus with 4'-6-Diamidino-2-phenylindole (DAPI) Control and stimulated/treated, 2 x 10^5 cells, grown in 10% FCS in RPMI medium on 2 well chamber slides (Nunc, Germany) and were fixed in 3% paraformaldehyde for 15 min than permeabilized with 0.2% Triton X-100 for 5 min. Cells were blocked with 1% BSA for 10 min, and incubated with mouse anti DAPK antibody at 1:50 dilution overnight at 4℃, followed by incubation with Cy3 anti-mouse secondary antibody (Sigma) at 1:400 dilution for 1 hour at room temperature. The subsequent reaction was carried out first by blocking step with 1% BSA than by incubating the cells with rabbit anti p-p38 or RSK at 1:1000 dilution for 2 hours at 37° C, followed by a 1:100 dilution of Flourescein anti-rabbit secondary antibody (Vector Labs) for 1 hour at room temperature. The slides were counterstained and mounted with DAPI +

mounting medium (Vector Labs) and were examined under a fluorescence microscope equipped with the appropriate filters.

5.2.6 Statistical analysis

Data are presented as the means of triplicates from three separate experiments +/- SEM. Statistical comparisons of experimental data were performed by Student's t test. The level of statistical significance was set at $P<0.05$.

6. Results

6.1 DAPK status in different colorectal cell lines

6.2 Macrophage ⟶ Tumor cell

6.2.1 Macrophage-mediated killing of HCT116 p53+/+ tumor cells

6.2.2 Macrophage-triggered up-regulation of DAPK expression

6.2.3 Increase in TNFα and IFNγ release upon macrophage a ctivation

6.2.4 TNFα but not IFNγ exposure induced apoptosis in HCT116 p53+/+ cells

6.2.5 TNFα mediated DAPK-dependent apoptosis in HCT116 p53+/+ cells.

6.2.6 Early activation of p38 in HCT116 p53+/+ tumor cells subjected to TNFα.

6.2.7 Identification of p-p38 as DAPK binding-protein

6.2.8 Triggering of DAPK-mediated apoptosis by p-p38

6.2.9 P53 acts down-stream of DAPK

6.2.10 TNFα alone induced cell death in HCT116p53-/-

6.2.11 P38 is also activated in the p53 deficient HCT116 cells upon TNFα exposure

6.2.12 Physiological relevance of DAPK regulation

6.2.12.1 DAPK co-localizes with p-p38 in human colorectal carcinoma

6.2.12.2 Apoptosis induction in the HCT116 p63+/+ cell and DAPK up-regulation after exposure to the supernatants of freshly isolated activated human macrophages

6.3 Tumor cell ⟶ Macrophage

6.3.1 Tumor cells-supernatants increased DAPK level but did not induce apoptosis in activated U937

6.3.2 DAPK participated in survival of the activated macrophages

6.3.3 RSK may be involved the DAPK-mediated cell survival of U937

6.1 DAPK status in different colorectal cell lines

Based on the findings that DAPK is one of p53 target genes (Martoriati et al., 2005), we aimed to verify the expression of DAPK and p53 in five different colorectal cancer cell lines (HCT116 p53+/+, HCT116 p53-/-, HT29, CaCo, and SW480), using *real-time* RT-PCR. As shown in Fig. 9A, no high correlation was found between DAPK and p53 transcripts in the normal status of the cell lines. This finding was further confirmed by analyzing protein levels of DAPK and p53, using Western Blotting (Fig. 9B). To investigate the relationship between DAPK expression pattern and its methylation status, methylation-specific PCR (MSP) was performed to examine the status of methylation in the promoter of DAPK in the selected colorectal cell lines and in the macrophage-like cell line U937. Partial hypermethylation of DAPK promoter was observed in the two colorectal cancer cell lines (HCT116 p53-/- and SW489), but not in HCT116 p53+/+, HT29, and CaCo cell lines (Fig. 9C). DAPK was unmethylated in monocytic, differentiated and activated U937 (Fig. 9D). To investigate DAPK expression and its possible regulation by p53 and because p53 is mutated in HT29, CaCo and SW480, we selected HCT116 p53+/+ and its counterpart HCT116 p53-/- cell lines.

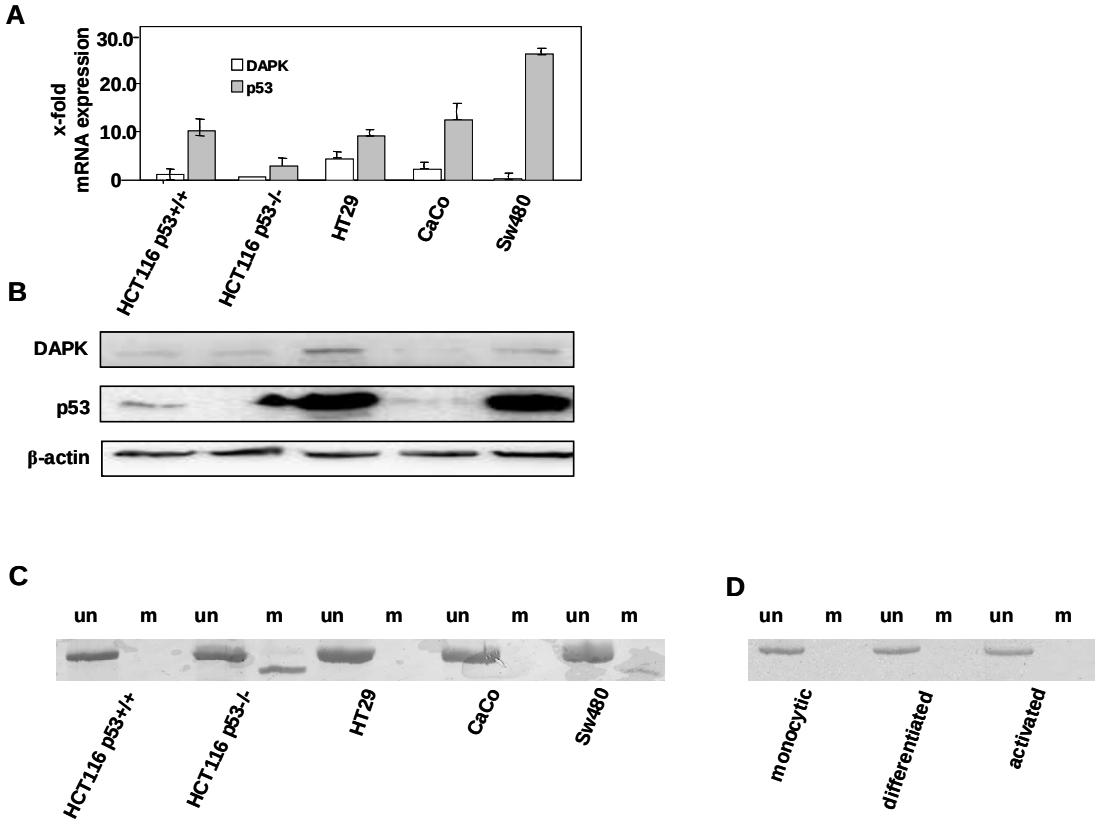

FIG. 9. DAPK status. (A) *real-time* RT-PCR analysis was performed using gene-specific primers for DAPK and p53. (B) Lysates prepared from five colorectal

cell lines were analyzed by anti-DAPK, anti-p53, or anti-ß-actin Western blotting for equal loading. (C) methylation status of DAPK promoter in five colorectal cell lines and different status of the macrophage-like cell line U937 (D).

6.2 Macrophage ⟶ Tumor cell

6.2.1 Macrophage-mediated killing of HCT116 p53+/+ tumor cells

Schneider-Stock et al., 2006 showed that, DAPK protein expression in colorectal tumor cells and their tumor-associated macrophages was found to be highly correlated. Furthermore, the increase in the DAPK level was associated with higher apoptosis in colorectal tumor cells.

To determine whether tumor-associated macrophages and their secretion of cytotoxic mediators might induce apoptosis in tumor cells, we used a cell culture assay to recapitulate events that might occur in the *in vivo* tumor setting. For this purpose, the conditioned media from the treated macrophage cell line U937 [differentiated with PMA (diffM) and differentiated + activated with LPS (actM)] were collected, filtered, and applied to HCT116 p53+/+ colorectal tumor cells. The apoptosis in tumor cells was assessed after 24-72 h of incubation with the macrophage-conditioned media, by Annexin-V-FITC binding, and after 48h by caspase-3/7 activity assays. There was a significant apoptosis induction (2.5-fold) in tumor cells treated with actM supernatants, starting early at 24 h (6.37% to 15.87%) and continuing until 72 h compared to untreated HCT116 p53+/+ cells (Fig. 10A). In contrast, diffM supernatants induced only an early increase in the percentage of apoptotic HCT116 p53+/+ cells at 24 h (6.37% to 17.87%), but cell death disappeared at later time points (Fig. 10A). Considering the 48 h time point, these findings were in accordance with caspase activity data, showing 3-fold up-regulation in caspase 3/7 activity in HCT116 p53+/+ cells treated with actM supernatants (Fig. 10B). Thus, our data suggest that actM may release a soluble factor into the media, which might be responsible for apoptosis induction in HCT116 p53+/+ tumor cells.

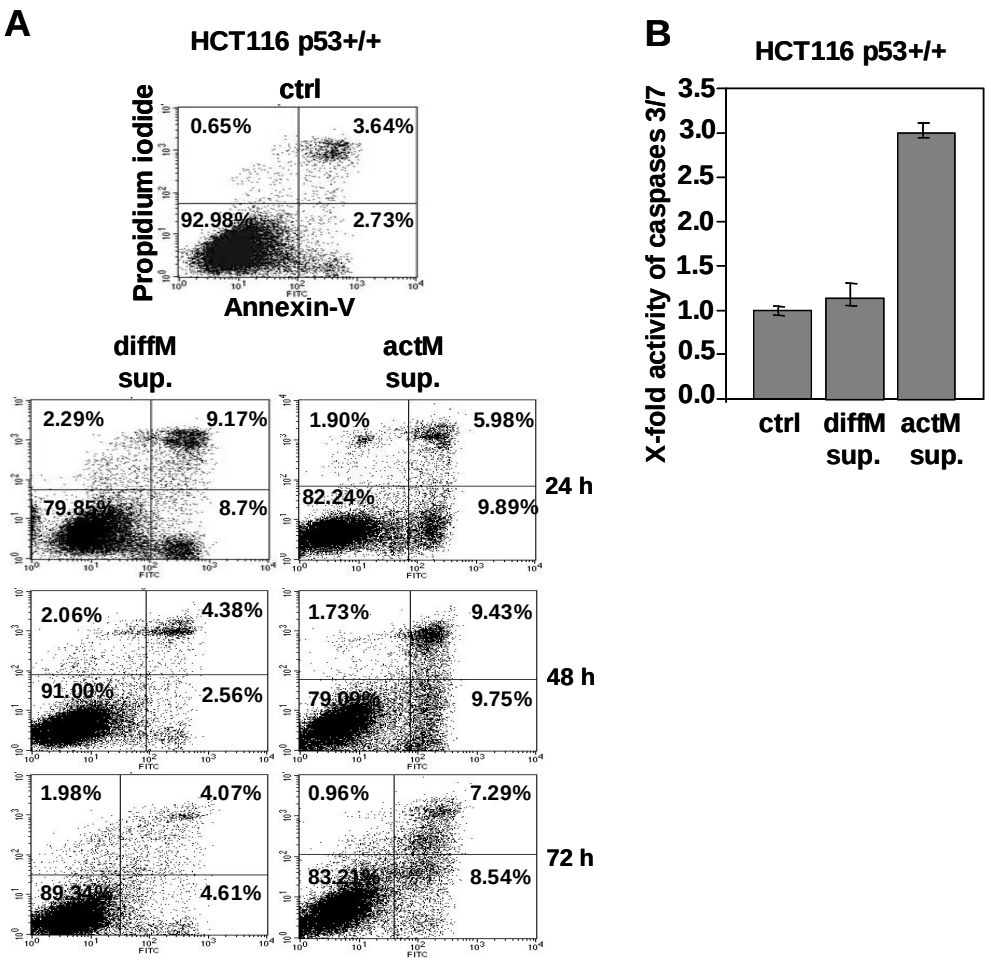

FIG. 10. Macrophages-induced cell death in HCT116 p53+/+ cells. (A) Annexin-V measurements of HCT116 p53+/+ cells (ctrl) and HCT116 p53+/+ cells subjected to diffM sup. or actM sup. for 24 h, 48 h, and 72 h. (B) HCT116 p53+/+ subjected to diffM sup. or actM sup. for 48 h were analyzed by caspase 3/7 activity assay. Ctrl, control; diffM sup., supernatant of PMA-differentiated macrophages U937; actM sup., supernatant of PMA-differentiated and PMA-activated macrophages U937.

6.2.2 Macrophage-triggered up-regulation of DAPK expression.

To investigate whether DAPK is involved in the observed apoptosis induction, we examined DAPK mRNA and protein expression. *Real-time* RT-PCR revealed that the steady state level of DAPK mRNA was unchanged during the experiment (Fig. 11A). However, there was an increase in the DAPK protein level even after 6 h of incubation with supernatants from diffM and actM (Fig. 11B). While the DAPK protein level was found to be increased only slightly at later time points after incubation with diffM supernatants, the DAPK protein level continued to increase markedly after incubation with actM supernatants, similarly to the time course of apoptosis induction (Fig. 10A). These data suggest that macrophage-mediated secretion of cytotoxic

factors by actM might induce DAPK protein accumulation without affecting its gene transcription.

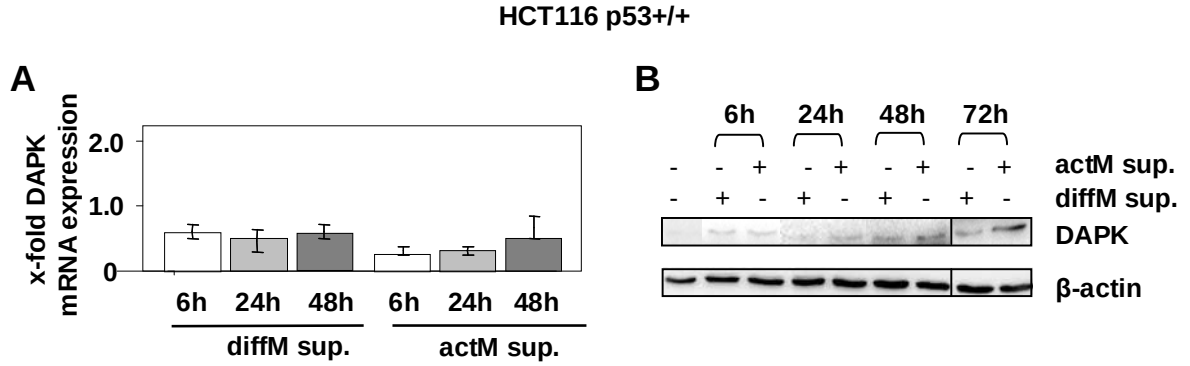

FIG. 11. Macrophages up-regulate DAPK protein levels. (A) For HCT116 p53+/+ cells, subjected to diffM sup. or actM sup., *real-time* RT-PCR analysis was performed using gene-specific primers for DAPK. (D) Lysates prepared from diffM sup.- and actM sup.-exposed HCT116 p53+/+ cells were analyzed by anti-DAPK, or anti-ß-actin Western blotting for equal loading. Control HCT116 p53+/+ cells served as control. Ctrl, control; diffM sup., supernatant of PMA-differentiated macrophages U937; actM sup., supernatant of PMA-differentiated and PMA-activated macrophages U937.

6.2.3 Increase in TNFα and IFNγ release upon macrophage activation

As earlier studies have shown that TNFα and IFNγ can promote DAPK-dependent apoptosis (Cohen et al., 1999; Deiss et al., 2001), they are potential candidates to be the cytotoxic factors secreted by actM in our experimental setting. Thus, we measured their release using an ELISA assay and determined the optimal time point and concentration of TNFα or IFNγ to be used in our further experiments.

The diffM did not show any time-dependent TNFα or IFNγ release (Fig. 12A, B). In contrast, in actM (LPS 1 ng/ml, 5 ng/ml, and 10 ng/ml), concentrations of TNFα were significantly elevated (0 to 0.65 ng/ml), reaching a maximal release at 3 h, whereas IFNγ secretion (0 to 0.002 ng/ml) was only minor affected (Fig. 12A, B). Because both cytokines were significantly released by macrophages upon their activation, they were further investigated for their apoptosis-inducing effects in HCT116 p53+/+ cells.

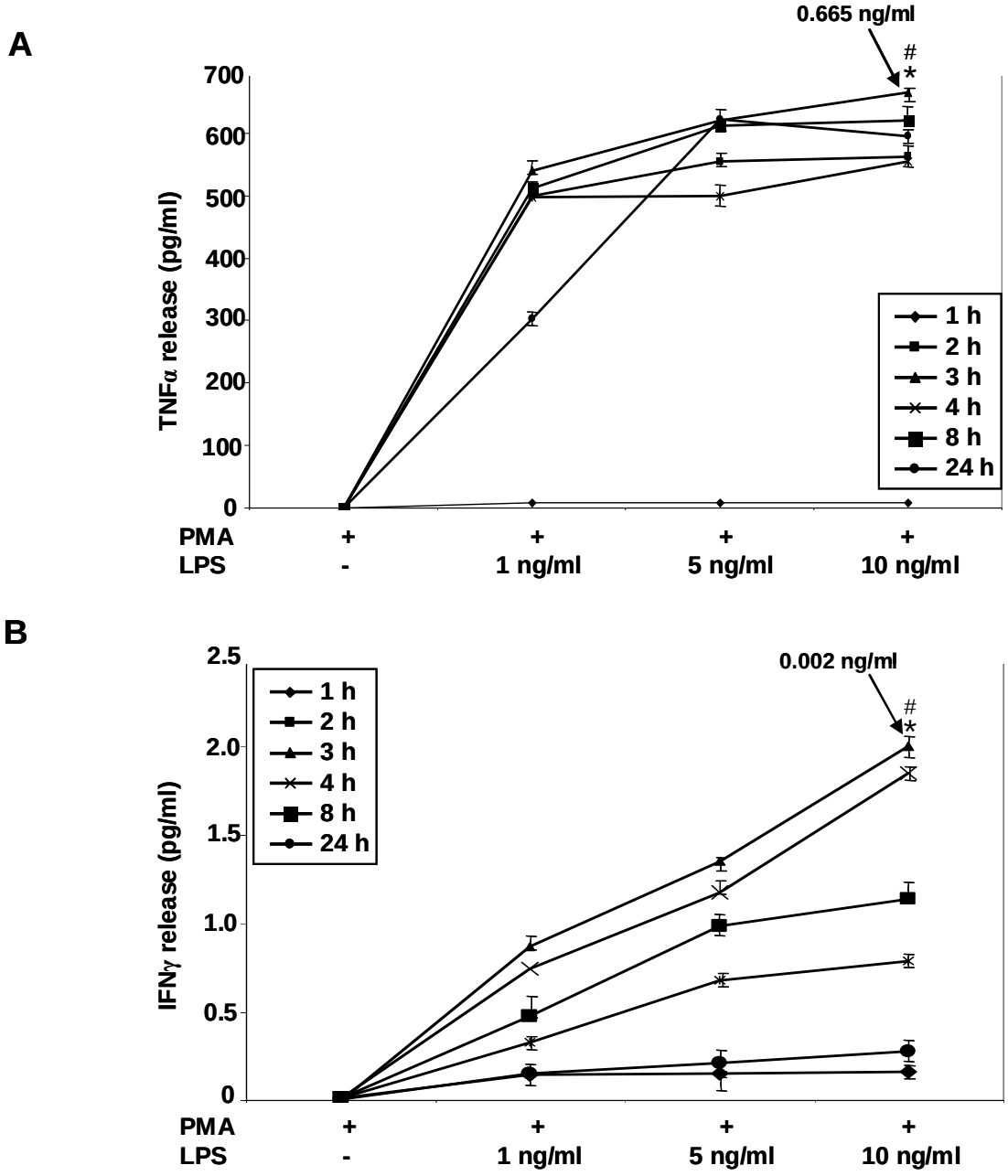

FIG. 12. TNFα and IFNγ are significantly released by macrophage cell line U937 upon their activation. (A) U937 cells were stimulated with PMA or stimulated and activated with PMA and LPS, and subsequently, the supernatants were analyzed by TNFα-ELISA (A) and IFNγ-ELISA (B).

6.2.4 TNFα but not IFNγ exposure induced apoptosis in HCT116 p53+/+ cells

We then proved whether TNFα or IFNγ exposure alone (measured in the supernatant upon LPS stimulation: 0.665 ng/ml or 0.002 ng/ml, Fig. 12) are capable of inducing apoptosis in HCT116 p53+/+ cells. IFNγ did neither alter the DAPK protein amounts during the time frame of 6 h to 72 h nor did it induce apoptosis (Fig. 13 A, B).

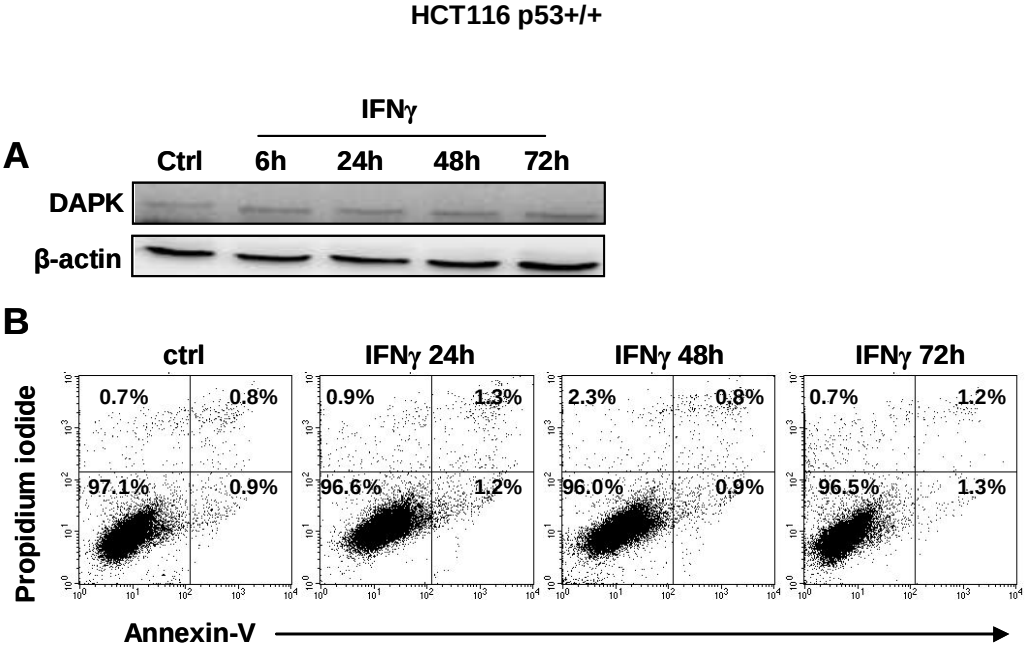

FIG 13. INFγ is not critical for macrophage-induced cell death in HCT116 p53+/+ cells. (A) Lysates prepared from HCT116 p53+/+ cells subjected to 0.002 ng/ml INFγ for 6 h, 24 h 48 h, and 72 h were analyzed by Western blotting using anti-DAPK, or anti-ß-actin for equal loading. Control HCT116 p53+/+ cells (ctrl) served as control. (B) Annexin-V measurements of HCT116 p53+/+ cells (ctrl) and HCT116 p53+/+ cells subjected to 0.002 ng/ml INFγ for 24 h, 48 h, and 72 h.

In contrast, TNFα administration resulted in a significant increase in the apoptotic cell population in the Annexin-V assay (maximal induction at 48 h: 3.94% to 19.2% apoptotic cells) accompanied by 2.8-fold up-regulation in caspase 3/7 activity (Fig. 14 A, B). Furthermore, TNFα exposure led to an elevated DAPK protein level in HCT116 p53+/+ cells (Fig. 14C), paralleled by DAPK catalytic activity induction measured by *in vitro* kinase assay (Fig. 14D). In further studies we focused on signal transduction upon 0.665 ng/ml which best reflected the events that occurred in our experimental settings, albeit the same results were also revealed when using higher TNFα concentration [30 ng/ml (Cohen et al., 1999), 60, and 100 ng/ml]. These data indicate that TNFα is capable of inducing apoptosis and simultaneously activating DAPK.

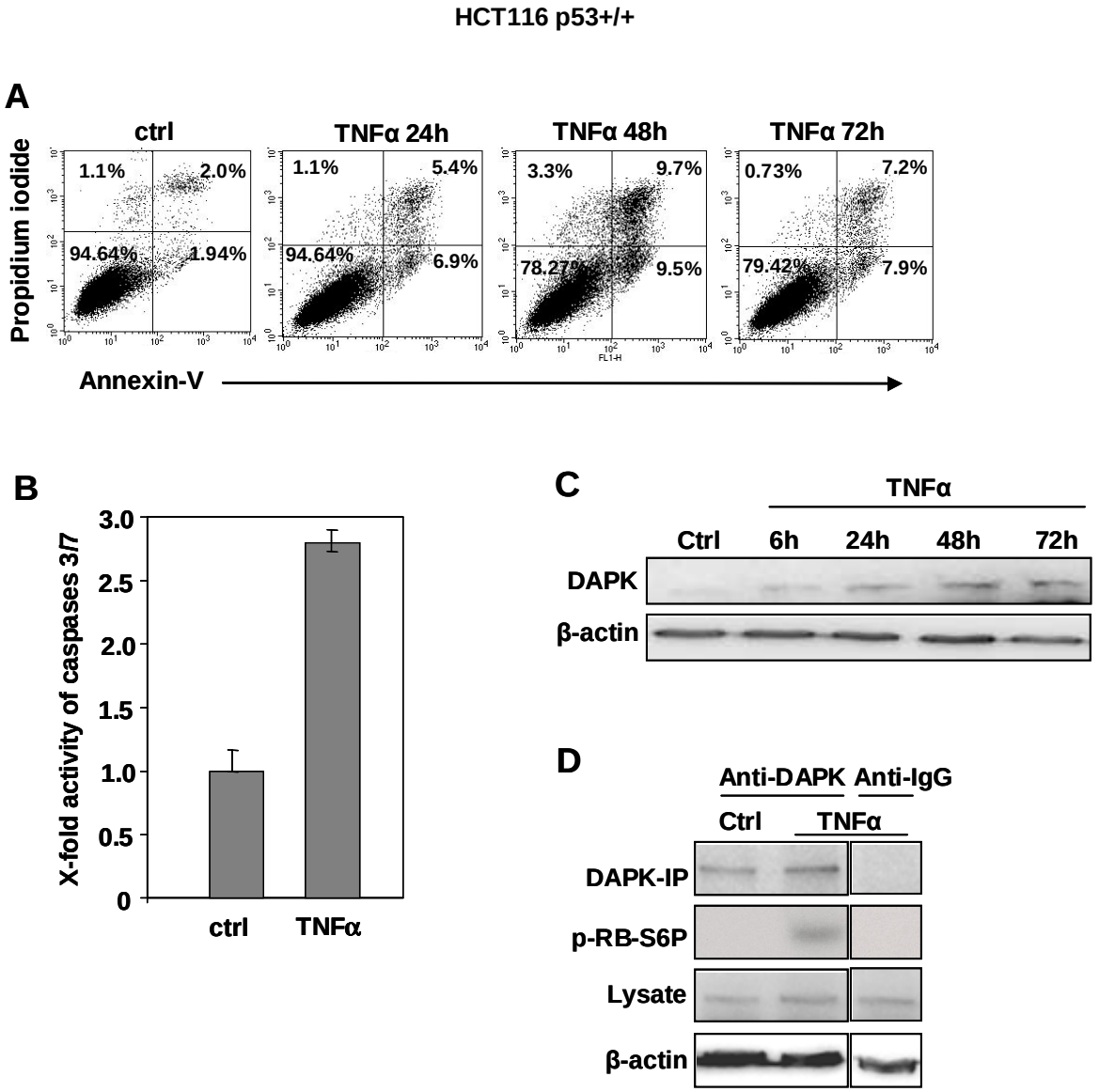

FIG. 14. TNFα is critical for macrophage-induced cell death in HCT116 p53+/+ cells. (A) Annexin-V measurements of control HCT116 p53+/+ cells (ctrl) and HCT116 p53+/+ cells subjected to 0.665 ng/ml TNFα for 24 h, 48 h, and 72 h. (B) Control HCT116 p53+/+ cells (ctrl) and HCT116 p53+/+ cells subjected to 0.665 ng/ml TNFα for 48 h were analyzed by caspase 3/7 activity assay. (C) Lysates prepared from HCT116 p53+/+ cells subjected to 0.665 ng/ml TNFα for 6 h, 24 h 48 h, and 72 h were analyzed by anti-DAPK or anti-ß-actin Western blotting for equal loading. Control HCT116 p53+/+ cells (ctrl) served as control. (D) DAPK-immunoprecipitate of HCT116 p53+/+ cells subjected to 0.665 ng/ml TNFα for 24 h was analyzed by *in vitro* kinase assay. DAPK-immunoprecipitate of control HCT116 p53+/+ cells (ctrl) and IgG-immunoprecipitate subjected to 0.665 ng/ml TNFα served as controls. IP, immunoprecipitation; ctrl, control

6.2.5 TNFα mediated DAPK-dependent apoptosis in HCT116 p53+/+ cells

To verify if DAPK contributes to the observed TNFα-triggered cell death, we transfected the HCT116 p53+/+ cells with DAPK-specific siRNA, resulting in a

complete loss of DAPK protein expression after TNFα administration at 48 h where the maximal apoptosis induction was observed (Fig. 15A). Performing an Annexin-V assay, we found that apoptosis was markedly reduced in HCT116 p53+/+ cells, the DAPK expression of which was inhibited (Fig. 15B), suggesting a role of DAPK in TNFα-mediated cell death.

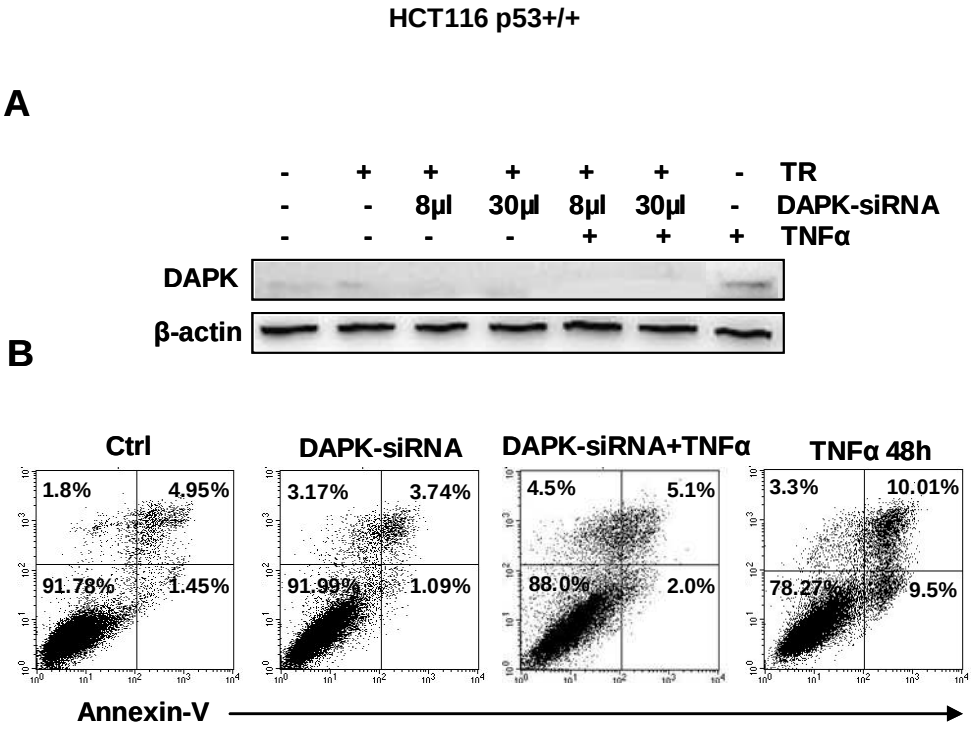

FIG 15. TNFα-induced apoptosis in HCT116 p53+/+ cells is mediated by DAPK (A) Lysates prepared from HCT116 p53+/+ cells knocked down for DAPK and subsequently subjected to 0.665 ng/ml TNFα for 48 h were analyzed by anti-DAPK or anti-ß-actin Western blotting for equal loading. HCT116 p53+/+ cells subjected to transfection reagent, DAPK-siRNA, and TNFα-treatment served as controls. (B) HCT116 p53+/+ cells were transfected with DAPK-siRNA, stimulated with 0.665 ng/ml TNFα for 48 h and subsequently analyzed for apoptosis by Annexin-V measurements. Control HCT116 p53+/+ cells (ctrl), transfected HCT116 p53+/+ cells (DAPK-siRNA), and TNFα-exposed HCT116 p53+/+ cells (TNFα 48h) served as controls. ctrl, control; TR, transfection reagent.

6.2.6 Early activation of p38 in HCT116 p53+/+ tumor cells subjected to TNFα

Previous studies (Chen et al., 2005; Eisenberg-Lerner A et al., 2007) have revealed, that members of the MAPK kinase family (ERK, JNK) are involved in DAPK-dependent apoptosis. To ascertain the role of ERK, JNK/SAPK, and p38 in TNFα-mediated apoptosis, we performed a western blot screen for the activation of these MAP kinases [total proteins and corresponding phosphorylated (activated) forms]. We found a time-dependent pattern of MAPK activation upon TNFα. The only marked

de novo induction was detected for p-p38 within 6 h after TNFα administration, and it disappeared at later time points (24, 48, 72 h). p-JNK/SAPK slightly increased at 6 h and dropped down to the basal level at later time points (Fig. 16).

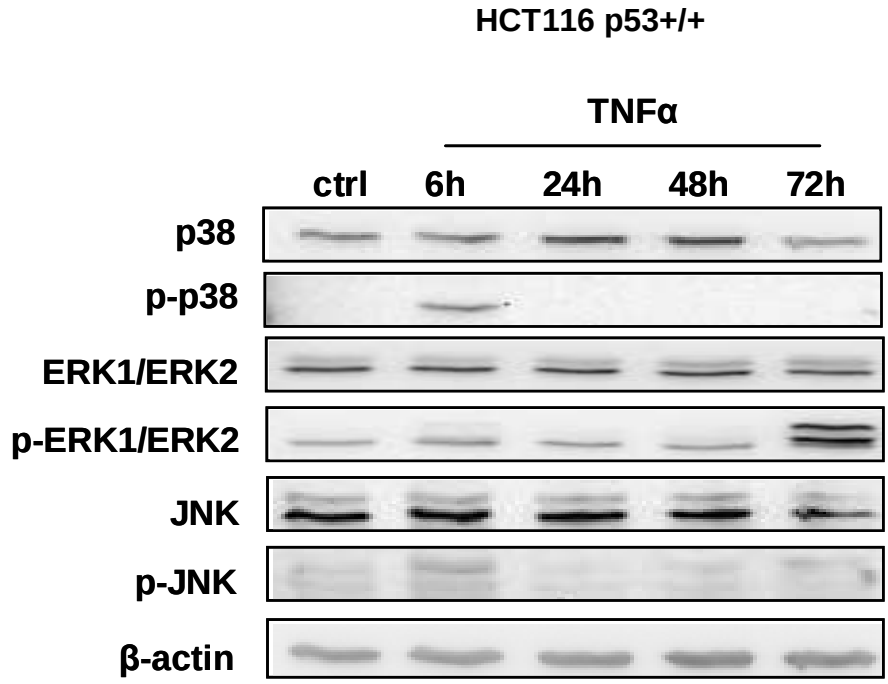

FIG 16. Early activation of p38 in HCT116 p53+/+ cells after TNFα exposure. Lysates prepared from HCT116 p53+/+ cells subjected to 0.665 ng/ml TNFα for 6 h, 24 h 48 h, and 72 h were analyzed by Western blotting using anti-p38, anti-p-p38, anti-ERK1/ERK2, anti-p-ERK1/ERK2, anti-JNK/SAPK, anti-p-JNK/SAPK, or anti-ß-actin for equal loading. HCT116 p53+/+ cells (ctrl) served as control.

To investigate whether JNK could affect the observed apoptosis in HCT116 p53+/+ cells we transfected the cells with JNK-siRNA in the presence or absence of TNFα. JNK siRNA knock down did not influence DAPK-dependent apoptosis in HCT116 p53+/+ cells subjected to TNFα (Fig. 17A, B). Thus, JNK signaling upon TNFα exposure was not further considered. In contrast to p-JNK, p-ERK1/2 was only activated at 72 h (Fig. 16). This very late activation seems not to be associated with DAPK-dependent apoptosis induction and therefore the p-ERK1/2 pathway was excluded in further experiments.

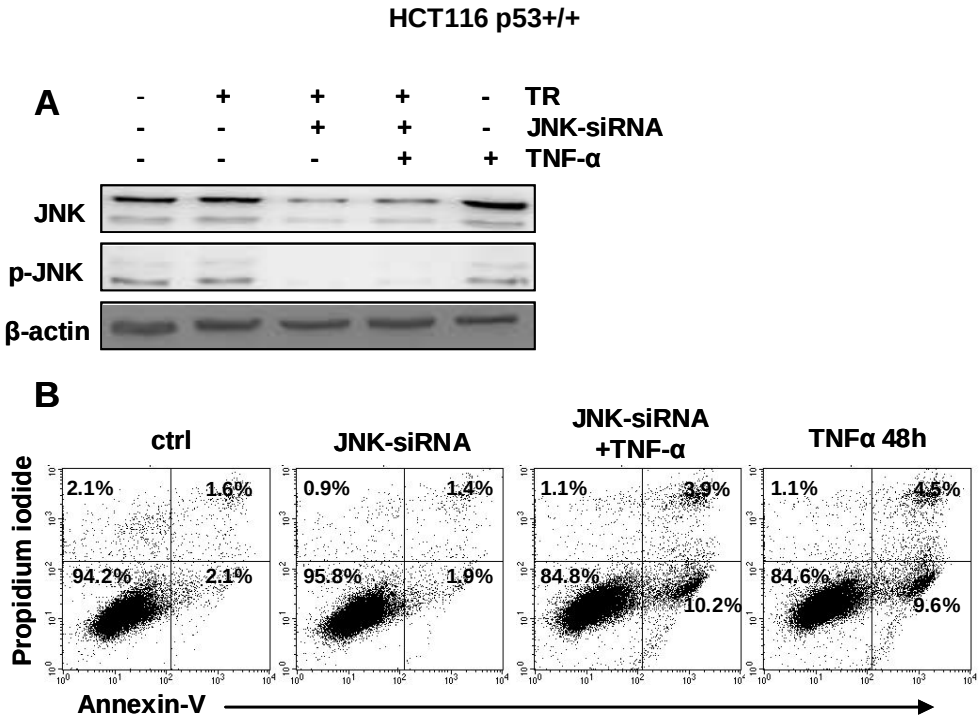

FIG 17. TNFα-induced cell death in HCT116 p53+/+ cells is not mediated by JNK. (A) Lysates prepared from HCT116 p53+/+ cells knocked down for JNK and subsequently subjected to 0.665 ng/ml TNFα for 48 h were analyzed by anti-JNK, anti-p-JNK, or anti-ß-actin Western blotting. HCT116 p53+/+ cells stimulated with transfection reagent alone and in combination with DAPK-siRNA or single TNFα-exposure served as controls together with unstimulated HCT116 p53+/+ cells.

Altogether, these data suggest that p38 seems to be the major player in DAPK-dependent apoptosis after TNFα exposure in HCT116 p53+/+ cells. This hitherto unknown early functional induction of p-p38 was further confirmed in a p38 activity ELISA assay (Fig. 18). For the first time, we identified p-p38 MAPK as target for TNFα-mediated apoptosis and the role of p38 in TNFα/DAPK mediated apoptosis was selected to be the subject for our further investigations.

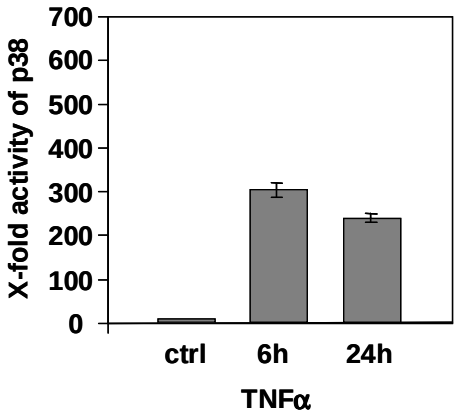

FIG. 18. HCT116 p53+/+ cells (ctrl) or subjected to 0.665 ng/ml TNFa for 6 h and 24 h were assayed for p38 MAPK activity, the control was adjusted to one.

6.2.7 Identification of p-p38 as DAPK binding-protein

To determine whether the p-p38 is interacting with DAPK, we first analyzed the localization of both proteins in HCT116 p53+/+ cells with or without TNFα. We selected the 6 h time point for co-immunofluorescence studies because p-p38 and DAPK were here simultaneously induced. In the absence of TNFα, DAPK was found in the cytoplasm of tumor cells, whereas p-p38 was not detectable in the cells. Upon TNFα exposure, both proteins were found to be co-localized in the cytoplasm of the HCT116 p53+/+ cells (Fig. 19A). The physical interaction between DAPK and p-p38 was further confirmed by co-immunoprecipitation studies. Performing a reverse immunoprecipitation with the anti-DAPK antibody followed by immunoblotting with anti-p-p38 antibody in the HCT116 p53+/+ cells subjected to TNFα (Fig. 19B), p-p38 was identified as DAPK-interacting protein. Altogether, our results strongly indicate p-p38 as a new DAPK binding partner in HCT116 p53+/+ cells upon TNFα exposure.

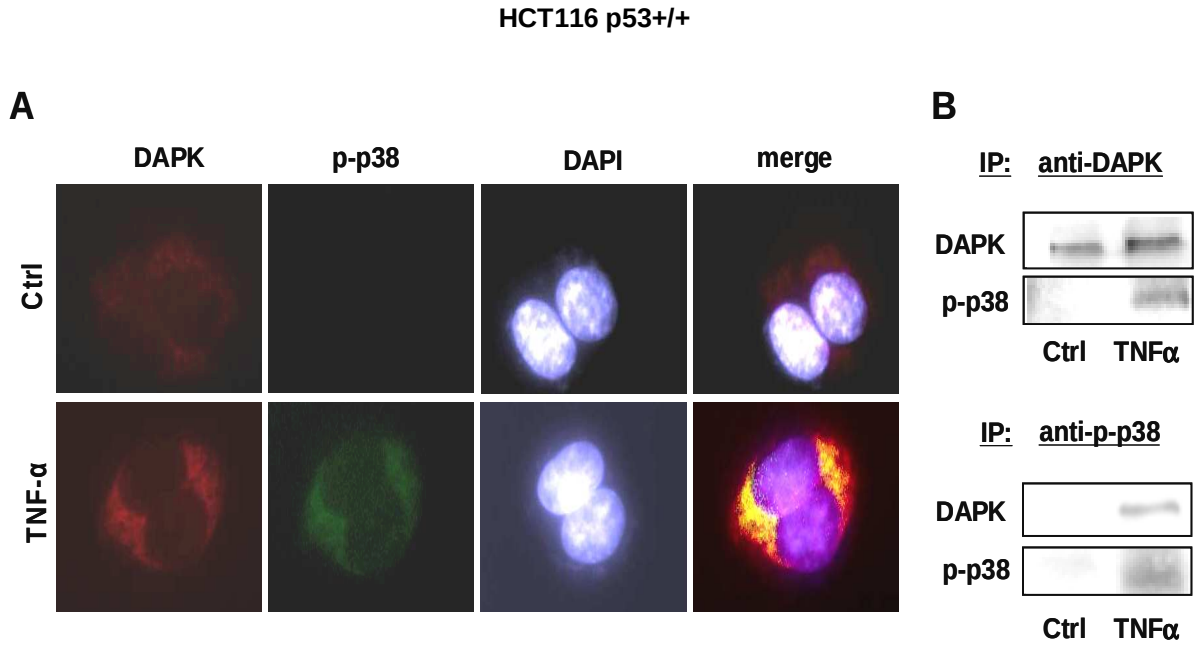

FIG. 19. p-p38 is a direct interacting partner of DAPK during TNFα-induced apoptosis. (A) TNFα-induced co-localization of DAPK and p-p38 after 6 h was determined by fluorescence immunolabeling analysis using anti-DAPK, anti-p-p38, and DAPI. (B) HCT116 p53+/+ cells subjected to 0.665 ng/ml TNFα were lysed, and DAPK or p38 proteins were immunoprecipitated using anti-DAPK or anti-p-p38. Precipitates were analyzed by Western blotting for the presence of p-p38 and DAPK. IP, immunoprecipitation; ctrl, control.

6.2.8 Triggering of DAPK-mediated apoptosis by p-p38

Having identified physical interaction between DAPK and p-p38, we then aimed to demonstrate the direct induction of DAPK catalytic activity by p-p38. For this, we used p38-siRNA to reduce the endogenous expression levels of p38 in HCT116 p53+/+ cells upon TNFα exposure. siRNA transfection resulted in 50% reduction of p38 protein levels, but caused a complete suppression of p-p38 protein (Fig. 20A) and p38 activity (Fig. 20A). Furthermore, siRNA-mediated loss in p-p38 protein did not influence the DAPK protein level in cell lysates (Fig. 20B), but resulted in a significant repression of TNFα-induced DAPK catalytic activity (Fig. 20B) which was accompanied by an efficient loss of TNFα-induced apoptosis in HCT116 p53+/+ cells (Fig. 20C). Altogether, these results suggest that p-p38 may be necessary for DAPK-activation and DAPK-mediated apoptosis in HCT116 p53+/+ cells upon TNFα exposure.

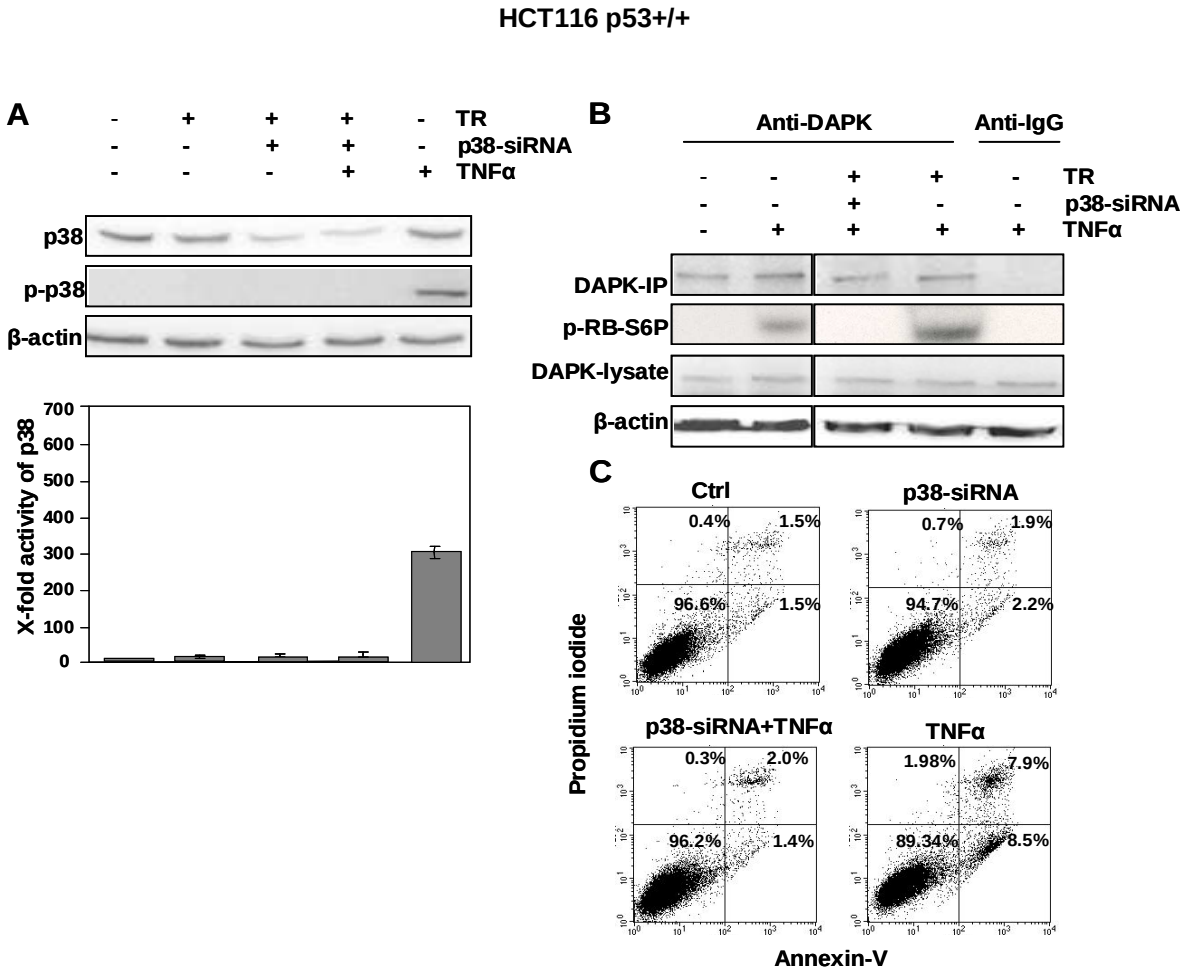

FIG. 20. TNFα-induced and DAPK-mediated apoptosis is triggered by p-p38. (A) Lysates prepared from HCT116 p53+/+ cells knocked down for p-38 and

subsequently subjected to 0.665 ng/ml TNFα for 48 h were analyzed by Western blotting using anti-p38, anti-p-38, or anti-ß-actin for equal loading and were then assayed for p38 MAPK activity, the control was adjusted to 1.0. Control HCT116 p53+/+ cells, HCT116 p53+/+ cells stimulated with transfection reagent, p38-siRNA, or TNFα served as controls. (B) DAPK-immunoprecipitate of HCT116 p53+/+ cells transfected with p38-siRNA prior to TNFα-exposure was analyzed by *in vitro* kinase assay. DAPK-immunoprecipitate of control HCT116 p53+/+ cells, of HCT116 p53+/+ cells transfected with p38-siRNA, or stimulated with transfection reagent or TNFα and IgG-immunoprecipitate subjected to 0.665 ng/ml TNFα served as controls. (C) HCT116 p53+/+ cells were transfected with p38-siRNA, subjected to 0.665 ng/ml TNFα for 48 h and subsequently analyzed for apoptosis by Annexin-V measurements. Control HCT116 p53+/+ cells (ctrl), transfected HCT116 p53+/+ cells (p38-siRNA), and TNFα-subjected HCT116 p53+/+ cells (TNFα 48h) served as controls. IP, immunoprecipitation; TR, transfection reagent.

6.2.9 P53 acts down-stream of DAPK

Recently, it was shown that p53 tumor suppressor is a DAPK upstream transcriptional regulator (Martoriati et al., 2005). Moreover, p53 is an effecter of DAPK-mediated apoptosis (Raveh et al., 2001). To investigate the role of p53 in the observed apoptosis after application of conditioned supernatants of diffM and actM we compared HCT116 cells having different p53 status.

Performing *real-time* RT-PCR in HCT116 p53+/+ cells, we did not find any alterations in the p53 transcript amounts in our experimental setting (Fig. 21A). Evaluating the Western Blots, the p53 protein expression level in the HCT116 p53+/+ cells first decreased at earlier time points (6h, 24h), but reached again the normal control expression level after 48h (Fig. 21B). This increase in p53 amounts, seen later, occurred with a time delay compared to the time course of DAPK protein increase (Fig. 11B). Investigating DAPK protein expression in HCT116 p53-/- cells subjected to the conditioned media of macrophages, we observed a similar pattern of DAPK protein amounts (Fig. 21C). Both findings suggest a down-stream action of p53.

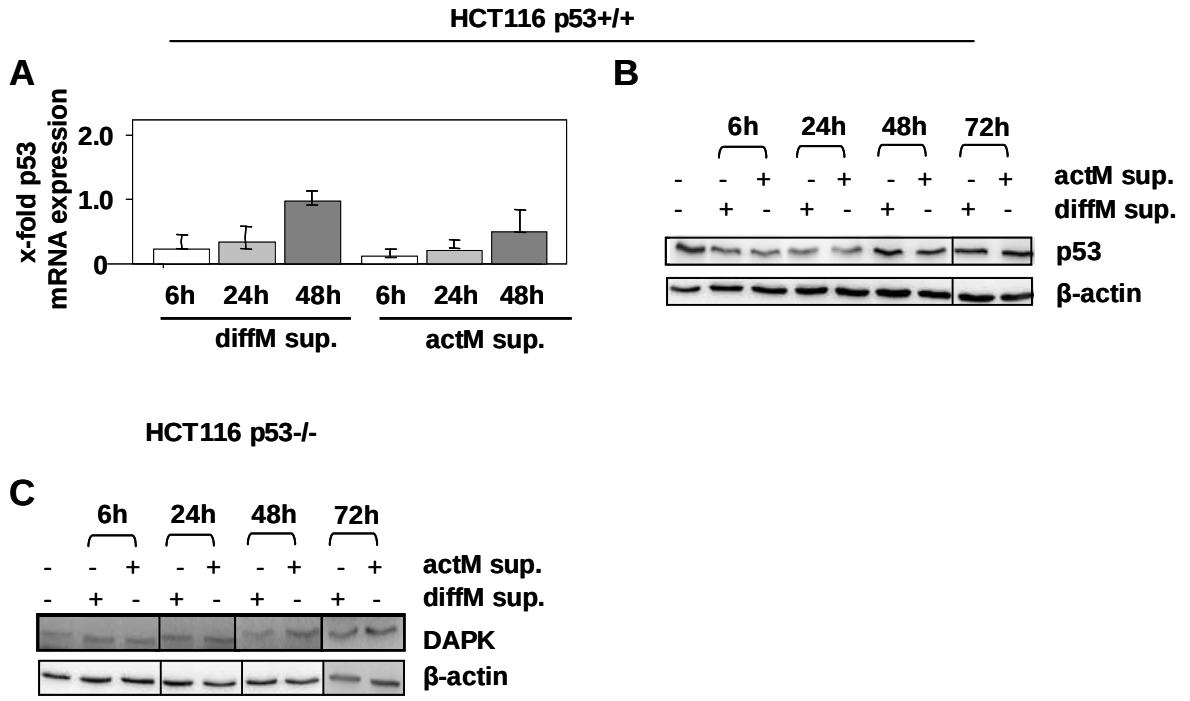

FIG 21. p53 acts downstream of DAPK. (A) For HCT116 p53+/+ cells, subjected to diffM sup. or actM sup., RT-PCR analysis was performed using cDNA-specific primers for DAPK. (B) Lysates prepared from diffM sup.- and actM sup.-exposed HCT116 p53+/+ cells were analyzed by anti-p53 or anti-ß-actin Western blotting for equal loading. Control HCT116 p53+/+ cells served as control. (C) HCT116 p53-/- cells were subjected to diffM sup. or actM sup. and subsequently DAPK protein levels were analyzed by anti-DAPK or anti-ß-actin Western blotting for equal loading. Ctrl, control; diffM sup., supernatant of PMA-differentiated macrophages U937; actM sup., supernatant of PMA-differentiated and PMA-activated macrophages U937.

In the HCT116 p53-/- cells, apoptosis measured by caspase 3/7 activity and Annexin staining assays revealed a lower cell death induction (10%, at 48 h) in comparison with the HCT116 p53+/+ (20%, at 48 h) after incubation with diffM and actM supernatants (Fig. 22A, B) compared to the HCT116 p53+/+ cells. Both cell lines showed a reinforcement of apoptosis after exposure to the actM supernatant. These data suggest that the observed apoptosis induction may partly be strengthened by p53.

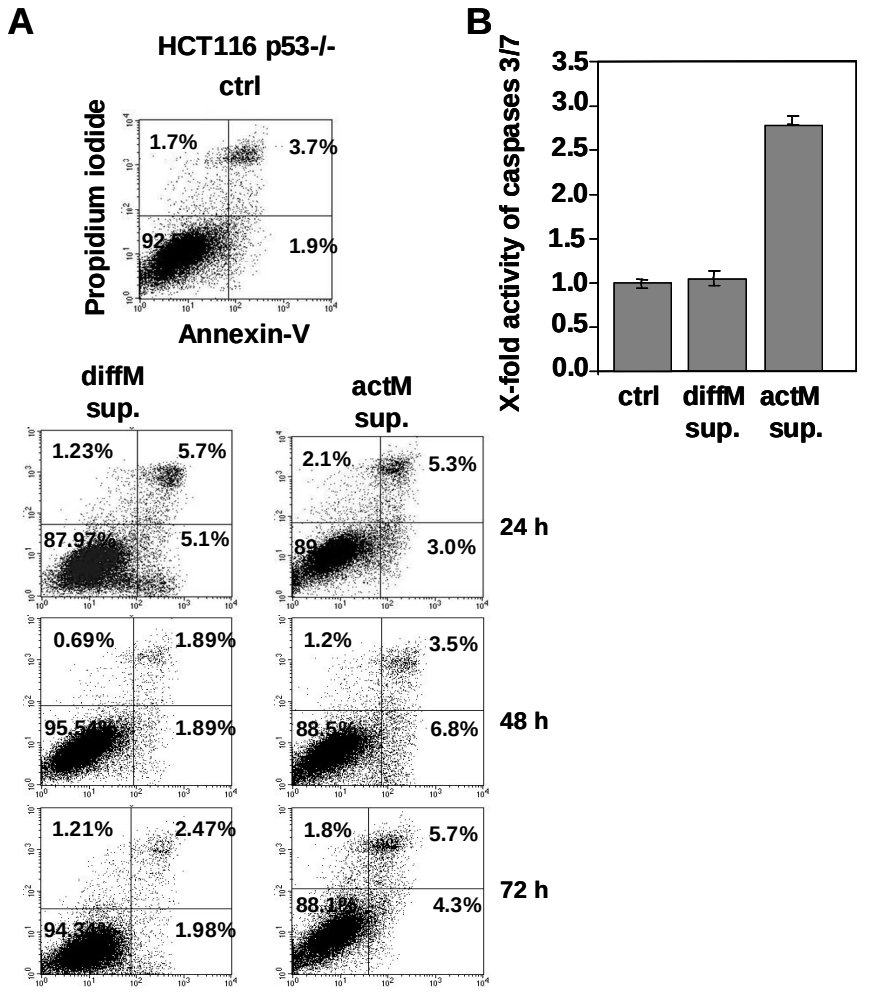

FIG. 22.The DAPK-induced apoptosis is partially p53-dependent. (A) Annexin-V measurements of HCT116 p53-/- cells (ctrl) and HCT116 p53-/- cells subjected to diffM sup. or actM sup. for 24 h, 48 h, and 72 h. (B) HCT116 p53-/- cells subjected to diffM sup. or actM sup. for 48 h were analyzed by caspase 3/7 activity assay. Ctrl, control; diffM sup., supernatant of PMA-differentiated macrophages U937; actM sup., supernatant of PMA-differentiated and PMA-activated macrophages U937.

6.2.10 TNFα induced cell death in HCT116 p53-/-

In the HCT116 p53-/- cells, TNFα induced early DAPK protein expression (6 h) which further increased till 72 h. this effect was accompanied by apoptosis induction but to a much lesser extent (9%, at 48 h) than in the p53+/+ cells (20%, at 48 h) (Fig. 23). As mentioned above, these data again suggest that p53 acts downstream of DAPK and participates in the observed TNFα-mediated cell death. Altogether, having differences in the annexin positive cells but relatively the same caspase 3/7 activity in HCT116 p53+/+ and HCT116 p53 -/- cells, suggest another apoptosis pathway in the HCT16 p53 deficient cells.

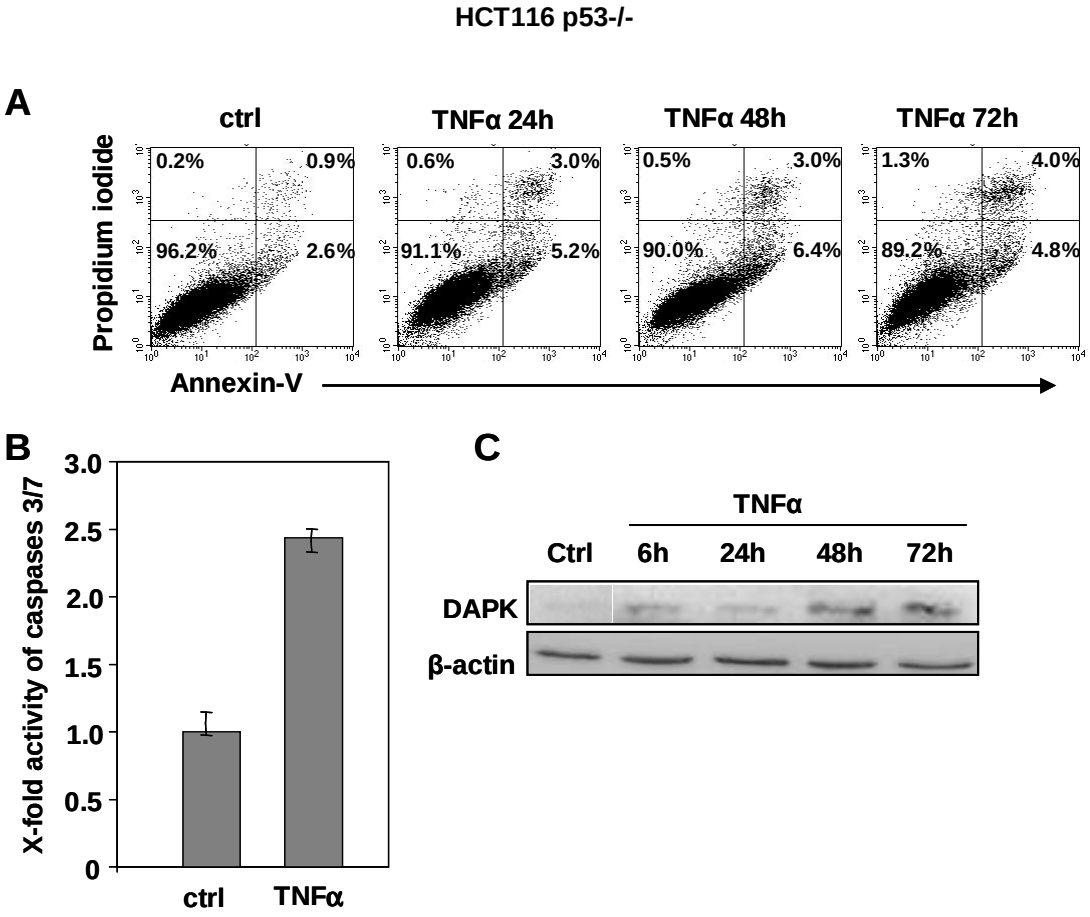

FIG. 23. TNFα-induced cell death in HCT116 p53-/- cells is accompanied by DAPK up-regulation. (A) Lysates prepared from HCT116 p53-/- cells subjected to 0.665 ng/ml TNFa for 6 h, 24 h 48 h, and 72 h were analyzed by Western blotting, using anti-DAPK, or anti-ß-actin for equal loading. Control HCT116 p53-/- cells (ctrl) served as control. (B) Annexin-V measurements of unstimulated HCT116 p53-/- cells (ctrl) and HCT116 p53-/- cells subjected to 0.665 ng/ml TNFα for 24 h, 48 h and 72 h. (C) HCT116 p53-/- cells (ctrl) and HCT116 p53-/- cells subjected to 0.665 ng/ml TNFα for 48 h were analyzed by caspase 3/7 activity assay.

6.2.11 P38 is also activated in the p53 deficient HCT116 cells upon TNFα exposure

To investigate whether p38 is activated in HCT116 p53-/- after TNFα administration, we performed Western Blotting of p38 and its phosphorylated form. Indeed, our analysis showed an increase in the p-p38 protein level at 6 h and its activity (Fig. 24A, B). Furthermore, double immunofluorescence analysis revealed a co-localization of DAPK and p-p38 in the cytoplasm of HCT116 p53-/- cells upon TNFα exposure (Fig. 24C).

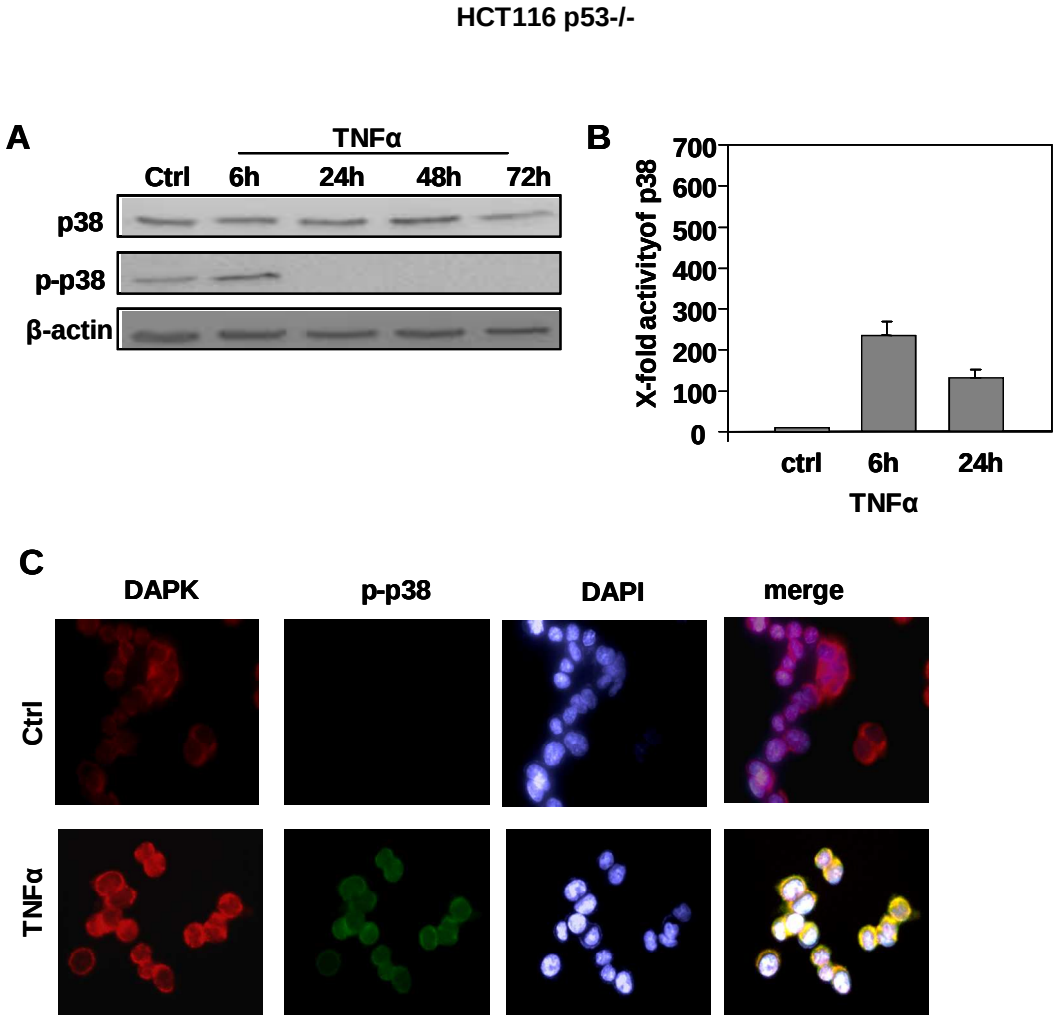

FIG. 24. Early activation of p38 and co-localization with DAPK in HCT116 p53 deficient cells after TNFα exposure. (A) Lysates prepared from HCT116 p53-/- cells subjected to 0.665 ng/ml TNFα for 6 h, 24 h, 48 h, and 72 h were analyzed by Western blotting using anti-p38, anti-p-p38, or anti-ß-actin for equal loading. HCT116 p53-/- cells (ctrl) served as control. (B) HCT116 p53-/- cells (ctrl) or subjected to 0.665 ng/ml TNFα for 6 h and 24 h were assayed for p38 MAPK activity, the control was adjusted to 1.0. (C) TNFα-induced co-localization of DAPK and p-p38 after 6 h was determined by fluorescence immunolabeling analysis using anti-DAPK, anti-p-p38, and DAPI.

6.2.12 Physiological relevance of DAPK regulation

6.2.12.1 DAPK co-localizes with p-p38 in human colorectal carcinoma

To investigate the physiological distribution of DAPK and p-p38 proteins, we performed an immunohistochemical analysis of the two proteins in serial sections of representative samples of normal colonic mucosa and colorectal carcinoma tissue with and without DAPK promoter methylation. As shown in Fig. 25, in the unmethylated tumors, the expression of DAPK was strongly associated with the presence of p-p38 expression. In contrast, the methylated carcinomas demonstrated a weak cytoplasmic p-p38 expression of the tumor with a nuclear expression of single tumor cell. In normal colorectal mucosa, nuclear expression of phospho-p38 MAPK was observed in the proliferative zone of the crypts was observed.

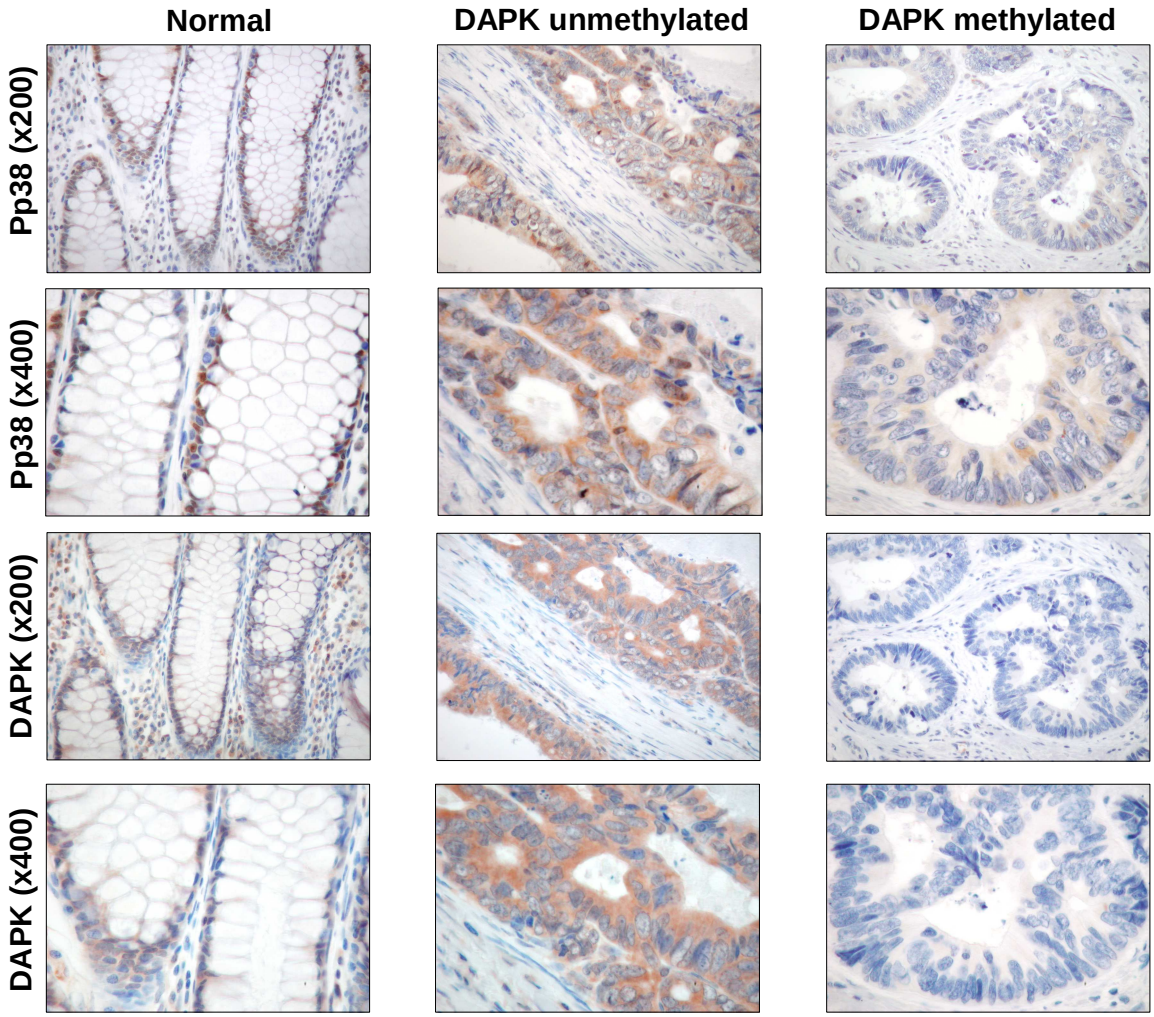

FIG. 25. DAPK co-localizes with p-p38 in human colorectal carcinoma. Immunohistochemical analysis of DAPK and p-p38 in normal colonic mucosa and colorectal carcinoma tissue with and without DAPK promoter methylation was detected by anti-DAPK and anti-p-p38. (Microscope: Zeiss Axioscope 50, camera: Nikon coolpix 990; magnification: x200, x400)

6.2.12.2 Apoptosis induction in the HCT116 p63+/+ cell and DAPK up-regulation after exposure to the supernatants of freshly isolated activated human macrophages

To gain further insight into the physiologic role of human macrophages, we stimulated the freshly isolated human macrophages with 10 ng/ml LPS, which induced TNFα release (0.352 ng/ml). Applying the activated macrophages-supernatants to the HCT116 p53+/+ cells up-regulated DAPK protein levels and induced p-p38 already at 6 h (Fig. 26). Simultaneously, as a sign of apoptosis induction, caspase 3 cleavage was detectable.

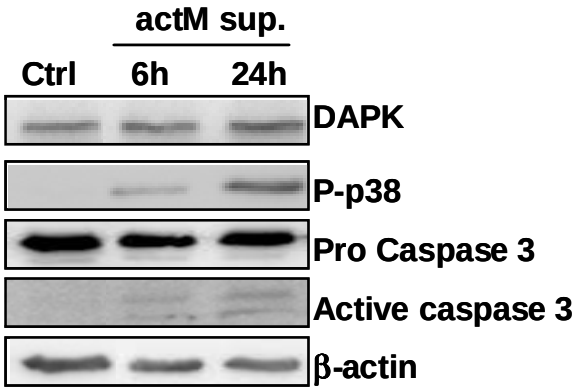

FIG. 26. Lysates from human actM spernatant-stimulated HCT116 p53+/+ were analyzed by anti-DAPK, anti p-P38, anti-Caspase3 and anti-β-actin Western blotting. Unstimulated HCT116 p53+/+ served as control.

6.3 Tumor cell ⟶ Macrophage

6.3.1 Tumor cell-supernatants increased DAPK level but did not induce apoptosis in activated U937

Schneider-Stock et al. (2006) showed that, by analysing human colorectal tumor sections, although DAPK levels were increased in the tumor-associated macrophages, no cell death was detected. Therefore, we aimed to test whether our experimental settings might recapitulate the *in vivo* observed events. Indeed, DAPK protein levels were increased after incubation the diffM and actM with either HCT116 p53+/+ or HCT116 p53-/- supernatants (Fig. 27A, B). Furthermore, no p53 protein expression was detected. Moreover, in contrast to the diffM the supernatants of HCT116 cells did not induce apoptosis in actM (Fig. 28A). The observed apoptosis resistance in the actM was further confirmed by measuring the caspase activity (Fig.

28B). Altogether, these findings indicate that DAPK might play a role in macrophages survival in a p53-independent pathway.

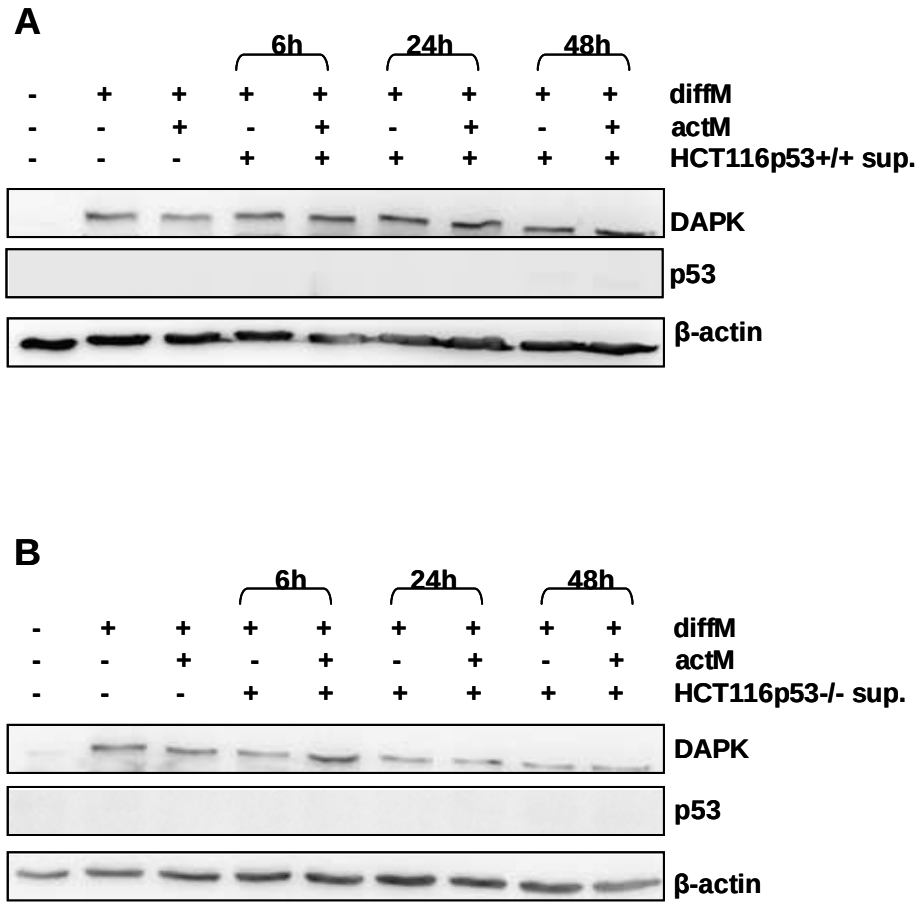

FIG. 27. Tumor cells-supernatants induced DAPK up-regulation in the macrophage-like cell line U937. (A) Lysates prepared from diffM and actM exposed to supernatants of HCT116 p53+/+ (A) or HCT116 p53-/- (B) cells were analyzed by anti-DAPK, anti-p53 or anti-ß-actin Western blotting for equal loading. diffM; PMA-differentiated macrophages U937; actM; PMA-differentiated and LPS-activated macrophages U937, HCT116 p53+/+ sup.; supernatants of HCT116 p53+/+, and HCT116 p53-/- sup.; supernatants of HCT116 p53-/-.

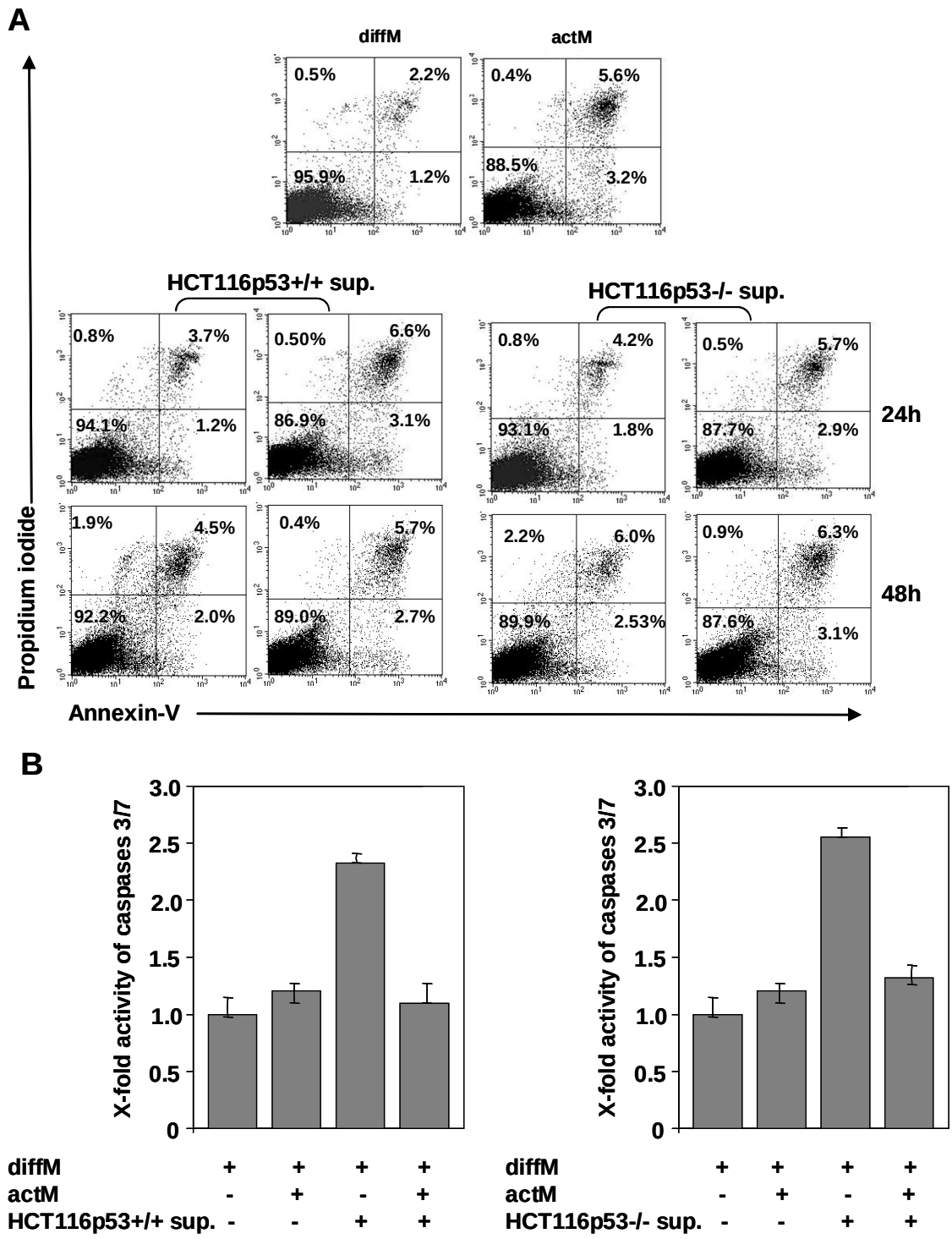

FIG. 28. Tumor cell-supernatants did not induce cell death in the activated macrophages. (A) Annexin-V measurements of diffM and actM subjected to the supernatants of HCT116 p53+/+ or HCT116 p53-/- for 24 h and 48 h. (B) diffM and actM subjected to the supernatants of HCT116 p53+/+ or HCT116 p53-/- for 48 h were analyzed by caspase 3/7 activity assay. diffM; PMA-differentiated macrophages U937; actM; PMA-differentiated and LPS-activated macrophages U937, HCT116 p53+/+ sup.; supernatants of HCT116 p53+/+, and HCT116 p53-/- sup.; supernatants of HCT116 p53-/-.

6.3.2 DAPK participated in survival of the activated macrophages.

Jin et al. (2005) demonstrated that, after overexpressing mouse DAPK β in HEK cells, it did not induce apoptosis and inhibited caspase 3 acitivty, suggesting an antiapoptotic effect of DAPK. In order to test if there is a relationship between the macrophages survival and DAPK up-regulation, siRNA to DAPK was used to suppress its expression in U937 subjected to HCT116 p53+/+ supernatants. As shown in fig. 29A there was a reduction of DAPK protein after siRNA transfection. Moreover, DAPK-siRNA transfected cells underwent apoptosis via reduction of BCL-2 potein expression and induction of Bax levels and the cleavage of caspase 3 (Fig. 29A). Application of DAPK-siRNA to actM exposed to HCT116 p53+/+ supernatants resulted in marked increase of apoptotic cells (Fig. 29B), indicating that DAPK is involved in the observed apoptosis resistance in the actM.

A

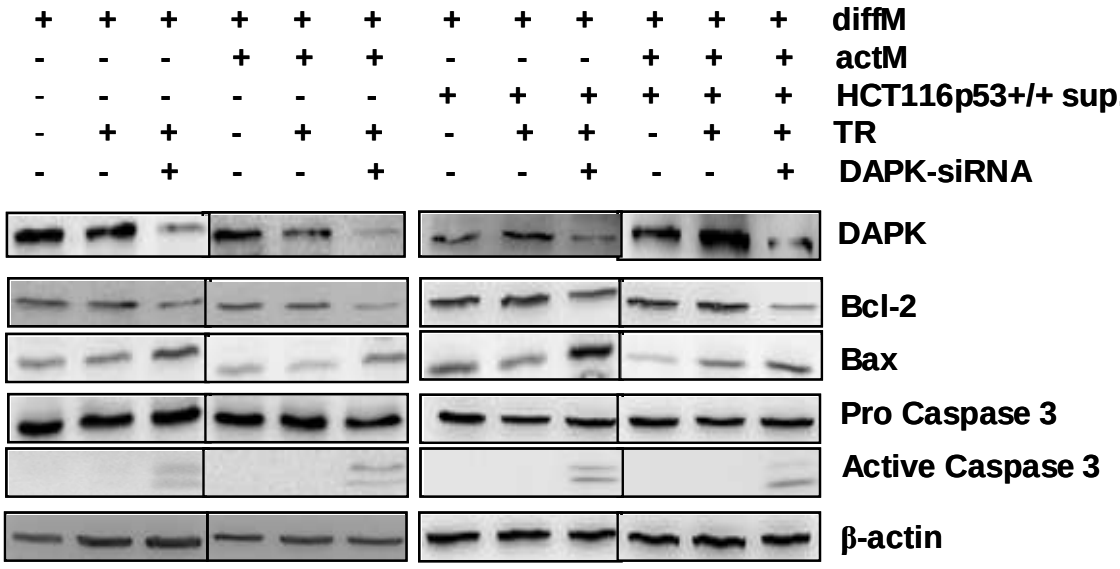

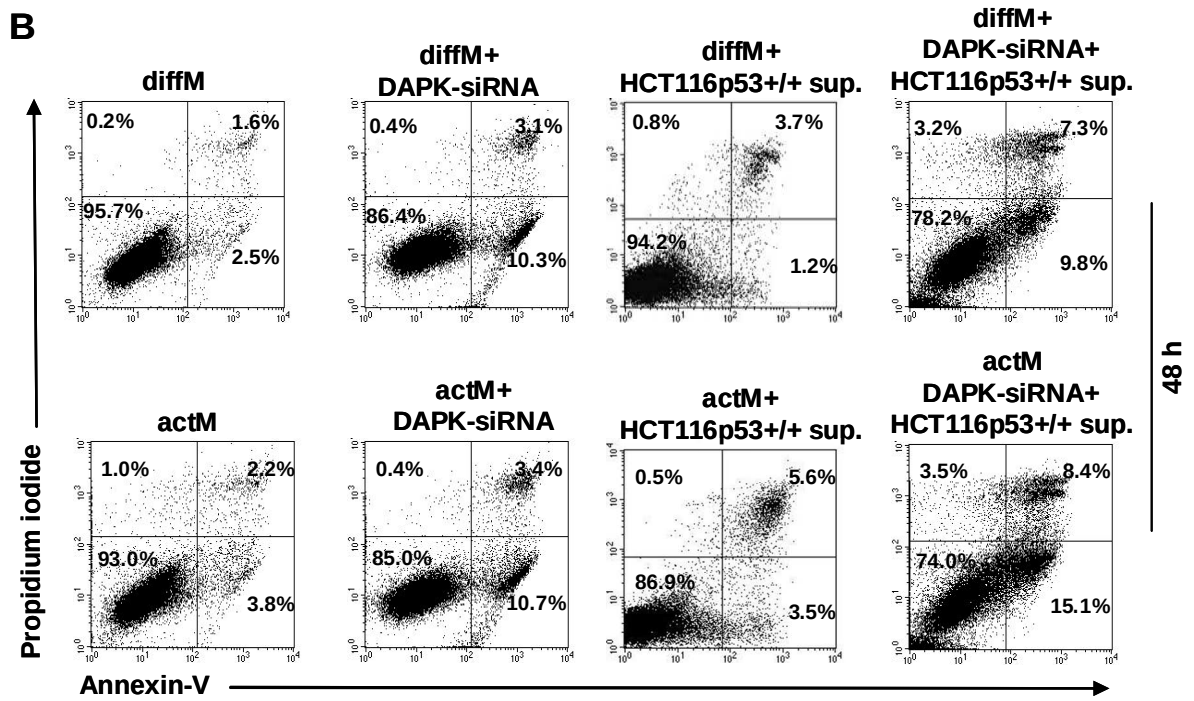

FIG 29. Cell survival in activated macrophages is mediated by DAPK. (A) Lysates prepared from U937 cells knocked down for DAPK and subsequently subjected to HCT116 p53+/+ were analyzed by anti-DAPK, anti-Bcl-2, anti-Bax, anti-caspase 3, or anti-ß-actin Western blotting for equal loading. U937 cells subjected to transfection reagent, DAPK-siRNA, and HCT116 p53+/+ supernatants served as controls. (B) U937 were transfected with DAPK-siRNA, subjected to HCT116 p53+/+ supernatants for 48 h and subsequently analyzed for apoptosis by Annexin-V measurements. diffM; PMA-differentiated macrophages U937; actM; PMA-differentiated and LPS-activated macrophages U937, HCT116 p53+/+ sup.; supernatants of HCT116 p53+/+.

6.3.3 RSK may be involved the DAPK-mediated cell survival of U937

Recently, it has been demonstrated that RSK phosphorylates DAPK, resulting in inhibiting its pro-apoptotic function (Anjum et al., 2005). Therefore, we aimed to analyze RSK protein level and whether it participates in the observed DAPK-mediated cell survival. Western Blotting analysis showed an increase of RSK protein levels (Fig. 30A). Moreover, performing double immunofluorescence revealed a co-localization of RSK and DAPK in U937 cells (Fig. 30B), suggesting that RSK may participate in the macrophage apoptosis resistance.

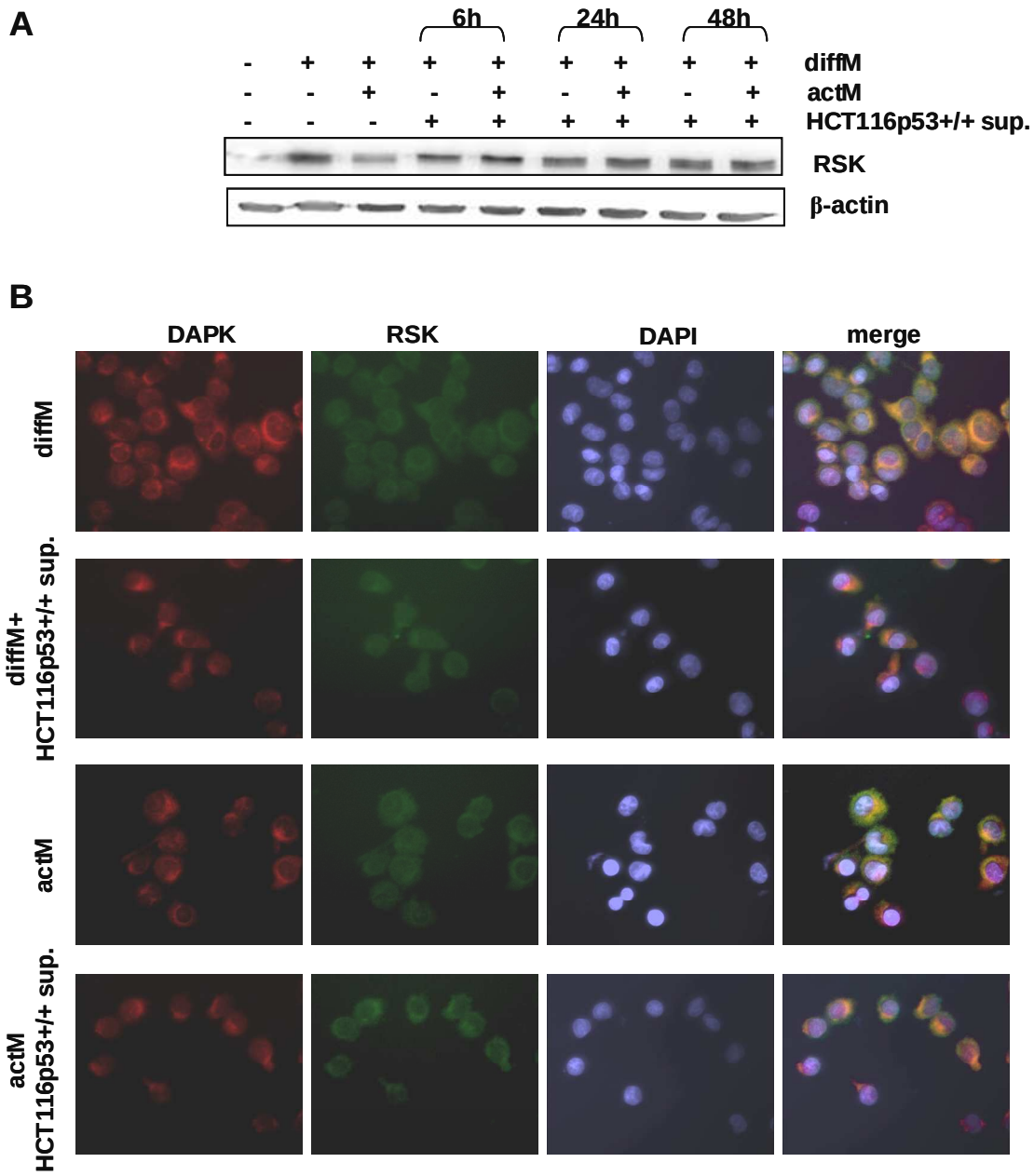

FIG. 30. RSK is up-regulated and co-localized with DAPK in U937. (A) Lysates prepared from diffM and actM exposed to supernatants of HCT116 p53+/+ cells were analyzed by anti-RSK, or anti-ß-actin Western blotting for equal loading. (B) Co-localization of DAPK and p-p38 after 6 h was determined by fluorescence immunolabeling analysis using anti-DAPK, anti-RSK, and DAPI. diffM; PMA-differentiated macrophages U937; actM; PMA-differentiated and LPS-activated macrophages U937, HCT116 p53+/+ sup.; supernatants of HCT116 p53+/+.

7. Discussion

There are a number of different methods used to treat cancer. Surgery, radiation and chemotherapy are three common forms of cancer treatment that have been used for a number of years. Recently, new strategies have been developed toward new therapeutic cancer approaches, namely immunotherapy.

The concept of immunotherapy is based on the body's natural defense system, which protects the human body against a variety of diseases. Although we are less aware of it, the immune system also works to aid our recovery from many illnesses. For many years, physicians believed that the immune system was effective only in combating infectious diseases caused by such invading agents as bacteria and viruses. More recently, we have learned that the immune system may play a central role in protecting the body against cancer and in combating cancer that has already developed. This latter role is not well understood, but there is evidence that in many cancer patients the immune system slows down the growth and spread of tumors. The body's ability to develop an immune reaction to tumors may help determine which patients are cured of cancer using conventional therapies, including surgery, radiation and drugs. One immediate goal of research in cancer immunology is the development of methods to harness and enhance the body's natural tendency to defend itself against malignant tumors. Immunotherapy represents a new and powerful approach in anticancer treatment. Immunotherapy seems to offer great promise as a new dimension in cancer treatment, but it is still very much in its infancy. Immunotherapies involving certain cytokines and antibodies have now become part of standard cancer treatment (Senzer et al., 2004, Ribas et al., 2005 Mazzolini et al., 2007). Other examples of immunotherapy remain experimental. Although many clinical trials of new forms of immunotherapy are in progress (Keilholz et al., 1997, Rubin et al., 1997, Morse et al., 1999), an enormous amount of research remains to be done before the findings can be widely applied. In this respect, targeting immune cells around tumors might be a promising approach in finding new alternatives of cancer treatments with less side affects.

The purpose of this study was to recapitulate the events observed by Schneider-Stock et al., (2006), to investigate the role of DAPK in tumor cells and macrophages, including apoptosis and survival, and to study which mechanisms involve DAPK regulation.

The current study identifies p-p38 MAPK as a novel interacting protein of DAPK during TNAα-induced apoptosis in colorectal cancer cells. p38 MAPK phoshorylation was found to be an upstream target for DAPK after TNFα exposure, providing new insights into the regulation of DAPK-mediated apoptosis. P-p38 regulates TNFα-mediated cell death by enhancing DAPK catalytic activity. The DAPK/p-p38 interaction was also evident in DAPK-unmethylated human colorectal cancer tissue. Furthermore, the physiological significance of our findings was verified by showing an increase in DAPK and p-p38 protein expression, as well as enhanced cell death after treatment of colorectal cancer cells with the conditioned supernatants of human freshly isolated and differentiated PBMCs.

The experimental setting was based on our previous findings which showed that the higher apoptotic rate in colorectal tumors was associated with an increase in DAPK protein expression (Schneider-Stock et al., 2006). Interestingly, the DAPK protein expression was similar between macrophages and tumor cells, suggesting a cross talk between these two cell types in DAPK-mediated tumor cell death (Schneider-Stock et al. 2006). To understand the effects that macrophages may have on colorectal cancer cells and DAPK expression, we developed a human cell culture model that simulates the physiologic conditions. Culture supernatants from diffM and actM macrophages were applied to the HCT116 colorectal tumor cell line. Our findings indicate that actM induced apoptosis in the tumor cells. In contrast, diffM (non-activated macrophages) were not able to mediate cell death in HCT116 cells. The observed cell death was associated with accumulation of DAPK protein rather than its gene transcription. As p53 was shown to transcriptionally transactivate the DAPK promoter in MEFs after tamoxifen treatment (Martoriati et al. 2005), we exclude this pathway for TNAα-driven, DAPK-dependent apoptosis. P53 also acts as a downstream effector of DAPK, contributing to an oncogene-driven $p19^{ARF}$-dependent checkpoint pathway (Raveh et al., 2001). The marginally lower apoptotic rate in the HCT116 p53-/- cells indicated that the TNFα-driven DAPK-dependent apoptosis was at least partially p53-dependent. This seems to be interesting against

the background of the fact that most of colon cancers bear p53 mutations that functionally inactivate the p53 protein and thus should be of therapeutical relevance.

The complex between both kinases may be regulated in a phosphorylation-dependent manner. P-p38 is known to phosphorylate its downstream targets at Ser and Thr residues. Activated p38 has been shown to phosphorylate several cellular targets, including transcription factors ATF1 and ATF2, MEF2A, Sap-1, NfkB, and p53 (Kyriakis and Avruch, 2001). For DAPK, activating and inactivating phosphorylation sites have been identified, but the endogenous DAPK status was never investigated: Chen et al. (2005) have shown that activated ERK phosphorylates DAPK at Ser735 after serum stimulation in HEK293T cells. On the other hand, RSK inactivates DAPK through phosphorylation at Ser289 after PMA exposure in HEK293E cells (Anjum et al. 2005). Recently, Wang et al. (2007) identified DAPK as a phosphorylation target of both tyrosine kinase Src and phosphatase LAR, which act in synergism to inactivate DAPK. In the case of p-p38, the activation of DAPK seems to have an apoptosis-promoting function. On way of p38-DAPK interaction is phosphorylation of DAPK by p38, thus enhancing its kinase activity. We found that p38 activation induces DAPK catalytic activity. Notably, DAPK possesses a serine-containing peptide (at Ser^{735}) that can be phosphorylated by p38 (for details see: www. scansite.mit.edu/cgi-bin/motifscan_seq). It is not clear which region of p-p38 interacts with DAPK domains. What is known is that p38 MAPK and ERK2 bind to D-domain peptides through a specific docking groove (Chang et al. 2002, Lee et al. 2004). Chen et al. (2005) reported that DAPK interacts with ERK through a D-domain within its death domain and promotes the cytoplasmic retention of ERK, thereby inhibiting ERK signaling in the nucleus. The significance of the death domain of DAPK in mediating its death-promoting function after TNFα exposure was documented by Cohen et al. (1999). In our experimental setting, endogenous DAPK was found to co-localize with p-p38 MAPK in the cytoplasm after TNFα exposure in colorectal cancer cells. Without the stimulus, p-p38 was not detectable in the nucleus or in the cytoplasm of the cancer cells. Most stimuli that activate p38 also activate JNK, as we have observed upon TNFα exposure in colon cancer cells. Nevertheless, for our scenario, JNK activation was not found to play a role in DAPK-dependent apoptosis upon TNFα exposure.

P38 was shown to be present in both the nucleus and cytoplasm of quiescent cells, but upon cell stimulation, the cellular localization of p38 is not well understood. Some

evidence suggests that following activation, p38 translocates from the cytoplasm to the nucleus (Raingeaud et al. 1995), but other data indicate that activated p38 is also present in the cytoplasm of stimulated cells (Ben-Levy et al. 1998). To the best of our knowledge, there is no report on p38 activation in the cytoplasm upon TNFα exposure. Here, we show for the first time an interaction of activated p38 MAPK and DAPK in the cytoplasm of TNFα-stimulated tumor cell death.

Furthermore, TNFα induces p38 activation and apoptotic cell death in endothelial cells through downregulation of the Bcl-x(L) protein (Grethe et al., 2004). Similarly, for the TNFα-induced DAPK-dependent apoptosis, it was verified that DAPK acts upstream of caspase 3, and that the death-promoting effects of DAPK are counteracted by Bcl2. The novel finding of our experimental setting is that we connect these previous studies by showing that TNFα induces a DAPK-dependent caspase-associated apoptosis by interacting with activated p38 MAPK in colon cancer cells.

Tumor-associated macrophages (TAMs) represent a prominent component of the leucocytic infiltrate in most malignant tumors (Balkwill and Mantovani, 2001). TAMs support tumor growth by secreting factors such as cytokines and matrix metalloproteases that promote proliferation, invasion, and metastasis of tumor cells as well as tumor vascularization (Sunderkotter C et al., 1994). In contrast, TAM-derived inflammatory cytokines including TNFα, IFNγ, or TGFβ can also induce apoptosis in tumor cells (Baron-Bodo et al., 2005; Karpoff et al., 1996; Ohta et al., 1996). We identified TNFα, but not IFNγ in supernatants derived from actM and diffM as the critical mediator for DAPK-dependent apoptosis in colon cancer cells. In our experimental setting, DAPK was up-regulated only at the posttranscriptional level. Therefore, TGF-β was excluded as a possible mediator, because it was found to transcriptionally activate DAPK through Smad binding-sites in its promoter (Jang et al., 2001).

In contrast to our observations in the colorectal cancer cells, we showed that DAPK up-regulation in the activated macrophage-like cell line U937 was not associated with cell death, confirming the findings reported by Schneider-Stock et al. (2006). ActM showed cell death resistance even after incubation with supernatants of HCT116 p53 wild type and deficient cells. Jin et al. (2005) demonstrated that, overexpressing mouse DAPK β in HEK cells did not induce apoptosis, by inhinbiting caspase 3 and 9 activity and delaying cytochrome C release. In our study we demonstrated that the

survival in the actM was mediated by DAPK. Furthermore, we showed the mechanism of action in which DAPK triggered cell survival, by inhibiting caspase 3 cleavage. It has been found that RSK inactivates DAPK-proapoptotic function (Anjum et al. 2005). Interestingly, RSK was up-regulated during differentiation and activation of macrophages. Moreover, RSK was co-localized with DAPK in the cytoplasm of the macrophages, suggesting that RSK may interact with DAPK and positively regulate the DAPK-antiapoptotic function. However, further studies has to be done, in order to clarify that exact mechanisms involved DAPK regulation and its role in cell survival and cytokines production in macrophages.

TNF-α has long been recognized as an agent capable of inducing marked tumor regression and has undergone considerable testing against tumors in patients and animal models. Local administration of TNF-α alone, or in combination with other drugs or cytokines, was effective at inhibiting tumor growth with minimal side effects in both tumor models and human patients (Baisch etl al., 1990; Asher et al., 1991; Lasek et al., 1995 ,1996; Lejeune et al., 1994). Our study showed the cytotoxic potential of TNFα released from activated macrophages on colon cancer cells. We demonstrated the TNFα mechanism of action on p38 MAPK activation, which in turns induced DAPK activity and triggered apoptosis in colon cancer cells. Our *In vivo* examinations confirmed this DAPK-regulatory circuit.

Taken together, further studies are required to define more precisely the interactions between the tumor-associated macrophages (TAMs) and their growing solid tumors. A better understanding of the regulation and function of TAMs or their secretory cytokines may help to establish more therapeutically efficacious novel therapies for cancer management.

8. Summary

In summary, using our *in vitro* model, we could recapitulate the in vivo events observed by Schneider-Stock et al. (2006). We addressed that, colon tumor cells incubated with activated supernatants showed DAPK protein accumulation and underwent apoptosis. In contrast, although DAPK protein level was elevated after incubating the activated macrophages with colon tumor cell-supernatants, cells were apoptosis resistant. Moreover, we suggest that RSK may participate in the DAPK-dependent cell survival in U937 cell line. We show that *in vitro* DAPK and apoptosis inductions were due to TNFα release from the macrophages. For the first time, we showed a co-localization and physical interaction between activated p38 MAPK and DAPK, a complex that triggers TNFα-mediated apoptosis in colorectal cancer cells. Finally, our study demonstrated the Physiological significance of DAPK regulation in colon cancer. Altogether, these results encourage further testing of TNFα for its role as an anti-cancer agent.

Our results of can be summarized as follows:

1- Macrophage ⟶ Tumor cell

- Supernatants of activated macrophages mediated killing of HCT116 p53+/+ tumor cells.
- Supernatants of activated macrophages triggered DAPK protein accumulation rather than affecting its gene transcription in HCT116 p53+/+ tumor cells.
- Increase in TNFα and IFNγ release upon macrophage activation.
- TNFα but not IFNγ exposure induced cell death and DAPK protein up-regulation in HCT116 p53+/+ cells.
- TNFα mediated DAPK-dependent apoptosis in HCT116 p53+/+ cells.
- TNFα induced early activation of p38 in HCT116 p53+/+ tumor cells.

- JNK and ERK1/ERK2 did not contribute to TNFα/DAPK-triggered apoptosis in HCT116 p53+/+ cells.

- P-p38 co-localized and interacted with DAPK, thus it is identified as a new DAPK binding-protein

- P-p38 induced DAPK catalytic activity, thus it triggers the DAPK-mediated apoptosis by p-p38

- P53 acted down-stream of DAPK and involved partially in the observed cell death.
- TNFα induced apoptosis in HCT116 p53 deficient cells.

- P-p38 was up-regulated in the p53 deficient HCT116 cells upon TNFα exposure.
- P-p38 co-localized with DAPK in primary human colon cancer tissues.
- Supernatants of freshly isolated activated human macrophages up-regulated DAPK, induced early activation of p38 and cleavage of caspase 3.

2- Tumor cell ⟶ Macrophage

- HCT116 p53 wild type and deficient cells-supernatants increased DAPK level but no apoptosis was indicated in the activated U937.

- DAPK was found to contribute to the cell survival of the activated macrophages, by inhibiting caspase-3 cleavage.

- RSK co-localized with DAPK in the macrophage-like-cell line U937, thus it may play a role in the observed macrophages DAPK-mediated apoptosis resistance.

9. References

Aaltonen LA, Peltomaki P, Leach FS, Sistonen P, Pylkkanen L, Mecklin JP, et al. Clues to the pathogenesis of familial colorectal cancer. Science 1993;260:812–6.

Alleva DG, Burger CJ, Elgert KD. Tumor-induced regulation of suppressor macrophage nitric oxide and TNF-alpha production. Role of tumor-derived IL-10, TGF-beta, and prostaglandin E2. J Immunol 1994; 153: 1674-86.

Alleva DG, Askew D, Burger CJ, Elgert KD. Fibrosarcoma-induced increase in macrophage tumor necrosis factor a synthesis suppresses T cell responses. J Leukoc Biol 1993; 54: 152-160

Allum WH, Hallissey MT, Ward LC, Hockey MS. A controlled, prospective, randomised trial of adjuvant chemotherapy or radiotherapy in resectable gastric cancer: interim report. British Stomach Cancer Group. Br J Cancer 1989;60:739-44.

Alvarado-Kristensson M., Po¨rn-Ares M.I., Grethe S., Smith D., Zheng L., Andersson T., p38 Mitogen-activated protein kinase and phosphatidylinositol 3-kinase activities have opposite effects on human neutrophil apoptosis, FASEB J. 2001 (10.1096/fj.01-0817fje).

Anderson NG, Maller JL, Tonks NK, Sturgill TW. (1990) Requirement for integration of signals from two distinct phosphorylation pathways for activation of MAP kinase. *Nature,* 343: 651-653.

Anjum R., Roux P., Ballif B., Gygi S., Blenis J. The tumor suppressor DAP kinase is a target of RSK-mediated survival signaling. Curr Biol. 2005 Oct 11;15(19):1762-7.

Aoe T, Saito T. Towards immuno-modulation through the molecular mechanism of lymphocyte activation. Nippon Rinsho; 1995; 53: 2331-9

Aso H, Tamura K, Yoshie O, Nakamura T, Kikuchi S, Ishida N. Impaired NK response of cancer patients to IFN-alpha but not to IL-2: correlation with serum immunosuppressive acidic protein (IAP) and role of suppressor macrophage. Microbiology & Immunology 1992; 36: 1087-97

Asher A L, Mule J J, Kasid A, Restifo N P, Salo J C, Reichert C M, Jaffe G, Fendly B, Kriegler M, Rosenberg S A. J Immunol. 1991;146:3227–3234.

Auger MJ, Ross JA. The biology of macrophage. In Lewis CE, McGee JO, eds. The Macrophage. Oxford: Oxford University Press, 1992; 2-74

Baisch H, Otto U, Kloppel G. Cancer Res. 1990;50:6389–6395.

Baron-Bodo V., P. Doceur, M. L. Lefebvre, K. Labroquere, C. Defaye, C. Cambouris, D. Prigent, M. Salcedo, A. Boyer & A. Nardin: Anti-tumour properties of human-

activated macrophages produced in large scale for clinical application. Immunobiology 210, 267-277 (2005).

Ben-Baruch A. Inflammation-associated immune suppression in cancer: the roles played by cytokines, chemokines and additional mediators. Semin Cancer Biol 2005

Ben-Efraim S, onta BL. Modulation of antitumour activity of macrophages by regulation of eicosanoids and cytokine production. International Journal of Immunopharmacology 1994; 16: 397-9

Ben-Levy, R., S. Hooper, R. Wilson, H. F. Paterson, and C. J. Marshall. 1998. Nuclear export of the stress-activated protein kinase p38 mediated by its substrate MAPKAP kinase-2. Curr. Biol. 8:1049–1057.

Beyaert, R. & Fiers, W. (1994) Molecular mechanisms of tumor necrosis factor-induced cytotoxicity. What we do understand and what we do not. FEBS Lett. 340, 9-16

Blachere NE, Li Z, Chandawarkar RY, Suto R, Jaikaria NS, Basu S, Udono H, Srivastava PK. Heat shock protein-peptide complexes, reconstituted in vitro, elicit peptide-specific cytotoxic T lymphocyte response and tumor immunity. J Exp Med 1997; 186: 1315-22

Bonta IL, Ben-Efraim S, Mozes T, Fieren MW. Tumour necrosis factor in inflammation: relation to other mediators and to macrophage antitumour defence. Pharmacological Research 1991; 24: 115-30

Breitschopf K., Haendeler J., Malchow P., Zeiher A.M., Dimmeler S., Posttranslational modification of Bcl-2 facilitates its proteasomedependent degradation: molecular characterization of the involved signaling pathway, Mol. Cell. Biol. 20 (2000) 1886–1896.

Bronner CE, Baker SM, Morrison PT, Warren G, Smith LG, Lescoe MK, et al. Mutation in the DNA mismatch repair gene homologue *hMLH1* is associated with hereditary non-polyposis colon cancer. Nature 1994;368:258–61.

Bulavin DV, Phillips C, Nannenga B, Timofeev O, Donehower LA, Anderson CW, Appella E, Fornace Jr AJ. Inactivation of the Wip1 phosphatase inhibits mammary tumorigenesis through *p38 MAPK*-mediated activation of the *p16(Ink4a)-p19(Arf)* pathway. Nat Genet 2004; 36:343-50.

Cappell MS, Friedel D. The role of esophagogastroduodenoscopy in the diagnosis and management of upper gastrointestinal disorders. Med Clin North Am 2002;86:1165-216.

Carswell EA, Old LJ, Kassel RL, Green S, Fiore N, Williamson B. An endotoxin-induced serum factor that causes necrosis of tumors. Proceedings of the National Academy of Sciences of the United States of America 1975; 72: 3666-70

Chen, Z., T. B. Gibson, F. Robinson, L. Silvestro, G. Pearson, B. Xu, A. Wright, C. Vanderbilt, and M. H. Cobb. 2001. MAP kinases. Chem. Rev. 101:2449–2476.

Chen CH, Wang WJ, Kuo JC, Tsai HC, Lin JR, Chang ZF, Chen RH. Bidirectional signals transduced by DAPK-ERK interaction promote the apoptotic effect of DAPK. EMBO J. 2005 Jan 26;24(2):294-304. Epub 2004 Dec 16.

Cheung LY, DelCore R. Stomach. In: Townsend CM, Sabiston DC. Sabiston Textbook of surgery: the biological basis of modern surgical practice. 16th ed. Philadelphia, Pa.: Saunders, 2001:855-65.

Cohen O, Feinstein E, Kimchi A (1997) DAP-kinase is a Ca^{2+}/calmodulin-dependent, cytoskeletal-associated protein kinase, with cell death-inducing functions that depend on its catalytic activity. *EMBO J* 16: 998–1008

Cohen O, Inbal B, Kissil JL, Raveh T, Berissi H, Spivak-Kroizaman T, Feinstein E, Kimchi A (1999) DAP-kinase participates in TNF-alpha- and Fas-induced apoptosis and its function requires the death domain. *J. Cell. Biol.* 146: 141-148

Cohen, O. et al. DAP-kinase participates in TNFα- and Fas-induced apoptosis and its function requires the death domain. J. Cell. Biol. 146, 141−148 (1999).

Cohen, O., Feinstein, E. & Kimchi, A. DAP-kinase is a Ca^{2+}/calmodulin-dependent kinase, with cell death-inducing functions that depend on its catalytic activity. EMBO J. 16, 998−1008 (1997).

Colombo MP, Modesti A, Parmiani G, Forni G. Local cytokine availability elicits tumor rejection and systemic immunity through granulocyte-T-lymphocyte cross-talk. Cancer Research 1992; 52: 4853-7

Colorectal Cancer. In: BW Steward and P Kleihues, Editors, *World Cancer Report*, IARC Press, Lyon (2003), pp. 198–202.

Deacon K, Mistry P, Chernoff J, Blank JL, Patel R. p38 Mitogen-activated protein kinase mediates cell death and p21-activated kinase mediates cell survival during chemotherapeutic drug-induced mitotic arrest. Mol Biol Cell 2003; 14:2071-87.

Deiss LP, Feinstein E, Berissi H, Cohen O, Kimchi A (1995) Identification of a novel serine/threonine kinase and a novel 15-kD protein as potential mediators of the gamma interferon-induced cell death. *Genes Dev* 9: 15–30

DeMarco R, Ensor JE, Hasday JD. Tumor-stimulated release of tumor necrosis factor-alpha by human monocyte-derived macrophages. Cellular Immunology 1992; 140: 304-18

Derijard B, Hibi M, Wu IH, Barrett T, Su B, Deng T, Karin M, Davis RJ. JNK1: A protein kinase stimulated by UV light and Ha-Ras that binds and phosphorylates the c-Jun activation domain. Cell 1994; 76:1025-37.

Elgert KD, Alleva DG, Mullins DW. Tumor-induced immune dysfunction: the macrophage connection. J Leukoc Biol 1998; 64:275-90

Eisenberg-Lerner A., Kimchi A. DAP kinase regulates JNK signaling by binding and activating protein kinase D under oxidative stress. (2007). Cell Death Differ. 2007 Nov;14(11):1908-15

Ellinger-Ziegelbauer H, Kelly K, Siebenlist U. Cell cycle arrest and reversion of Rasinduced transformation by a conditionally activated form of mitogen-activated protein kinase kinase kinase 3. Mol Cell Biol 1999; 19:3857-68.

Erickson SL, de-Sauvage FJ, Kikly K, Carver-Moore K, Pitts-Meek S, Gillett N, Sheehan KC, Schreiber RD, Goeddel DV, Moore MW. Decreased sensitivity to tumour-necrosis factor but normal T-cell development in TNF receptor-2-deficient mice. Nature 1994; 372: 560-3

Fearon ER, Vogelstein B. A genetic model for colorectal tumorigenesis. Cell 1990;61:759–67.

Fidler IJ. Eradication of cancer metastasis by tumoricidal macrophages. Advances in Experimental Medicine & Biology 1988; 233: 415-23

Fishel R, Lescoe MK, Rao MR, Copeland NG, Jenkins NA, Garber J, et al. The human mutator gene homolog *MSH2* and its association with hereditary nonpolyposis colon cancer. Cell 1993;75:1027–38.

Freshney, N. W. *et al.* Interleukin-1 activates a novel protein kinase cascade that results in the phosphorylation of Hsp27. *Cell* 78, 1039–1049 (1994).

Fuchs CS, Mayer RJ. Gastric carcinoma. N Engl J Med 1995;333:32-41.

Gardner A.M., Johnson G.L. Fibroblast growth factor-2 suppression of tumor necrosis factor alpha-mediated apoptosis requires Ras and the activation of mitogen-activated protein kinase, J. Biol. Chem. 271 (1996) 14560–14566.

Ghiara P, Boraschi D, Villa L, Scapigliati G, Taddei C, Tagliabue A. *In vitro* generated mast cells express natural cytotoxicity against tumour cells. Immunology 1985; 55: 317324

Grethe S, Ares MP, Andersson T, Porn-Ares MI. p38 MAPK mediates TNF-induced apoptosis in endothelial cells via phosphorylation and down-regulation of Bcl-x(L). Exp Cell Res 2004;298:632–42.

Gunderson LL, Donohue JH, Burch PA. Stomach. In: Abeloff MD. Clinical oncology. 2d ed. New York, N.Y.: Churchill Livingstone, 2000:1545-79.

Grabbe S, Bruvers S, Beissert S, Granstein RD. Interferon-gamma inhibits tumor antigen presentation by epidermal antigen-presenting cells. J Leukoc Biol 1994; 55: 695-701

Hale K.K., Trollinger D., Rihanek M., Manthey C.L., Differential expression and activation of p38 mitogen-activated protein kinase alpha, beta, gamma, and delta in inflammatory cell lineages, J. Immunol. 162 (1999) 4246– 4252.

Han J, Lee JD, Bibbs L, Ulevitch RJ. A MAP kinase targeted by endotoxin and hyperosmolarity in mammalian cells. Science 1994; 265:808-11.
Huynh ML, Fadok VA, Henson PM (2002) Phosphatidylserine-dependent ingestion of apoptotic cells promotes TGF-beta1 secretion and the resolution of inflammation. J Clin Invest 1:41–50

Hannigan, M., Zhan, L., Ai, Y. & Huang, C. K. The role of p38 MAP kinase in TGF-β1-induced signal transduction in human neutrophils. Biochem. Biophys. Res. Commun. 246, 55–58 (1998).

Huang J, Wu L, Tashiro S, Onodera S, Ikejima T. comparison of the signal pathways between the TNF alpha- and oridonin-induced murine L929 fibrosarcoma cell death. Acta Med Okayama. 2005 Dec;59(6):261-70.

Henderson WR, Chi EY, Jong EC, Klebanoff SJ. Mast cell-mediated tumor-cell cytotoxicity. Role of the peroxidase system. J Exp Med 1981; 153: 520533

Huynh ML, Fadok VA, Henson PM (2002) Phosphatidylserine-dependent ingestion of apoptotic cells promotes TGF-beta1 secretion and the resolution of inflammation. J Clin Invest 1:41–50

Ichinose Y, Tsao JY, Fidler IJ. Destruction of tumor cells by monokines released from activated human blood monocytes: evidence for parallel and additive effects of IL-1 and TNFα. Cancer Immunology, Immunotherapy 1988; 27: 7-12

Inbal B, Cohen O, Polak-Charcon S, Kopolovic J, Vadai E, Eisenbach L, Kimchi A. DAP kinase links the control of apoptosis to metastasis. Nature 1997; 390:180-4.

Inbal, B., Shani, G., Cohen, O., Kissil, J.L. & Kimchi, A. Death-associated protein kinase-related protein 1, a novel serine/threonine kinase involved in apoptosis. Mol. Cell Biol. 18, 1642−1651 (2000).

Inbal, B., Bialik S., Sabanay I., Shani G., and Kimchi A. DAP kinase and DRP-1 mediate membrane blebbing and the formation of autophagic vesicles during programmed cell death J. Cell Biol., April 29, 2002; 157(3): 455 - 468.

Imanishi T, Han DK, Hofstra L, Hano T, Nishio I, Conrad LW, Gorden AM, Schwartz SM (2002) Apoptosis of vascular smooth muscle cells is induced by Fas ligand derived from monocytes/macrophage. Atherosclerosis 1:143–151

Ionov Y, Peinado MA, Malkhosyan S, Shibata D, Perucho M. Ubiquitous somatic mutations in simple repeated sequences reveal a new mechanism for colonic carcinogenesis. Nature 1993;363:558–61.

Iyoda K, Sasaki Y, Horimoto M, Toyama T, Yakushijin T, Sakakibara M, Takehara T, Fujimoto J, Hori M, Wands JR, Hayashi N. Involvement of the p38 mitogen-activated protein kinase cascade in hepatocellular carcinoma. Cancer 2003; 97:3017-26.

Jang CW, Chen CH, Chen CC, Chen JY, Su YH, Chen RH (2001) TGF-beta induces apoptosis through Smad-mediated expression of DAP-kinase. *Nat Cell Biol* 4: 51–58

Kankaanranta H., DeSouza P.M, Barnes P.J., Salmon M., Giembycz M.A., Lindsay M.A., SB 203580, an inhibitor of p38 mitogenactivated protein kinase, enhances constitutive apoptosis of cytokinedeprived human eosinophils, J. Pharmacol. Exp. Ther. 290 (1999) 621–628.

Karpoff HM, Tung C, Ng B, Fong Y. Interferon gamma protects against hepatic tumor growth in rats by increasing Kupffer cell tumoricidal activity. *Hepatology.* 1996 Aug;24(2):374–379

Keilholz U, Goey SH, Punt CJ, et al. Interferon α-2a and interleukin-2 with or without cisplatin in metastatic melanoma: a randomized trial of the European Organization for Research and Treatment of Cancer Melanoma Cooperative Group. J Clin Oncol 1997;15:2579–88.

Keranen LM, Dutil EM, Newton AC. (1995) Protein kinase C is regulated in vivo by three functionally distinct phosphorylations. *Curr. Biol.,* 5: 1394-1403

Killion JJ, Fidler IJ. Therapy of cancer metastasis by tumoricidal activation of tissue macrophages using liposome-encapsulated immunomodulators. Pharmacology & Therapeutics 1998; 78: 141-54

Kimchi, A. DAP genes: novel apoptotic genes isolated by a functional approach to gene cloning. Biochim. Biophys. Acta 1377, 13−33 (1998).

Klostergaard J, Leroux SM, Ezell SM, Kull FCJ. Tumoricidal effector mechanisms of murine Bacillus Calmette-Guerin-activated macrophages: mediation of cytolysis, mitochondrial respiration inhibition, and release of intracellular iron by distinct mechanisms. Cancer Research 1987; 47: 2014-9

Koh TJ, Wang TC. Tumors of the stomach. In: Feldman M, Friedman LS, Sleisenger MH. Sleisenger & Fordtran's Gastrointestinal and liver disease. 7th ed. Philadelphia, Pa.: Saunders, 2002:829-44.

Konishi H, Tanaka M, Takemura Y, Matsuzaki H, Ono Y, Kikkawa U, Nishizuka Y. (1997) Activation of protein kinase C by tyrosine phosphorylation in response to H2O2. *Proc. Natl. Acad. Sci. USA,* 94: 11233-11237

Kuo, J.-C., J.-R. Lin, J.M. Staddon, H. Hosoya, and R.-H. Chen. 2003. Uncoordinated regulation of stress fibers and focal adhesions by DAP-kinase. J. Cell Sci. 116:4777–4790

Kuo JC, Wang WJ, Yao CC, Wu PR, Chen RH. The tumor suppressor DAPK inhibits cell motility by blocking the integrin-mediated polarity pathway. J Cell Biol. 2006 Feb 13;172

Kyriakis, J. M., and J. Avruch. 2001. Mammalian mitogen-activated protein kinase signal transduction pathways activated by stress and inflammation. Physiol. Rev. 81:807–869.

Lasek W, Sora M, Wankowicz A, Jakobisiak M. Cancer Lett. 1995;89:137–143.

Lasek W, Wankowicz A, Kuc K, Feleszko W, Giermasz A, Jakobisiak M. *Oncology.* 1996;53:31–37.

Leek RD, Lewis CE, Whitehouse R, Greenall M, Clarke J, Harris AL. Association of macrophage infiltration with angiogenesis and prognosis in invasive breast carcinoma. Cancer Research 1996; 56: 4625-9

Lejeune F, Lienard D, Eggermont A, Schraffordt Koops H, Rosenkaimer F, Gerain J, Klaase J, Kroon B, Vanderveken J, Schmitz P. J Cell Biochem. 1994;56:52–61.

Liguo Zhang, Kenneth P. Nephew, and Patricia J. Gallagher. Regulation of death-associated protein kinase. Stabilization by HSP90 heterocomplexes. J Biol Chem. 2007 Apr 20;282(16):11795-804. Epub 2007 Feb 26.

Lin Y, Stevens C, Hupp T. Identification of a dominant negative functional domain on DAPK-1 that degrades DAPK-1 protein and stimulates TNFR-1-mediated apoptosis. J Biol Chem. 2007 Jun 8;282(23):16792-802. Epub 2007 Feb 26.

Liversidge J, Dick A, Gordon S (2002) Nitric oxide mediates apoptosis through formation of peroxynitrite and fas/fas-ligand interactions in experimental autoimmune uveitis. Am J Pathol 3:905–916

Losa JH, Parada Cobo C, Viniegra JG, Sanchez-Arevalo Lobo VJ, Ramon y Cajal S, Sanchez-Prieto R. Role of the p38 MAPK pathway in cisplatin-based therapy. Oncogene 2003; 22:3998-4006.

Madhani, H. D., and G. R. Fink. 1998. The riddle of MAP kinase signalling specificity. Trends Genet. 14:151–155.

Mantovani A, Ming WJ, Balotta C, Abdeljalil B, Bottazzi B. Origin and regulation of tumor-associated macrophages: the role of tumor-derived chemotactic factor.Biochim Biophys Acta 1986; 865:59-67

Markowitz S, Wang J, Myeroff L, Parsons R, Sun L, Lutterbaugh J, et al. Inactivation of the type II TGF-beta receptor in colon cancer cells with microsatellite instability. Science 1995;268:1336–8.

Martoriati A, Doumont G, Alcalay M, Bellefroid E, Pelicci PG, Marine JC (2005) *dapk1***,** encoding an activator of a p19ARF-p53 mediated apoptotic checkpoint, is a transcription target of p53**.** *Oncogene* 24**:** 1461–1466

Mayne ST, Risch HA, Dubrow R, Chow WH, Gammon MD, Vaughan TL, et al. Nutrient intake and risk of subtypes of esophageal and gastric cancer. Cancer Epidemiol Biomarkers Prev 2001;10:1055-62.

Mazzolini G, Murillo O, Atorrasagasti C, Dubrot J, Tirapu I, Rizzo M, Arina A, Alfaro C, Azpilicueta A, Berasain C, Perez-Gracia J, Gonzalez A, Melero I. Immunotherapy and immunoescape in colorectal cancer. World J Gastroenterol 200713: 5822-31

Mills CD, Shearer J, Evans R, Caldwell MD. Macrophage arginine metabolism and the inhibition or stimulation of cancer. J Immunol 1992; 149: 2709-14

Mittag F, Kuester D, Vieth M, Peters B, Stolte B, Roessner A, Schneider-Srock R, DAPK promoter methylation is an early event in colorectal carcinogenesis. Cancer Lett. 2006; 240: 69-75

Morse MA, Deng Y, Coleman D, Hull S, Kitrell-Fisher E, Nair S, Schlom J, Ryback ME, Lyerly HK. A Phase I study of active immunotherapy with carcinoembryonic antigen peptide (CAP-1)-pulsed, autologous human cultured dendritic cells in patients with metastatic malignancies expressing carcinoembryonic antigen. Clin Cancer Res 1999; 5: 1331-1338

Mosmann T. (1983).Rapid colorimetric assay for cellular growth and survival: application to proliferation and cytotoxicity assays. J Immunol Methods. 16; 65(1-2):55-63

Nicolaides NC, Papadopoulos N, Liu B, Wei YF, Carter KC, Ruben SM, et al. Mutations of two PMS homologues in hereditary nonpolyposis colon cancer. Nature 1994;371:75–80.

Nicolaides NC, Carter KC, Shell BK, Papadopoulos N, Vogelstein B, Kinzler KW. Genomic organization of the human PMS2 gene family. Genomics 1995;30:195–206.

Ohno S, Inagawa H, Dhar DK, et al. The degree of macrophage infiltration into the cancer cell nest is a significant predictor of survival in gastric cancer patients. Anticancer Res 2003;23:5015–22

Ohta K, Pang XP, Berg L, Hershman JM. Antitumor actions of cytokines on new human papillary thyroid carcinoma cell lines. J Clin Endocrinol Metab 1996;81:2607–12.

Opdenakker G, Van-Damme J. Cytokines and proteases in invasive processes: molecular similarities between inflammation and cancer. Cytokine 1992; 4: 251-8

Owen MR, Sherratt JA. Modelling the macrophage invasion of tumours: effects on growth and composition. IMA Journal of Mathematics Applied in Medicine & Biology 1998; 15: 165-85

Parajuli P, Singh SM. Alteration in IL-1 and arginase activity of tumor-associated macrophages: a role in the promotion of tumor growth. Cancer Lett 1996; 107: 249-56

Park JM, Greten FR, Li ZW, Karin M. Macrophage apoptosis by anthrax lethal factor through p38 MAP kinase inhibition. Science 2002; 297:2048-51.

Papadopoulos N, Nicolaides NC, Liu B, Parsons R, Lengauer C, Palombo F, et al. Mutations of *GTBP* in genetically unstable cells. Science 1995;268:1915–7.

Pawson, T. and Nash, P. (2000) Protein–protein interactions define specificity in signal transduction. Genes Dev. 14, 1027–1047

Pearson, G., F. Robinson, T. Beers Gibson, B. E. Xu, M. Karandikar, K. Berman, and M. H. Cobb. 2001. Mitogen-activated protein (MAP) kinase pathways: regulation and physiological functions. Endocrinol. Rev. 22:153–183.

Pruitt K, Pruitt WM, Bilter GK, Westwick JK, Der CJ. Raf-independent deregulation of p38 and JNK mitogen-activated protein kinases are critical for Ras transformation. J Biol Chem 2002; 277:31808-17.

Puri PL, Wu Z, Zhang P, Wood LD, Bhakta KS, Han J, Feramisco JR, Karin M, Wang JY. Induction of terminal differentiation by constitutive activation of *p38 MAP* kinase in human rhabdomyosarcoma cells. Genes Dev 2000; 14:574-84.

Raveh, T., Berissi, H., Eisenstein, M., Spivak, T. & Kimchi, A. A functional genetic screen identifies regions at the C-terminal tail and death-domain of death-associated protein kinase that are critical for its proapoptotic activity. Proc. Natl. Acad. Sci. USA 97, 1572−1577 (2000).

Raingeaud, J., S. Gupta, J. S. Rogers, M. Dickens, J. Han, R. J. Ulevitch, and R. J. Davis. 1995. Pro-inflammatory cytokines and environmental stress cause p38 mitogen-activated protein kinase activation by dual phosphorylation on tyrosine and threonine. J. Biol. Chem. 270:7420–7426

Raingeaud J, Gupta S, Rogers JS, Dickens M, Han J, Ulevitch RJ, Davis RJ. Pro-inflammatory cytokines and environmental stress cause p38 mitogen-activated protein kinase activation by dual phosphorylation on tyrosine and threonine. J Biol Chem 1995; 270:7420-6.

Raveh T, Droguett G, Horwitz MS, DePinho RA, Kimchi A (2001) DAP kinase activates a p19ARF/p53-mediated apoptotic checkpoint to suppress oncogenic transformation. *Nat Cell Biol* 3: 1–7

Raveh T, Kimchi A. DAP *kinase*-a proapoptotic gene that functions as a tumor suppressor. Exp Cell Res 2001; 264:185-92.

Redel CA, Zweiner RJ. Stomach. In: Feldman M, Friedman LS, Sleisenger MH. Sleisenger & Fordtran's Gastrointestinal and liver disease. 7th ed. Philadelphia, Pa.: W.B. Saunders, 2002:557-60.

Ricardo SD, Diamond JR (1998) The role of macrophages and reactive oxygen species in experimental hydronephrosis. Semin Nephrol 6:612–621

Ribas A, Camacho LH, Lopez-Berenstein G, et al. Antitumor activity in melanoma and anti-self responses in a phase I trial with the anti-cytotoxic T lymphocyte-associated antigen 4 monoclonal antibody CP-675, 206. J Clin Oncol 2005;23:8968–77.

Roulston A., Reinhard C., Amiri P., Williams P.T., Early activation of c-Jun N-terminal kinase and p38 kinase regulate cell survival in response to tumor necrosis factor a, J. Biol. Chem. 273 (1998) 10232– 10239.

Rubin J, Galanis E, Pitot HC, Richardson RL, Burch PA, Charboneau JW, Reading CC, Lewis BD, Stahl S, Akporiaye ET, Harris DT. Phase I study of immunotherapy of hepatic metastases of colorectal carcinoma by direct gene transfer of an allogeneic histocompatibility antigen, HLA-B7. Gene Ther 1997; 4: 419-425

Rustgi AK. Neoplasms of the stomach. In: Cecil RL, Goldman L, Bennett JC. Cecil Textbook of Medicine. 21st ed. Philadelphia, Pa.: W.B. Saunders, 2000: 738-41.

Salvesen H, Akslen L. Significance of tumour-associated macrophages, vascular endothelial growth factor and thrombospondin-1 expression for tumour angiogenesis and prognosis in endometrial carcinomas. Int J Cancer1999; 84: 539-43

Schaeffer EM, Broussard C, Debnath J, Anderson S, McVicar DW, Schwartzberg PL. Tec family kinases modulate thresholds for thymocyte development and selection. J Exp Med 2000; 192:987-1000.

Schneider-Stock R., Kuester D., Ullrich O., Mittag F., Habold C., Boltze C., Peters B., Krueger S., Hintze C., Meyer F.. Close localization of DAP-kinase positive tumor-associated macrophages and apoptotic colorectal cancer cells. *J* Pathol. 2006;209:95–105

Senzer N, Mani S, Rosemurgy A, Nemunaitis J, Cunningham C, Guha C, Bayol N, Gillen M, Chu K, Rasmussen C, Rasmussen H, Kufe D, Weichselbaum R, Hanna N. TNFerade biologic, an adenovector with a radiation-inducible promoter, carrying the human tumor necrosis factor alpha gene: a phase I study in patients with solid tumors. J Clin Oncol 2004; 22: 592-601

Shani, G., S. Henis-Korenblit, G. Jona, O. Gileadi, M. Eisenstein, T. Ziv, A. Admon, and A. Kimchi. 2001. Autophosphorylation restrains the apoptotic activity of DRP-1 kinase by controlling dimerization and calmodulin binding. EMBO J. 20:1099–1113.

Siewert JR, Fink U, Sendler A, Becker K, Bottcher K, Feldmann HJ, et al. Gastric cancer. Curr Probl Surg 1997;34:835-939.

Siewert JR, Bottcher K, Stein HJ, Roder JD. Relevant prognostic factors in gastric cancer: ten-year results of the German Gastric Cancer Study. Ann Surg 1998; 228:449-61.

Silverman MA, Zaidi U, Barnett S, Robles C, Khurana V, Manten H, et al. Cancer screening in the elderly population. Hematol Oncol Clin North Am 2000;14:89- 112.

Simpson DJ, Clayton RN & Farrell WE 2002 Preferential loss of Death Associated Protein kinase expression in invasive pituitary tumours is associated with either CpG island methylation or homozygous deletion. Oncogene 21 1217–1224.

Smith SJ, Fenwick PS, Nicholson AG, Kirschenbaum F, Finney-Hayward TK, Higgins LS, Giembycz MA, Barnes PJ, Donnelly LE. nhibitory effect of p38 mitogen-activated protein kinase inhibitors on cytokine release from human macrophages. Br J Pharmacol. 2006 Oct;149(4):393-404.

Spriggs, D.; Yates, S. Tumor Necrosis Factors: Their Emerging Role in Medicine. Beutler B. , editor. New York: Raven; 1992. pp. 383–405.

Sunderkotter C, Goebeler M, Schulze-Osthoff K, et al. Macrophage-derived angiogenesis factors. Pharmacol Ther 1991;51:195–216

Sunderkotter C, Steinbrink K, Goebeler M, Bhardwaj R, Sorg C. Macrophages and angiogenesis. J Leukoc Biol 1994; 55: 410-22

Takanami I, Takeuchi K, Kodaira S. Tumor-associated macrophage infiltration in pulmonary adenocarcinoma: association with angiogenesis and poor prognosis. Oncology 1999; 57: 138-42

Tani K, Ogushi F, Shimizu T, Sone S. Protease-induced leukocyte chemotaxis and activation: Roles in host defense and inflammation. J Med Invest 2001; 48: 133-141

Thibodeau SN, Bren G, Schaid D. Microsatellite instability in cancer of the proximal colon. Science 1993;260:816–9.

Timofeev O, Lee TY, Bulavin DV. A subtle change in *p38 MAPK* activity is sufficient to suppress in vivo tumorigenesis. Cell Cycle 2005; 4:118-20.

Urban JL, Shepard HM, Rothstein JL, Sugarman BJ, Schreiber H. Tumor necrosis factor: a potent effector molecule for tumor cell killing by activated macrophages. Proceedings of the National Academy of Sciences of the United States of America 1986; 83: 5233-7

Volodko N, Reiner A, Rudas M, Jakesz R. Tumour-associated macrophages in breast cancer and their prognostic correlations. Breast 1998; 7: 99-105

Wang W., Kuo J., Ku W., Lee Y., Lin F., Chang Y., Lin Y., Chen C., Huang Y., Chiang M., Yeh S., Wu P., Shen C., Wu C., Chen R. The tumor suppressor DAPK is reciprocally regulated by tyrosine kinase Src and phosphatase LAR. Mol Cell. 2007 Sep 7;27(5):701-16

Zarubin T, Han J. Activation and signaling of the p38 MAP kinase pathway. Cell Res 2005; 15:11-8.

Zechner D., Craig R., Hanford D.S., McDonough P.M, Sabbadini R.A., Glembotski C.C., MKK6 activates myocardial cell NF-kappaB and inhibits apoptosis in a p38 mitogen-activated protein kinasedependent manner, J. Biol. Chem. 273 (1998) 8232–8239.

10. Abbreviations

APS	Ammonium-persulfate
ATCC	American Type Culture Collection
ATF	Activating transcription factor
ATP	Adenosine triphosphate
BSA	Bovine serum albumine
cDNA	Complementary deoxyribonucleic acid
CGI	CpG island
Da	Dalton
DAPK	Death associated protein kinase
DAPI	4',6-diamino-2-phenylindole
DMEM	Dulbecco's modified Eagles medium
DMSO	Dimethylsulfoxide
DNA	Deoxyribonucleic acid
DRAK	DAPK-related protein
DTT	D,1-Dithiothreitol
ECL	Enhanced chemiluminescence
EDTA	Ethylenediamine-tetra acetic acid
EGF	Epidermal growth factor
ELISA	Enzyme-Linked ImmunoSorbent Assay
ERK	Extracellular regulated kinase
FACS	Fluorescence-activated cell sorting
FBS	Fetal bovine serum
FCS	Fetal calf serum
FITC	fluorescein isothiocyanate
HRP	Horseradish peroxidise
HSP90	Heat shock protein 90
IFNγ	Interferon gamma
Ig	Immunoglobulin
IL	Interleukin
kDa	Kilo dalton
JNK	c-Jun amino terminal kinase

LAR	Leukocyte common antigen-related tyrosine phasphatse
LPS	lipopolysaccharide
M	Molarity
MAPK	Mitogen-activated protein kinase
MEK	Mitogen-activated protein kinase kinase
MLC	Myosin light chain
MLCK	Myosin light chain kinase
mRNA	Messenger ribonucleic acid
MSP	Methylation-specific PCR
NF-κB	Nuclear factor-κB
OD	Optical density
PAGE	Polyacrylamid gel electrophoresis
PDGF	Plateled-derived growth factor
P.E.G	Polyethylenglycol 6000
PI	Propidium iodide
PMA	phorbol 12-myristate 13-acetate
PKB	Protein kinase B
PKD	Protein kinase D
PKC	Protein kinase C
PMSF	Phenylmethylsulfonyl fluoride
PS	phosphatidylserine
RNA	Ribonucleic acid
rpm	Rotation per minute
RPMI	Roswell Park Memorial Institute medium
RSK	Ribosomal S6 kinase
RT-PCR	Reverse transcription polymerase chain reaction
SAPK	Stress-activated protein kinase
SDS	Sodium dodecyl sulphate
siRNA	Small interfering RNA
Src	Raus sarcoma virus proto-oncogene product
STAT	Signal transducers and activators of transcription
TAM	Tumor associated macrophages
TBS	Tris Buffered Saline

TEMED	N,N,N',N'-Tetra-methylethylenediamine
TGFβ	Transforming growth facto beta
TMB	3,3′,5,5′-Tetramethylbenzidine tablets
TNFα	Tumor necrosis factor alpha
TNFR	Tumor necrosis factor receptor
TR	Transfection reagent
Tris	Trishydroxymethylaminomethane
TUNEL	Terminal uridine deoxynucleotidyl transferase dUTP nick end labeling
WHO	World health organization
ZIP	Zipper interacting protein
ZIPK	Zipper interacting protein kinase

11. Lebenslauf

Name:	Khuloud Bajbouj
Geburtsdatum und -ort:	10.03.1980 – Om AlQwain / Vereinigte arabische Emirate
Geschlecht:	weiblich
Staatsangehörigkeit:	syrisch
Familienstand:	verheiratet
Wohnsitz:	Fermersleber Weg 45a, 39112 Magdeburg
Schulausbildung:	1986-1989: Grundschule, Om AlQwain
	1989-1995: ‚Primary'-Schule, Om AlQwain
	1995-1998: Sekundarschule, Om AlQwain
Schulabschluss:	Zertifikat der "Secondery High School" am 07.07.1998
Studium:	1998-2002: Universität der vereinigten arabischen Emirate, Fachrichtung Biologie-Bachelor, Hauptfach: Zelluläre und Molekulare Biologie
Studienabschluss:	Bachelor am 02.2002, Prädikat: gut Abschlussprojekt: Molecluar diagnosis of β-Thalasimia disease.
Studium:	2004-2006: Otto-von-Guericke-Universität Magdeburg. Fachrichtung Neurobiologie-Diplom, Hauptfach: Zelluläre Grundlagen der Neurobiologie Nebenfach: Neuroimmunologie
Studienabschluss:	Diplom am 07.2006, Prädikat: gut

Diplomarbeit: “Epigenetische Regulation von $p21^{WAF1}$ nach Behandlung mit dem Histon-Deacetylase Inhibitor Trichostatin A in Glioblastoma Zelllinie (U87) Tumorzellen“

Berufstätigkeit:

2004, wissenschaftliche Hilfskraft, Leibniz-Institut für Neurobiologie Magdeburg

2004, wissenschaftliche Hilfskraft, Institut für Biophysik, Fakultät für Naturwissenschaften, Otto-von-Guericke-Universität Magdeburg

2005, wissenschaftliche Hilfskraft, Institut für Neurobiochemie, Medizinischen Fakultät, Otto-von-Guericke-Universität Magdeburg

2005, wissenschaftliche Hilfskraft, Institut für Pathologie, Otto-von-Guericke Universität Magdeburg

Promotionsarbeit:

seit 1.04.2006: Wissenschaftliche Mitarbeiterin des Instituts für Pathologie der Medizinischen Fakultät der Otto-von-Guericke-Universität Magdeburg

12. Own publications

1- Roepke M, Diestel A, **Bajbouj K**, Walluscheck D, Schonfeld P, Roessner A, Schneider-Stock R, Gali-Muhtasib H. 2007. Lack of p53 Augments Thymoquinone-Induced Apoptosis and Caspase Activation in Human Osteosarcoma Cells. Cancer Biology and Therapy 6(2):160-169.

2- Habold C, Poehlmann A, **Bajbouj K**, Hartig R, Korkmaz K S, Roessner A, Schneider-Stock R. 2007. Trichostatin A causes p53 to switch oxidative-damaged colorectal cancer cells from cell cycle arrest into apoptosis. http://www.blackwell-synergy.com/doi/abs/10.1111/j.1582-4934.2007.00136.x